AN INVESTIGATION INTO THE ERROR PERFORMANCE OF VERTICAL-BELL LABS LAYERED SPACE-TIME ARCHITECTURE V-BLAST

SAJID ANWAR KHAN

Electrical Engineering

May 2003

KING FAHD UNIVERSITY OF PETROLEUM AND MINERALS

DHAHRAN 31261, SAUDI ARABIA

DEANSHIP OF GRADUATE STUDIES

This thesis, written by **Sajid Anwar Khan** under the direction of his thesis advisor and approved by his thesis committee, has been presented to and accepted by the Dean of Graduate Studies, in partial fulfillment of the requirements for the degree of

MASTER OF SCIENCE IN ELECTRICAL ENGINEERING.

THESIS COMMITTEE

Dr. A.U.H. Sheikh (Chairman)

Dr. Saud A. Al – Semari (Member)

Dr. Maan Kousa (Member)

Dr. Jamil M. Bakhashwain
Department Chairman

Prof. Osama Ahmed Jannadi
Dean of Graduate Studies

Date

Dedicated to

My Beloved Parents

and

Caring Brothers

ACKNOWLEDGEMENTS

In the name of ALLAH, The Most Gracious, Merciful and Beneficent. First and foremost all the praise goes to ALLAH subhana-wa-ta' ala, The Almighty, and The Creator of the universe, who granted me the grace and strength to complete this work. Peace and blessing of ALLAH be upon His last Prophet Hazrat Muhammad sallallaho-alaihe-wassalam, and his family, and all his righteous followers till the day of judgement.

I would like to express my profound gratitude and appreciation to my thesis committee chairman Dr. Asrar U. H. Sheikh for his guidance, sincere advice, and continuous support throughout my thesis. Working with him was indeed a wonderful learning experience, which I thoroughly enjoyed. Thanks are also to Dr. Maan Kousa and Dr. S. A. Al Semari for their support and valuable suggestions they made to improve the work.

I shall ever remain indebted to my parents for their socio-religious guidance they gave to me. Their support and prayers led to this accomplishment. I pray ALLAH (SWT) to forgive their souls and admit them to Al-Jannah. I am also thankful to

my brothers and their children for their moral support.

Acknowledgement is due to King Fahd University of Petroleum and Minerals, Dhahran, Saudi Arabia for providing the support and facilities in carrying out this research.

I owe my deep appreciation to my seniors Moin Uddin, Saad Azhar and Ajmal Khan for helping me on issues relating to LaTeX. I also appreciate the support provided by my fellow Kamran and Ahmar.

Finally, I would like to thank my fellow graduate students and all my friends in the campus, especially Aamir, Shiraz, Asif, Naveed, Saad Mansoor, Shafayat, Mahmood, Fareed, Arshad and Owais for providing me a wonderful company.

My heartfelt thanks to my days old friends Atif, Wasif, Ali Khan, Aijaz and Ghufran . They truly are my great friends, I wish we could be together again.

Contents

List of Tables

List of Figures

THESIS ABSTRACT

Name: Sajid Anwar Khan

Title: An Investigation into the Error Performance of Vertical Bell-Labs Layered Space Time Architecture V-BLAST

Degree: MASTER OF SCIENCE

Major Field: Electrical Engineering

Date of Degree: May 2003

Recent information theory research has shown that the rich-scattering wireless channel is cable of enormous theoretical capabilities if the multipath is properly exploited. In effect, the unavoidable multipath is exploited to provide a very useful spatial parallelism that is used to greatly improve data transmission rates.

The study of statistical distribution of errors is a prerequisite in the design of appropriate coding techniques to effectively control errors. The V-BLAST architecture is analyzed and compared for two transmitter-receiver arrangements (3×3), and (6×6). (3×3) utilizes 9 channel paths while (6×6) utilizes 36 channel paths. Utilization of more channel paths improves the overall performance. We analyzed the system performance over Rayleigh and Nakagami channels along with statistical analysis of errors.

For correlated Channel paths (higher m), V-BLAST performance is limited by error propagation. Frequency of occurrences of Error Burst Lengths and Error Free Intervals are determined. Modelling of the distribution of Error Burst Lengths and Error Free Lengths is performed. We also analyzed all the above parameters when well renowned Turbo Coding is applied. We evaluated the effects of different interleaver depths where the interleavers used are cyclic shift interleavers. It is shown that the increase in the number of transmitters and receivers, and de-correlation in channel paths give improved performance.

Keywords: *Multipath, V-BLAST, Channel Capacity, Rayleigh, Nakagami, Turbo Coding, Interleaver Depth,*

King Fahd University of Petroleum and Minerals, Dhahran.

May 2003

Chapter 1

Introduction

1.1 Background of Mobile Radio Channels

Wireless communication is enjoying its fastest growth period in history, due to enabling technologies which permit widespread development. Historically, growth in the mobile communication field has come slowly, and has been coupled closely to technological improvements. The ability to provide wireless communications to an entire population was not even conceived until Bell-Laboratories developed the cellular concept in the 1960s and 1970s [1]. With the development of highly reliable, miniature, solid-state radio frequency hardware in the 1970s, the wireless communications era was born. The recent exponential growth in cellular radio and personal communication systems throughout the world is directly attributable to new technologies of the 1970s, which are mature today. The future growth of consumer-based

mobile and portable communication systems will be tied more closely to radio spectrum allocations and regulatory decisions which affect or support new or extended services, as well as to consumer needs and technology advances in the signal processing, access, and network areas.

1.2 Trends in Mobile Radio Systems

Since 1989, there has been enormous activity throughout the world to develop personal wireless systems that combine the network intelligence of today's PSTN with modern digital signal processing and RF technology. Indoor wireless networking products are steadily emerging and promise to become a major part of the telecommunications infrastructure within the next decade. An international standards body is developing standards, IEEE 802.11, for wireless access between computers inside buildings. The European Telecommunications Standard Institute (ETSI) is also developing the 20 Mbps HIPERLAN standard for indoor wireless networks.

A world wide standard, the Future Public Land Mobile Telephone System (FPLMTS)-renamed International Mobile Telecommunication 2000 (IMT-2000) in mid-1995 - is being formulated by the International Telecommunications Union (ITU) which is the standards body for the United Nations. FPLMTS (now IMT-2000) is a third generation universal Multi-function, globally compatible digital mobile radio system that would integrate paging, cordless, and cellular systems, as well as low earth orbit

satellites, into one universal mobile system. A total of 230 MHz in frequency bands 1885 MHz to 2025 MHz and 2110 MHz to 2200 MHz has been targeted by the ITU's 1992 World Administrative Radio Conference (WARC).

1.3 3G Systems

The Third Generation (3G) is a digital mobile multimedia offering broadband mobile communications with voice, video, graphics, audio and other information. 3G facilitates several new applications that have not previously been readily available over mobile networks due to the limitations in data transmission speeds. These applications range from Web Browsing to file transfer to Home Automation (the ability to remotely access and control in-house appliances and machines). Because of the bandwidth increase, these applications will be even more easily available with 3G than they were previously with interim technologies. The mobile communications industry has evolved in three stages, and correspondingly three generations of mobile phones have emerged thus far. Each one has provided more flexibility and usability than the previous ones.

1. (1G) Analog: Analog phones helped to make voice calls inside one's country without roaming facilities.

2. (2G) Digital mobile phone systems added fax, data and messaging capabilities as well as voice telephone service in many countries offering worldwide

roaming.

3. (3G) Multimedia services add high speed data transfer to mobile devices, allowing new video, audio and other applications (including Internet services) through mobile phones.

During the first and second generations, different regions of the world pursued different mobile phone standards, such as NMT and TACS for analog and GSM for digital. North America pursued AMPS for analog and a mix of TDMA, CDMA and GSM for digital. The aim of IMT-2000 is to harmonize worldwide 3G systems to provide global roaming. However, harmonizing so many different standards proved extremely difficult. As a result, five different standards grouped together under the IMT-2000 label:

- IMT-DS
- IMT-ML
- IMT-FT
- IMT-TC
- IMT-SC

Some of the 3G features are listed below.

1. With 3G, the information is split into packets before being transmitted and reassembled at the receiving end. Packet switched data formats are much more common than their circuit switched counterparts.

2. The World Wide Web (WWW) is becoming the primary communications interface. People access the Internet for entertainment, services, and information collection, the intranet for accessing enterprize information and connecting with colleagues and the extranet for accessing customers and suppliers. These are all derivatives of the World Wide Web aimed at connecting different communities of interest. Information and other resources are being stored in remote Web servers, which serves the various needs of human beings through Web browsers at their ends.

3. Speeds of up to 2 Megabits per second (Mbps) are achievable with 3G. The data transmission rates will depend upon the environment, the call is being made in, however, only indoors and in stationary environments that these types of data rates will be available. For high mobility, data rates of 144 kbps are expected to be available.

1.4 Need for Higher Capacity for Higher Speed Services

During the past ten years, there has been an explosive growth of personal and mobile wireless services whose ultimate goal is to support universal personal and multimedia services. The future services are intended to provide image, video, and local area network applications which require high-speed data transmission that can be more than 1000 times faster than present systems [2]. Applications such as CD audio, VCR quality TV require over 1 megabit per second (Mbps), while broadcast quality television or real-time video would require 5 megabits per second (Mbps). New advanced applications like tele-health, distance learning, the delivery of government services and e-business require large channel capacity. Physical limits imposed by the mobile radio channel cause performance degradation and make it very difficult to achieve high bit rates at low error rates over the time dispersive wireless channels. Another key limitation is co-channel interference (CCI) which can also significantly decrease the capacity of wireless and personal communications systems.

1.5 High Speed Data and Coding

Various techniques have been studied for reliable high-rate wireless-data transmissions. Recently, space-time coding is introduced as an alternative and attractive solution for high data rate transmission in wireless communications systems [3]. In this scheme multiple transmit antennas combined with optional receive antenna are

employed to spread encoded information across the antennas. This is done by combining signal processing at the receiver with coding techniques at multiple transmit antennas for providing high data rate wireless communications.

1.6 Motivation for Present Work

Vertical Bell-Labs Layered Space Time Architecture VBLAST proposed by G.J.Foshini *et al* [4], is capable of realizing extraordinary spectral efficiencies over rich scattering wireless channel. VBLAST suffers from the problem of error propagation. Also, wireless channel is inherently bursty channel. Therefore, VBLAST on wireless channel produces errors in bursts along with random errors. Therein lies the motivation for finding the ways and means of reflecting the statistical structure of error occurrences. By applying iterative turbo decoding, a very low bit error probability can be achieved at a signal to noise ratio close to the Shannon's capacity limit. The statistical structures of errors before and after applying turbo coding is compared to evaluate the impact of coding.

1.7 Literature Survey

The literature related to this work encompasses the research pertaining to layered space-time architecture BLAST proposed by Foschini [5]. G.J. Foschini *et al.* [6] constrain the channel bandwidth and total transmitted power and show that by

forming a channel using increased spatial dimensions one can get extraordinarily large capacity.

Number of detection algorithms are proposed for BLAST architecture. P.W. Wolniansky *et al.* [4, 7] implemented linear combinatorial nulling, in which each substream in turn is considered to be the desired signal one after another, and the remaining substreams are considered as "interferers". Nulling is performed linearly weighting the received signals so as to satisfy zero-forcing (ZF) criterion. Stephen Baro *et al* [8] provided another way to improve detection performance especially for mid-range SNR values and to replace the zero-forcing (ZF) nulling by the more powerful minimum mean-square error (MMSE) algorithm. In [9],Won-Joon, Rohit Negi and John M. Cioffi proposed to combine maximum likelihood (ML) decoding and decision feedback equalization for VBLAST. It performed ML decoding for the first p subchannels, and used the DFE procedure for the remaining subchannels. Babak Hassibi [10], developed a square-root algorithm for the nulling-vector optimal-ordering step. Xiaodong Li *et al* [11] studied coding architectures constructed from conventional codes including convolutional codes and Reed-Solomon codes. Their focus was on the performance and complexity trade-offs involved in the design of coding/decoding and signal detection algorithms. M.O. Damen *et al* [12], presented a detection algorithm that is based on QR decomposition of the channel transfer matrix which is then used to perform hard or soft inter-substream interference cancellation.

Different coding schemes are implemented to achieve the great potential of BLAST. Stephen Baro *et al* applied transmit diversity with space-time block codes in [8] and showed that the number of receive antennas can be reduced and the diversity level increased compared to the original BLAST. In [13], Mathini Sellathurai *et al* proposed a BLAST scheme termed T-BLAST which uses an inter-substream interleaver following a vector encoder with each substream utilizes the same forward error correction (FEC) code. They introduced two iterative receiver schemes for T-BLAST architecture :(1) an optimal MAP receiver with a computational complexity exponential in the number of transmitting antennas, and (2) a suboptimal nonlinear scheme obtained by replacing the actual co-antenna interference (CAI) with their expectations that leads to an iterative parallel soft interference canceller.

BLAST technique is also applied in CDMA systems to achieve high data rates. Howard Huang, Harish Viswanathan, and G.J. Foschini evaluated the capacity of a down link cellular CDMA system in [14]. They discussed a family of transmission techniques using multiple antennas and orthogonal codes which combine transit diversity and multicode transmission for achieving high data rates. Higher system spectral efficiencies (greater than one) can potentially be achieved if the same spreading code is used on different antennas to transmit independent substreams.

Seong Taek Chung *et al* [15] used feedback of Rate and/or power information to the transmitter and showed that, with per antenna rate adaptation, V-BLAST can achieve the same capacity available to much more complex structures. Dmitry

Chizhik *et al* [16] worked out the correlation between base station antennas for different antenna spacings. The result is used to derive link capacity, when there is correlation among receive antennas and among transmit antennas. F.R. Farrokhi *et al* [17] presented a generalization of BLAST that is optimal, in the sense of maximizing the link spectral efficiency, in the presence of spatially colored interference. In this general scheme, the channel and interference covariance are made available to the transmitter, which find the channel eigenmodes in the presence of the interference and sends multiple data streams through those eigenmodes.

1.8 Thesis Contribution

The objective of this work is to contribute towards better understanding of statistical analysis of errors occurred in a newly proposed Vertical Bell-Labs Layered Space Time Architecture. Study of statistical distribution of errors is a pre-requisite in the design of appropriate coding techniques to effectively control errors. The thesis investigates statistical analysis of errors along with bit error rate. Distributions of error burst lengths and error free lengths are evaluated and their modelling is performed for clear understanding of statistical structure of errors. Average error burst lengths and error free lengths are also measured. Bit error rate is a decisive criterion to judge a system. It is also calculated for V-BLAST system. All of the these analysis are performed over Rayleigh, Nakagami1.33, and Nakagami2.77

channels. This gives system performance over uncorrelated and correlated channels. Two transmitter-receiver arrangements are employed (Tx = 3, Rx = 3, and Tx = 6, Rx = 6) for all the channels. This gives system performance when different number of channel paths are utilized. The analysis is performed for different mobile speeds covering Doppler frequencies 10, 20, 50 Hz.

The thesis also covers the statistical analysis of errors and BER performance and the variation of these parameters with the application of Turbo coding over 10 Hz Doppler frequency channel. Iterative decoding using *maximum a posteriori probability* (MAP) algorithm is employed. The MAP decoding criterion is used to minimize the symbol or bit error probability. Interleavers are used to increase code length and decorrelate the inputs. Cyclic shift interleavers of depths 64, 512, 1024 are used in this work. In addition to the good performance of cyclic shift interleaver, it has the advantages of low design complexity and memory requirements. For all the above channels and transmitter-receiver arrangements, distribution of error burst lengths and error free lengths are evaluated after decoding. Modelling of the distributions is also performed. Average error burst lengths and average error free lengths are measured. Bit error rate of the system after decoding is also calculated that gives coding gain.

1.9 Thesis Organization

The next chapter describes the characteristics of mobile radio channel like fading and multipath. Discrete time channel model of mobile radio channel is studied. Performance degradation due to transmission over mobile radio channel is discussed.

Mobile radio channel characteristics and channel capacity are discussed in chapter 3. Channel memory and error characterization are studied. A separate section is devoted for methods to increase channel capacity.

In chapter 4, Bell-Labs Layered Space Time Architecture (BLAST) is introduced. Transmission and reception of BLAST and Vertical-BLAST is explained. VBLAST receiver structures are also described. Issues regarding Turbo Coding are also discussed.

Chapter 5 presents simulation results. Simulation model of mobile radio channel is described first. Simulation experiment design is discussed. Error characteristics and modelling is illustrated. Finally error characterization without and with turbo coding is presented.

The conclusion of the thesis is summarized in chapter 6, where some suggestions are also stated for direct extension of this work to further research.

Chapter 2

Mobile Radio Channel Model & Impairments

2.1 Fading

The rapid fluctuation of the amplitude of radio signal describes fading when the terminal travels through scattering and diffracting media. Fading channels are characterized as having randomly time-variant impulse responses because the physical characteristics of the media around the terminal continuously change[18].

2.1.1 Factors Influencing Fading

The extent of fading experienced by a signal propagating through a mobile radio channel depends on the nature of the transmitted signal and the signal propagating environment [19]. The two important factors that determine the type of fading are:

Multipath Propagation

The movement of mobile terminal relative to the reflecting and scattering objects in the propagating medium create a continuously changing environment that disperses the signal energy in magnitude, phase, and time, that is the signal is in the form of multiple signal replicas, which are displaced at the receiving antenna in time.

Doppler Shift

The time variations in the channel are evidenced as a Doppler broadening. Doppler spread is used to quantify the signal fading due to random *Doppler shifts*.

2.1.2 Types of Fading

The type of fading experienced by a signal propagating through a mobile radio channel depends on the nature of the transmitted signal with respect to the characteristics of the channel.

Flat Fading

If all the spectral components of the signal fade in unison, then the channel undergoes *flat fading*. Flat fading channel are also known as amplitude varying channels [1] and are sometimes referred to as a narrowband channels [2].

[1]The phase is usually considered to remain linear
[2]This implies that signal bandwidth is smaller than channel coherence bandwidth

Frequency Selective Fading

In *frequency selective fading*, the spectrum $S(f)$ of the transmitted signal has a bandwidth which is greater than the coherence bandwidth B_C of the channel and the signal spectral components may fade independently.

Fast Fading

In a *fast fading channel*, the channel impulse response changes rapidly even over a symbol duration. That is, the coherence time of the channel is shorter than the symbol period of the transmitted signal. Fading causes frequency dispersion (also called time selective fading) which leads to signal distortion. A signal undergoes fast fading if

$$T_S > T_C \tag{2.1}$$

and

$$B_S < B_D \tag{2.2}$$

Slow Fading

In a *slow fading channel*, the channel impulse response changes at a rate much slower than the transmitted baseband signal $s(t)$. A signal undergoes slow fading if

$$T_S \ll T_C \tag{2.3}$$

$$B_S \gg B_D \tag{2.4}$$

2.2 Discrete-Time Channel Model

Over many years, a large number of experiments have been carried out to understand the nature of fading channels. Earlier work in this area includes contributions from Bello[20], Clarke[21] and Jakes[22].

Assuming low-pass equivalent model for the channel as shown in [1], the received signal $r(t)$ over a fading multipath channel can be represented by

$$r(t) = \int_{-\infty}^{\infty} h(\tau, t)s(t-\tau)d\tau \tag{2.5}$$

where $s(t)$ is the transmitted signal and $h(\tau, t)$ is the time-variant channel impulse response at delay τ and time instant t. In discrete form

$$r(n) = \sum_{i=-\infty}^{\infty} h(iT_c, n)s(n - iT_c) \tag{2.6}$$

where T_c is the chip duration and n represents the sampling index. Defining a compact notation for the time varying channel coefficients in the form $h_i(n) = h(iT_c, n)$, (2.6) can be written as

$$r(n) = \sum_{i=-\infty}^{\infty} h_i(n)s(n - iT_c) \tag{2.7}$$

The time varying complex coefficients $h_i(n)$ are random processes that define the statistical characterization of the channel. For example, in case of typical fading the magnitude of $h_i(n)$ has Rayleigh distribution and the phase has uniform distribution. Clark developed a model of fading channel in [21] that accommodates the Doppler spread, having spectrum as

$$S(f) \propto \left[\frac{1}{1 - f/f_m}\right]^{1/2} \tag{2.8}$$

where f_m is the maximum Doppler frequency. Jakes presented a realization for the simulation of the fading channel model that generates real and imaginary parts of the channel tap coefficients as weighted sum of sinusoids. In mobile radio channels, the Rayleigh distribution is commonly used to describe the statistical time varying nature of the received envelope of a flat fading signal, or the envelope of an individual multipath component. It is well known that the envelope of the sum of two quadrature Gaussian noise signals obeys a Rayleigh distribution. Hence $h_i(n)$ are random processes.

$$h_i(n) = \sqrt{\rho_i} G_i(n) \tag{2.9}$$

where ρ_i is the strength of the signal of ith path.

2.3 Error Characteristics in Mobile Radio Channels

Errors occur in a communication system not only due to noise but also due to a variety of transmission impairments that are, in some cases, peculiar to a channel. On most wireless communication channels, the combined effect of error-producing mechanisms is such that errors occur in clusters or bunches separated by fairly long error free gaps. It is this biased behavior of channels to be either too good or too bad, that has come to be known as memory. To control the errors effectively through some coding techniques, the study of relative occurrences of the errors is a prerequisite. The fact that errors tend to occur in clusters, i.e., somewhat predictably, should prove to be advantageous. In information theory parlance, this means memory increases capacity. But this additional capacity can only be realized through some intelligent exploitation of the memory.

2.4 Channel Impairments that limit Capacity

Capacity is cited as the maximum information rate for error free transmission. In practice one is always willing to allow a certain error-rate though it must be as small as possible. It is usually reasonable and meaningful to compare information rates of practical systems at some non-vanishing error-rate to the channel capacity for error free transmission. Several useful interpretations follow from the channel capacity

formulas. One qualitative statement is that practical systems tend to operate at some 'information-rate efficiency' relative to channel capacity, the efficiency being somewhat characteristic of the system type and in many instances the change in channel capacity resulting from a change in the channel parameters is very similar to the change in performance of an actual system operating over the same channel [23]. This view of relating channel capacity with error rate gives an understanding that any means of channel impairment affects the system capacity. Some of the mobile radio impairment that affect the system capacity are described in the following.

2.4.1 Multipath

Multipath results in multiple versions of the transmitted signal that arrive at the receiving antenna, displaced with respect to one another in time and space. The random phase and amplitudes of the different multipath components cause fluctuations in signal strength, thereby inducing small scale fading, signal distortion, or both. Multipath propagation often lengthens the signal pulses which causes intersymbol interference and signal distortion. As a result the capacity of the channel reduces.

2.4.2 Coherent Bandwidth

The coherent bandwidth is a measure of the maximum frequency difference for which signals are still strongly correlated in amplitude. Two sinusoids with frequency separation greater than coherent bandwidth are affected quite differently

by the channel. If the transmission bandwidth is much greater than the coherence bandwidth than the channel varies greatly over its entire bandwidth and we get what's called "frequency-selective fading." If the transmission bandwidth is very small in relation to the coherence bandwidth than the channel is relatively flat over its entire bandwidth and we get what's called "Frequency-nonselective fading."

2.4.3 Channel Memory

Errors encountered in digital transmission over most real communications channels are not independent but appear in clusters. Such channels are said to exhibit memory, i.e., statistical dependence in the occurrence of errors; and thus cannot be adequately represented by the classical memoryless binary channel. Since memory increases capacity for a communications channel, how one can exploit the memory to realize the additional capacity? This basic question spurred the work in the area of statistical analysis of errors and their application to evaluation of error control techniques.

A typical digital communication system can be represented as shown in figure Fig. 2.1. In the performance analysis of the modulator-demodulator (modem), where the average error rate is considered as the key parameter, the physical sources of errors are reasonably mathematically tractable. For the coding channel involving the modem and the medium, any meaningful analytical description of channel memory in terms of the characteristics of the individual physical causes of errors is quite diffi-

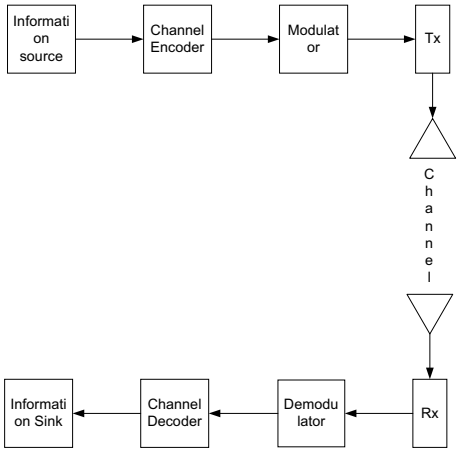

Figure 2.1: Block diagram of a typical communication system

cult. It is more convenient to work with sample error sequences obtained from test runs of data transmitted on a given coding channel to obtain statistical description of the error structure and use them in the design of error control systems. The required statistical parameters in this work are obtained from error sequences by direct processing of the sequences.

2.5 Methods to combat Channel Capacity limiting Impairments

Mobile radio channel impairments cause the signal at the receiver to distort or fade significantly as compared to AWGN channels. Diversity, channel coding, and equalization are three techniques which can be used independently or in tandem to improve received signal quality as well as capacity.

2.5.1 Diversity

Diversity is another technique used to compensate for fading channel impairments [24]. Diversity is usually employed to reduce the depth and duration of the fades experienced by a receiver in a flat fading (narrowband) channel. The most common diversity technique is called *spatial diversity*, whereby multiple antennas are strategically spaced and connected to a common receiving system. While one antenna sees a signal null, one of the other antennas may see a signal peak, and the receiver is able to select the antenna with the best signal at any time or combine signals on all antennas in a certain manner. Other diversity techniques include antenna polarization diversity, frequency diversity, and time diversity.

2.5.2 Channel Coding

Channel coding improves mobile communication link reliability and capacity by adding redundant data bits in the transmitted message [25, 26, 27] . At the baseband portion of the transmitter, a channel coder maps a digital message sequence into another specific code sequence containing a greater number of bits than originally contained in the message [28]. The coded message is then modulated for transmission in the wireless channel. Channel coding is used by the receiver to detect or correct some (or all) of the errors introduced by the channel in a particular sequence of message bits.

2.5.3 Equalization

Equalization compensates for *intersymbol interference* (ISI) created by multipath time dispersive channels [29]. If the modulation bandwidth exceeds the coherence bandwidth of the radio channel, ISI occurs and modulation pulses are spread in time. An equalizer within a receiver compensates for the average range of expected channel amplitude and delay characteristics. Equalizer must be adaptive since the channel is generally unknown and time varying.

Chapter 3

Bell-Labs Layered Space Time Architecture

3.1 Basic Concepts of BLAST

Bell Labs Layered Space Time Architecture (BLAST) is an extraordinary bandwidth-efficient approach to wireless communication which takes advantage of the spatial dimension by transmitting and detecting a number of independent co-channel data streams using multiple but essentially co-located antennas. This new communication structure targets application in future generations of wireless systems, bringing high bit rates to the office and home.

In wireless systems, radio waves do not propagate directly from transmit antenna to receive antenna, but bounce and scatter randomly off objects in the environment. This scattering of radio waves create, what we call multipath, as it results in the arrival of multiple copies (images) of the transmitted signal via different scattered paths at the receiver. In conventional wireless systems, multipath represents a sig-

nificant impediment to reliable reception, because the images arrive at the receiver at slightly different times and can thus in generally interfere destructively, cancelling each other out. For this reason, multipath is traditionally viewed as a serious impairment. Using the BLAST approach however, it is possible to exploit multipath, that is, to use the fading characteristics of the propagation environment to enhance, rather than degrade, reception accuracy by treating the multiplicity of scattering paths as separate parallel subchannels.

BLAST accomplishes this by splitting a single user's data stream into multiple substreams and using an array of transmitter antennas to simultaneously launch the parallel substreams. All substreams are transmitted in the same frequency band, so spectrum is used very efficiently. Since the user's data is being sent in parallel over multiple antennas, the effective transmission rate is increased in roughly in proportion to the number of transmitter antennas used.

At the receiver, an array of antennas is again used to pick up the multiple transmitted substreams and their scattered images. Each receive antenna "sees" all of the transmitted substreams superimposed, not separately. However, if the multipath scattering is sufficient, then the multiple substreams are all scattered slightly differently. To get uncorrelated scattering, they must originate from different transmit antennas that are located at different points in space. Using sophisticated signal processing, differences in scattering allow the substreams to be identified and recovered. In effect, the unavoidable multipath is exploited to provide a very useful

spatial parallelism that is used to greatly improve data transmission rates. Thus, when using the BLAST technique, the more distinct are the multipath, the better performance is achieved, just the opposite of conventional systems.

The BLAST signal processing algorithms used at the receiver are the heart of the technique. At the bank of receiving antennas, high-speed signal processors look at the signals from all the receiver antennas simultaneously, first extracting the strongest substream from the morass, then proceeding with the remaining weaker signals, which are easier to recover once the stronger signals have been removed as a source of interference. Again, the ability to separate the substreams depends on the slight differences in the way the different substreams propagate through the environment.

Under the widely used theoretical assumption of independent Rayleigh scattering, the theoretical capacity of the BLAST architecture grows roughly linearly with the number of antennas, even when the total transmitted power is held constant. In the real world of course, scattering will be less favorable than the independent Rayleigh assumption, and it remains to be seen how much capacity is actually available in various propagation environments. Nevertheless, even in relatively poor scattering environments, BLAST should be able to provide significantly higher capacities than conventional architectures.

3.1.1 Mathematical Notations for The System

The particular notation used in the literature [6], is introduced here to familiarize the reader to the system operation and its analysis. The point to point channel is discussed. The channels are considered baseband, complex Gaussian with unit variance. The following are the basic assumptions used in the thesis:

1. Number of Antennas: The multi-element array(MEA) at the transmitter has n_T transmitters. The MEA at the receiver has n_R receivers. For convenience, the pair(n_T, n_R) denotes a communication system with n_T transmit elements and n_R receive elements. There are $n_R \times n_T$ number of paths.

2. Noise at Receiver $v(t)$ is complex n_R dimensional AWGN. The components are statistically independent and of identical power N at each of the n_R antenna outputs.

3. Transmitted signal $s(t)$: The total power is constrained to $\widehat{P}$ regardless of the value of n_T (the dimension of $s(t)$). The bandwidth is narrow enough *w.r.t.* channel coherent bandwidth that we can treat the channel frequency characteristic as flat. This assumption does not take into account the channel frequency selectivity.

4. Received signal $r(t)$: This is n_R dimensional received signal. At each point in time there is one complex vector component per receive antenna. The average

power at the output of each of the receiving antenna is denoted by P.

5. Average signal to noise ratio (SNR) at each receive antenna: This is $\rho = P/N$, independent of n_T.

6. Matrix Channel Impulse Response g(t): When considering single path channel (see assumption 3), this matrix has n_T columns and n_R rows. In case of frequency selectivity, number of paths will be increased.

Consistent with the narrow band assumption ($B_T \leq B_C$ of channel), the basic vector equation describing the channel operation on the signal is

$$r(t) = g(t) \times s(t) + v(t) \tag{3.1}$$

These three vectors are complex n_R-dimensional vectors($2n_R$ real dimensions). Often, it is convenient to represent the matrix channel response in normalized form, $h(t)$. Specifically related to G (fourier transform of $g(t)$), we have the matrix H, where the equation $\widehat{P}^{1/2} \times G = P^{1/2} \times H$ defines the relationship so, $g(t) = (P/\widehat{P})^{1/2} \times h(t)$. Thus, in normalized form, (1) becomes

$$r(t) = (\rho/n_T)^{1/2} \cdot h(t) \cdot s(t) + v(t) \tag{3.2}$$

3.1.2 Mathematical Background

Let the channel transfer characteristic matrix H_{nn} has n rows and n columns. The vector space spanned by the H with n columns is $H_{:[1:n]}$. Where $H_{:1}$ is the first column vector i.e. first column and all rows ($n \times 1$ dimension vector). If a matrix say $'G'$ has k independent column vectors out of n total columns, then it has a rank of k and span a vector space of $G_{:k}$ (the k independent column vectors). Since the entries of H are complex n^2-dimensional independent Gaussians, therefore all the columns of H are independent and H has full rank (for independent fading on each path). It also means that for $k \leq n$ columns of H has k dimensions. For an example of (6×6), $H_{:[1:3]}$ has dimensions 3 and the vector space perpendicular to it is the space spanned by the remainder of columns i.e. $H_{:[4:6]}$ (columns 4 to 6).

3.2 Capacity for Space Time Diversity

Shannon made a tremendous contribution by defining and analyzing channel capacity expressions. Capacity formula as expressed in [6] in bps/Hz is

$$C = log_2(1 + \rho \cdot |H|^2) \tag{3.3}$$

where $|H|^2$ is the normalized channel transfer characteristic and ρ is SNR. It can be observed that for high SNRs a $3dB$ increase in ρ gives another bit/cycle capacity.

Bell Labs Layered Space Time Architecture (BLAST) technique uses space and time diversity. Multiple Element Antenna (MEA) are used at both transmitter and receiver ends. The capacity that this architecture delivers is enormous, provided that the multipath scattering is sufficiently rich and is properly exploited. The generalized capacity formula for the (n_T, n_R) case is shown in [6].

$$C = log_2 det[I_{n_R} + (\rho/n_T)\dot{H}H^T] \qquad b/s/Hz \tag{3.4}$$

where "det" means determinant, I_{n_R} is $n_R \times n_R$ identity matrix and "T" is transpose conjugate. Since the entries of the channel characteristic matrix "H" are zero mean unit variance complex Gaussians, therefore the above expression can also be written as

$$C > \sum_{k=1}^{n} log_2 det[I_{n_R} + (\rho/n_T)\chi^2_{2k} \qquad b/s/Hz \tag{3.5}$$

where χ^2_{2k} is a chi squared variate with $2k$ degrees of freedom.

The above expression clearly shows the huge capacity promised by the architecture, which is essentially impossible to obtain using traditional approaches in which a single transmitter is used. As per Bell laboratory testbed, their BLAST team demonstrated what they believe to be unprecedented wireless spectral efficiencies, ranging from 20 - 40 bps/Hz. By comparison, the efficiencies achieved using traditional wireless modulation techniques range from around 1 - 5 bps/Hz (mobile cellular) to around 10 - 12 bps/Hz (point-to-point fixed microwave systems). In the

30 kHz bandwidth utilized by their research testbed, the raw spectral efficiencies realized thus far in the lab correspond to payload data rates ranging from roughly 0.5 Mb/s to 1 Mb/s. By contrast, the data rate achievable in this bandwidth using typical traditional methods is only about 50 kbps. Although the practical capacity results are obtained for wireless LAN, this also gives motivation for applying BLAST approach to improve spectral efficiencies in wireless system.

3.3 BLAST Types and their Difference (Transmission and Reception)

Two types of BLAST architectures, Diagonal-BLAST and Vertical-BLAST, are discussed in literature. The first BLAST proposed in the literature is the Diagonal-BLAST (D-BLAST) architecture [5], which has a diagonal layering space-time coding [30] with sequential nulling and interference cancellation decoding. D-BLAST suffers from boundary wastage at the start and end of each packet, which becomes significant for a small packet size. Designing elegant diagonal layered space-time decoding techniques that eliminate the boundary wastage present an open research problem; indeed, they have become a popular research topic. Vertical-BLAST (V-BLAST) overcomes the limitations of D-BLAST by using independent horizontal layered space-time coding scheme; unfortunately, it does not utilize the time diversity and, therefore, suffers from the problem of reduced information capacity [4].

D-BLAST and V-BLAST are described below.

3.3.1 D-BLAST: Diagonal Bell-Labs Layered Space Time Architecture

As introduced in [5], this section provides a high level description of a form of the new architecture having an equal number of antenna elements at both ends of the link.

Transmission

The transmission process of the BLAST is described in Fig. 3.1. An input data stream is demultiplexed into n_T substreams. Each data stream has the same data rate which is equal to $1/n_T$ of the input data. Each substream is encoded using a specific code separately. Then all the substreams are transmitted through all n_T transmitting antennas cyclically. Each substream is transmitted from all the transmit antennas one by one. If 1 bit/cycle take τ seconds to transmit then n_T cycles take $n_T \times \tau$ seconds.

In one cycle each substream is transmitted via n_T subchannels. Therefore in n_T cycles, each substream utilize $n_T \times n_R$ subchannels. This ensures each substream to has same capacity. The balance sharing of all subchannels drastically reduces the deep fade stuck of any substream.

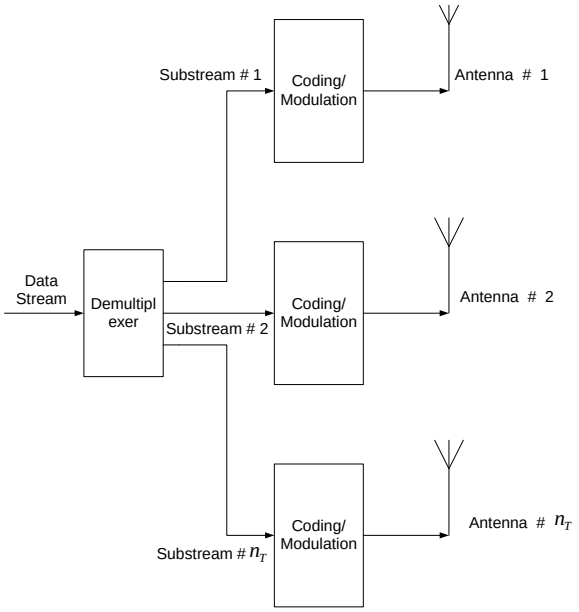

Figure 3.1: Transmission process using space-time layering

Processing at the Receiver

In describing the processing of (n, n) case at the receiver; a $(4, 4)$ is used as an example. The channel transfer characteristic matrix H is accurately known to receiver, that is accurate channel estimates are available. The transmitter, however does not know the channel.

Fig. 3.2 illustrates the details of processing steps in the diagonal layer in D-BLAST. X-axis represents the time axis in blocks. Each block has the duration of τ seconds, which is the time period of data substreams of one transmitter. Y-axis represents space dimension. This space dimension can be visualize as transmitter elements numbered $1, 2, 3, 4$. Data substreams (layers) are represented as $\alpha_i, \beta_i, \gamma_i$, and ζ_i. Where α, β, γ, and ζ are four substreams and i is the index to represent data sym-

bol in that substream.

$$\alpha_{-k}, \alpha_{-k+1}, \cdots, \alpha_0, \alpha_1, \cdots, \alpha_k$$

$$\beta_{-k}, \beta_{-k+1}, \cdots, \beta_0, \beta_1, \cdots, \beta_k$$

$$\gamma_{-k}, \gamma_{-k+1}, \cdots, \gamma_0, \gamma_1, \cdots, \gamma_k$$

$$\zeta_{-k}, \zeta_{-k+1}, \cdots, \zeta_0, \zeta_1, \cdots, \zeta_k$$

Entities shown in the blocks are layers at the specific time (in x-axis) and transmitted from the specific transmitter element (in y-axis). The signal received in any receiver is 4-D vector. The received vector at all the receivers at a time instance is the sum of vertical data symbols after passing through different fading channel at that time instance. For example, at $1\tau \leq t \leq 2\tau$, the received vector is:

$$r(t) = \alpha_{j+1}h' + \zeta_j h'' + \gamma_j h''' + \beta_j h'''' \tag{3.6}$$

All the layers disposed to be located underneath the α_{j+1} layer are assumed already successfully detected. While all the layers disposed to be located above the α_{j+1} layer are yet to be detected. For the ease of understanding, we described the processing for α_{j+1} layer at a specified time instance. Consider the instance $2\tau \leq t \leq 3\tau$. Layer α_{j+1} is transmitted from antenna 3. Layers ζ_j and layer γ_j are already detected. These detected layers are subtracted out from the received vector. The interferences from these layers are cancelled out. The remaining interference β_{j+1} is nulled out by

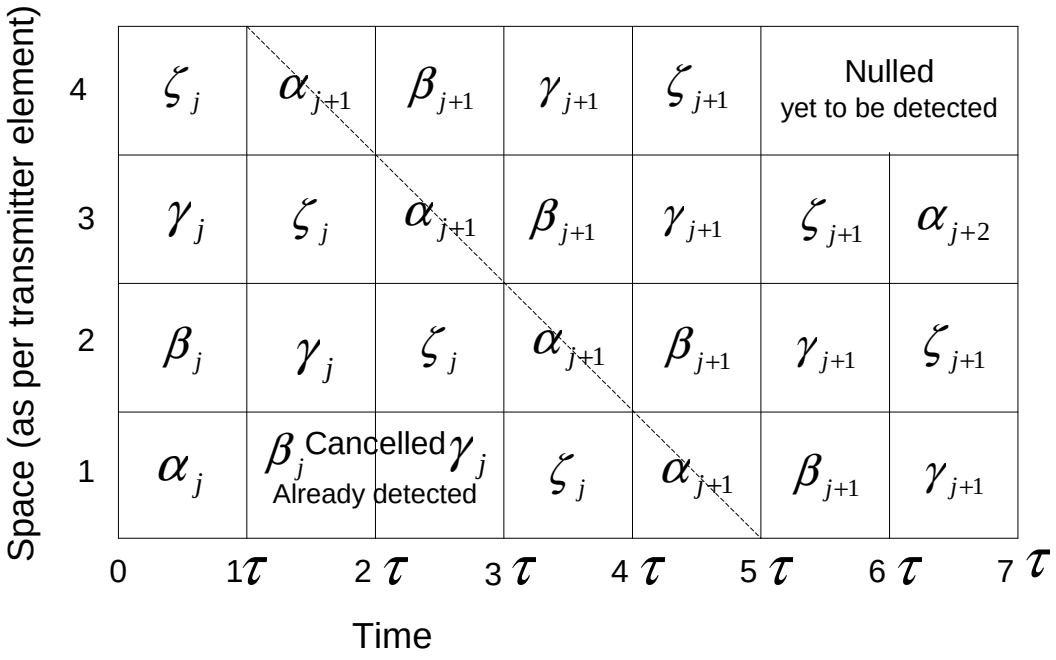

Figure 3.2: Flow of nominal processing time for a received signal

projecting the signal onto the subspace $H_{:4}^{\perp}$ i.e. $H_{:[1:3]}$. It is previously described in the mathematical background section that the space spanned by $H_{:4}^{\perp}$ is the maximal subspace orthogonal to the subspace spanned by signals received from transmitter 4. This will leave the data streams transmitted from 1, 2, 3 transmitter elements. Since the data transmitted from 1, and 2 i.e. γ_j and ζ_j are already subtracted out, so we can detect α_{j+1}. The remaining layers are detected in the same way. The flow diagram for the processing at the receiver is shown in Fig. 3.3. The capacity lower bound for an D-BLAST (n, n) system is proved in [5], which is

$$C > \sum_{k=1}^{n} log_2[1 + (\rho/n) \cdot \chi_{2k}^2] \qquad b/s/Hz \tag{3.7}$$

3.4 V-BLAST: Vertical Bell-Labs Layered Space Time Architecture

A high level block diagram of a BLAST system is shown in Fig. 3.4. A single data stream is demultiplexed into n_T substreams, and each substream is encoded and fed to its respective transmitter from 1 to n_T. Transmitters 1 to n_T operate co-channel at symbol rate 1/T symbols/sec. The power launched by each transmitter

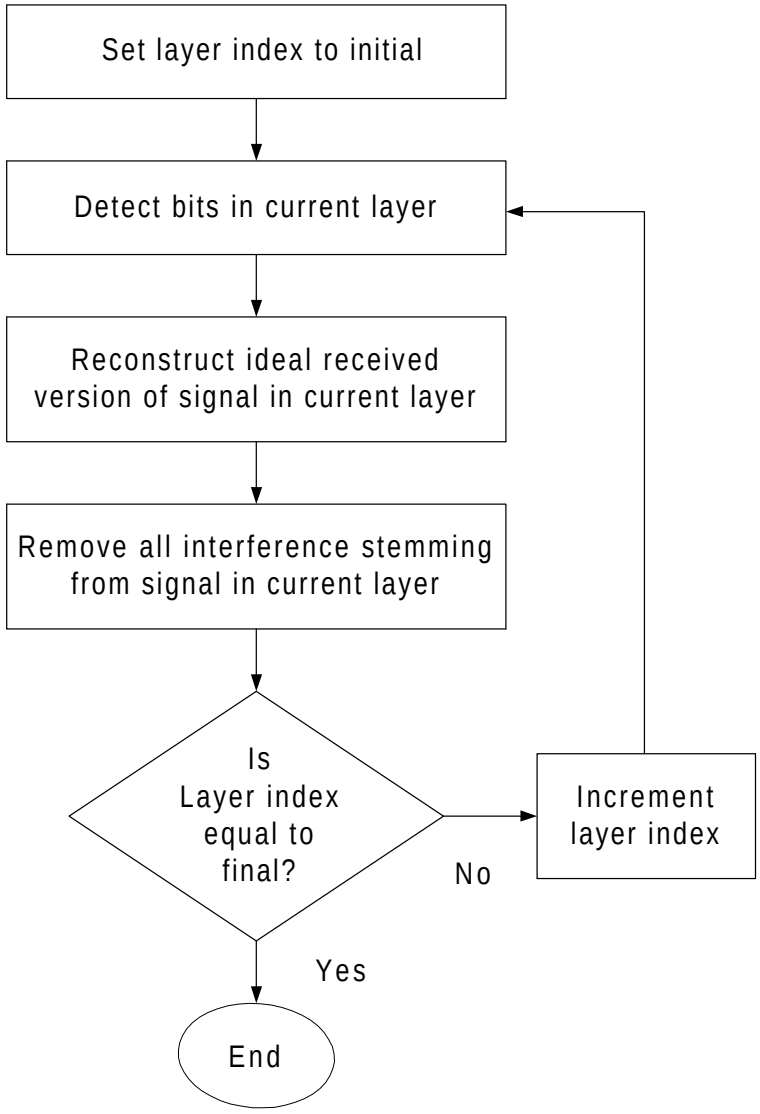

Figure 3.3: Temporal view of the processing of successive space-time layers

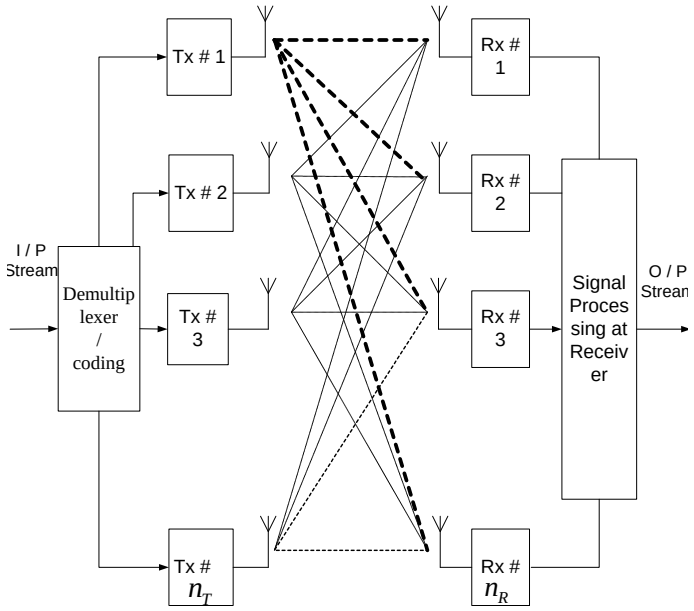

Figure 3.4: A V-BLAST system diagram

is proportional to $1/n_T$ so that the total radiated power is constant.

Receivers are from 1 to n_R. These receivers also operate co-channel, each receiving the signals radiated from all n_T transmit antennas. The matrix channel transfer function is $H_{n_R \times n_T}$, where h_{ij} is the (complex) transfer function from transmitter j to receiver i, and $n_T \leq n_R$. The essential difference between D-BLAST and V-BLAST is that D-BLAST utilizes both space and time diversity while V-BLAST utilizes only space diversity. So the layers that has to be cancelled out (or already detected layers) are not in order as in D-BLAST, where these layers are underneath the desired layer. Since V-BLAST does not utilize time diversity therefore the capacity of V-BLAST is lower than the D-BLAST.

In V-BLAST, the receiver looks at the signals from all the receiver antennas simultaneously and first extract the strongest substream from the morass. This is done by projecting the received vector on the subspace perpendicular to all other substreams. This operation is called nulling. Nulling is performed by linearly weighing the received signals so as to satisfy zero-forcing criterion. As shown in [4], a zero-forcing nulling can be performed by choosing weight vector w_i, $i = 1, 2, ..., n_T$, such that

$$w_i^T (H)_j = \delta_{ij} \tag{3.8}$$

where $(H)_j$ is the j^{th} column of H, and δ is the Kronecker delta. Thus the decision statistic for the i^{th} substream is $y_i = w_i^T r$.

After detecting the strongest layer, this strongest layer is subtracted out from the received signal vector. This subtraction removes the biggest interference from the received vector. The entries of the column of H respective to the substream detected are made zeros. This is called nulling operation. Nulling avoids any projection on the subspace spanned by this detected substream. The nulling process of the remaining substreams continue as per descending order of received signal powers until all layers are detected.

3.5 Turbo Coding

Convolutional error correcting or channel coding has become widespread in the design of digital transmission systems. One major reason for this is the possibility of achieving real-time decoding without noticeable information losses [31]. Two kinds of convolutional codes are of practical interest: nonsystematic convolutional (NSC) and recursive systematic convolutional (RSC) codes. Though RSC codes have the same free distance d_f as NSC codes, but they exhibit better performance at low signal to noise ratios (SNR's).

For a given rate, the error-correcting power of convolutional codes, measured as the coding gain at a certain binary error rate (BER) in comparison with the uncoded transmission, grows more or less linearly with code memory ν. Unfortunately, the complexity of the decoder is not a linear function of ν and it grows exponentially as $\nu \cdot 2^{\nu}$. The factor 2 represents the number of states processed by the decoder and the multiplying factor ν accounts for the complexity of the memory part.

In order to obtain high coding gains with moderate decoding complexity, concatenation has proved to be an attractive scheme. Classically, concatenation has considered in cascading a block code (the outer code, typically a Reed-Solomon code) and a convolutional code (the inner code) in a serial structure. Another concatenated code, presented in [32], which has been given the familiar name of *turbo-code*, is originally a parallel organization of two RSC elementary codes. These elementary

codes are called constituent codes [33].

There are two convolutional encoders in parallel. The information bits are scrambled before entering the second encoder. This scrambling is called interleaving. Interleaving is a process of rearranging the ordering of the data sequence in a one-to-one deterministic format. The inverse of this process is deinterleaving which restores the received sequence to its original order. The main role of interleavers is to decorrelate the inputs to the two decoders so that an iterative suboptimum decoding algorithm based on information exchange between the two component decoders can be applied [34, 35]. If the input sequences to the two component decoders are decorrelated, there is a high probability that after correction of some of the errors in one decoder, some of the remaining errors should become correctable in the second decoder. When decoded by an iterative process, turbo-codes offer near optimum performance.

3.6 Performance Measures

The analysis used in this work for performance measurement of the V-BLAST system are discussed below.

3.6.1 Error Burst Length Histogram

A error burst length profile shows the distribution of error events of different lengths. The length of an error event is determined by the distance between the first error and the last error in a burst. An error burst is preceded and followed by a long string of no errors. The characterization of a burst varies depending upon application. The analysis parameters like Burst error free threshold, minimum burst length, etc can be adjusted to match the need e.g. channel coding. In particular, the minimum burst length (which is 2 here) should be set to the smallest number of errors occurring in close proximity to one another that one wants to be defined as a burst. The "close proximity" is then defined by choosing a burst error free threshold; when this number of good bits is exceeded, one error event is concluded and counting begins for the next. In this work the burst error free threshold is 10. If 10 good bits occur then new error is accommodated in the next burst i.e. error burst counter is reset. This interval is long enough to reduce the effect of memory of the channel. Occurrence of an error after this burst error free threshold has no dependence on the previous error.

3.6.2 Error Free Length Histogram

The error free interval histogram looks like inter-burst interval. One bit between errors is most likely; two bits is next most likely; etc.

3.6.3 Average Error Burst Length

Average error burst length is the average of error burst lengths. This gives an idea whether a coding scheme is economical to be applied with such an average error bursts.

3.6.4 Average Error Free Length

Average error free length is average of error free gaps those are greater than error free threshold. This gives the mean of error free gaps where errors in bursts can be spread during interleaving.

3.6.5 Bit Error Rate

Bit error rate is bits in error per bits transmitted. It is an standard criterion to show the performance of any system.

Chapter 4

Simulation Results

4.1 Simulation Model of Fading Channels

This section describes the method that will be used to simulate the channel. Basically, we need colored Gaussian noise to realize fading channel statistics which may be Rayleigh, Rician or any other. These colored Gaussian processes can be generated either by *filtering* white Gaussian noise [21] or by *deterministic* methods [22, 36] or by *Monte Carlo* approach [37].

Jakes has given a sum-of-sinusoids (SOS) based fading channel simulator design [22] that has been widely used for almost three decades. Recently, an important design shortcoming in Jake′s model is found in [38], namely, that rays experiencing the same Doppler frequency shift are correlated. This causes the generated signal to be non-stationary. It is introduced in [38] that random phases in the low fre-

quency oscillators ensures the generation of a wide-sense stationary signal.In this thesis, modified semi-deterministic Jakes model as fading channel simulator is implemented.

The real and the imaginary components of the channel tap are generated by

$$\begin{aligned} g_I(t) &= 2\sum_{n=1}^{N_o} \cos\beta_n \cos(\omega_n t + \phi_n) + \sqrt{2}\cos\alpha\cos(\omega_m t + \psi_n) \\ g_Q(t) &= 2\sum_{n=1}^{N_o} \sin\beta_n \cos(\omega_n t + \phi_n) + \sqrt{2}\sin\alpha\cos(\omega_m t + \psi_n) \end{aligned} \tag{4.1}$$

$$\beta_n = \frac{n\pi}{N_o + 1} \qquad \omega_n = \omega_m \cos\left(\frac{2\pi n}{N}\right) \qquad N_o = \frac{1}{2}\left(\frac{N}{2} - 1\right) \tag{4.2}$$

where $t = kT_s$ and $\phi_1, \cdots, \phi_{N_o}$ and $\psi_1, \cdots, \psi_{N_o}$ are uniformly distributed random variables over $[0, 2\pi]$. For multipath uncorrelated scattering, we have implemented the technique proposed by Jakes [22] whose modified version is available in [39, p 80]. In this technique, the nth oscillator is given an additional phase shift $\gamma_{nl} + \beta_n$ with gains as before. The envelope fading is understood to be a random phenomenon and as a consequence statistical description is needed to characterize it. Performance of any system is affected by correlated paths. Channels with correlated paths are also analyzed. These correlated paths are simulated as Nakagami-m distributed channels. In general, a Nakagami distributed fading is specified in terms of two parameters, namely the mean power Ω and m the so called fading figure. Aun Abbas and Asrar Sheikh showed in [40] that the physical model used for Rice distribution can as

well be applied for Nakagami distribution with slight modification. A relationship is also given in [40] between K parameter of Rice distribution and m parameter of Nakagami distribution and i.e.

$$m = \frac{1}{1 - \frac{K^2}{(1+K)^2}} \tag{4.3}$$

In this thesis work the same method is employed to get the Nakagami distribution from the Rice distribution. For simulation Flat fading Rayleigh, Nakagami1.33, Nakagami2.77 channels are used with carrier frequency 2.1 GHz and with 10, 20, and 50 Hz Doppler frequencies.

4.2 Channel characterization

In most applications, no complete direct line of sight propagation exists between the base station and mobile terminal. When a signal is transmitted from a base station in a wireless fading channel, it experiences reflections and scattering from local and distance objects. These reflected signal components combine vectorially at the receiver antenna, and can cause the signal received by the mobile to fluctuate. The signal fluctuations around the receiver threshold produce fade and non fade intervals. Even when a mobile is stationary, the received signal may fade due to the movement of surrounding objects in the radio channel. These fades result in occurrences of error bursts while inter-fade intervals result in error free intervals.

If a line-of-sight component is present then it produce the effect of adding a dc component to the received vector. This dc component reduces the depth of durations of fades of mobile channel. The error burst and error free intervals are modelled by Gilbert model and Fritchman model. Fade and non-fade intervals are shown in Fig. 4.1.

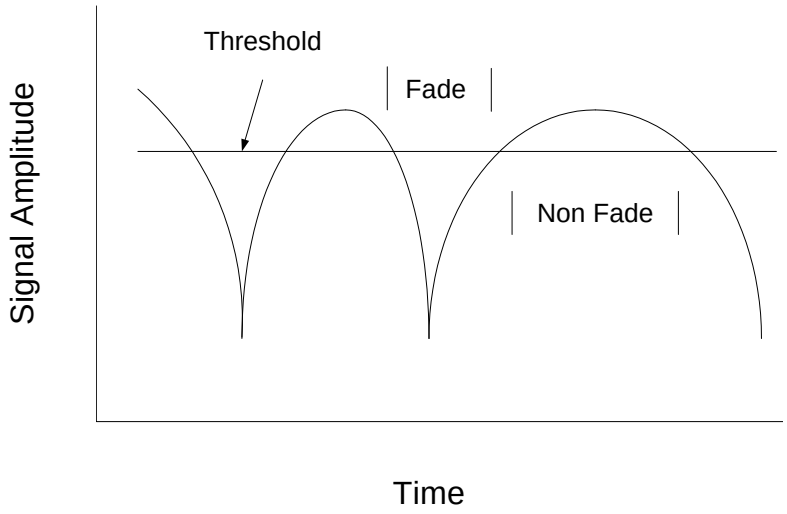

Figure 4.1: Fade and non-fade intervals for a sample of a fading signal

Fade durations depend on the speed of the mobile. The effectiveness of these schemes varies considerably as a function of mobile velocity. Increase in mobile velocity reduces fade and non-fade durations. Fading envelopes at 10 Doppler and 20 Doppler are shown in Figs. 4.2 and 4.3. Average fade and non-fade(interfade) durations are shown in Figs. 4.4 to 4.9 for Doppler frequencies 10, 20, 50 Hz at signal to noise ratios 3, 6, 9 dB. The average duration of fades is average length (in time or bits) for which the signal envelope remains below the threshold of reception.

While average duration of non fade is average length (in time or bits) for which the signal envelope remains above the threshold of reception. An examination of the figures reveals that fade and non-fade durations closely approximate exponential distributions. Shallower fades occur more frequently than deep fades. Very deep fades are rare. These variation in the durations in fade and non-fade intervals result in variation in error burst lengths and error free lengths.

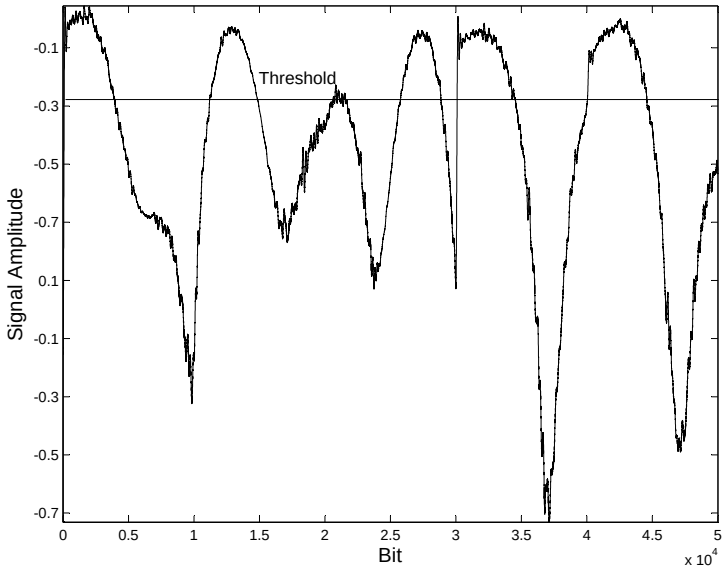

Figure 4.2: Typical fading envelope at 10 Hz Doppler

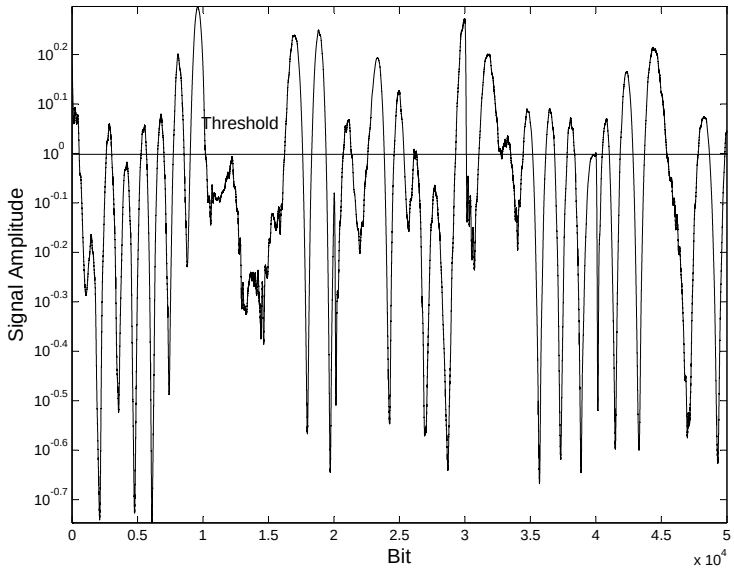

Figure 4.3: Typical fading envelope at 50 Hz Doppler

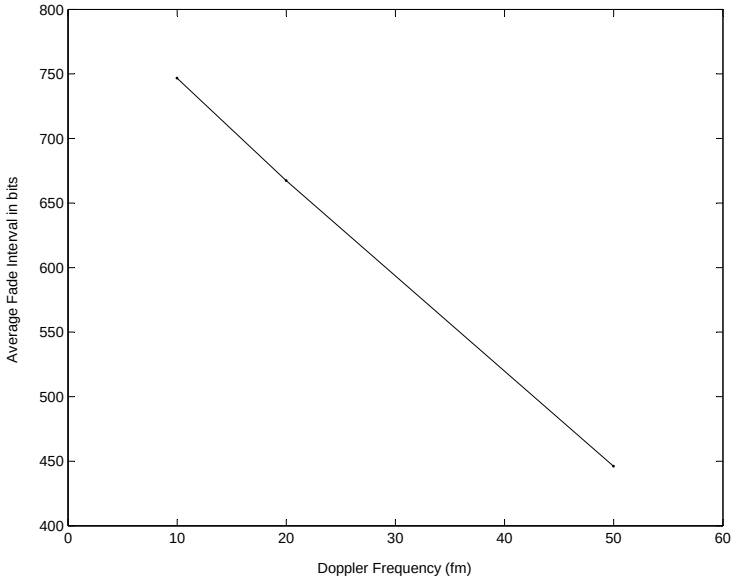

Figure 4.4: Average fade interval at SNR = 3 dB

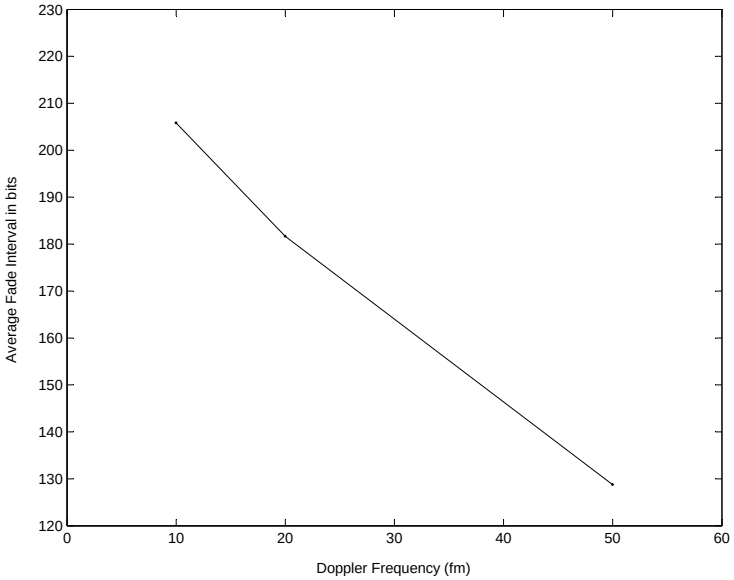

Figure 4.5: Average fade interval at SNR = 6 dB

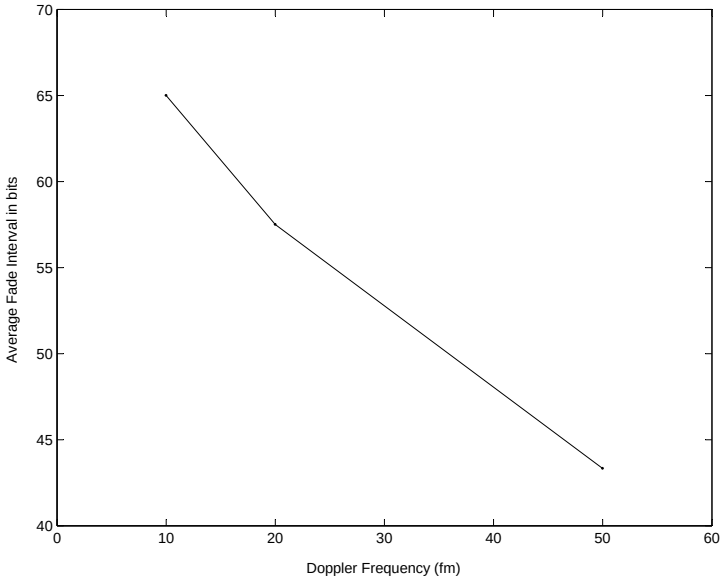

Figure 4.6: Average fade interval at SNR = 9 dB

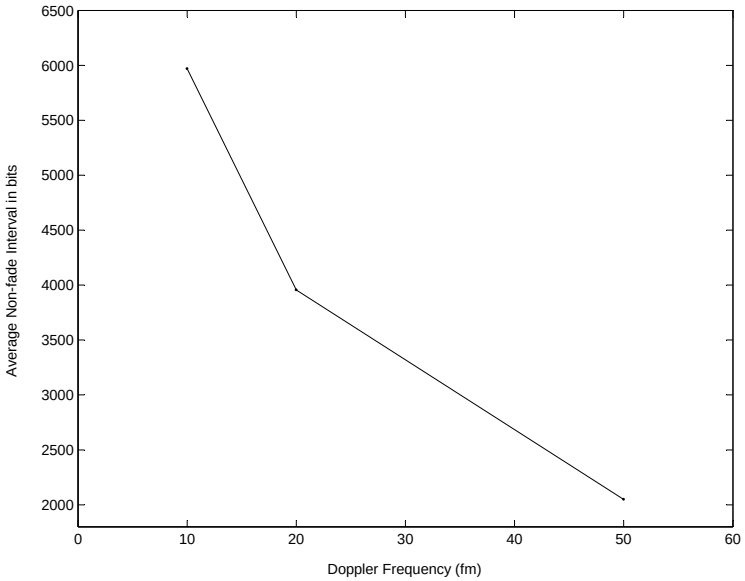

Figure 4.7: Average non-fade interval at SNR = 3 dB

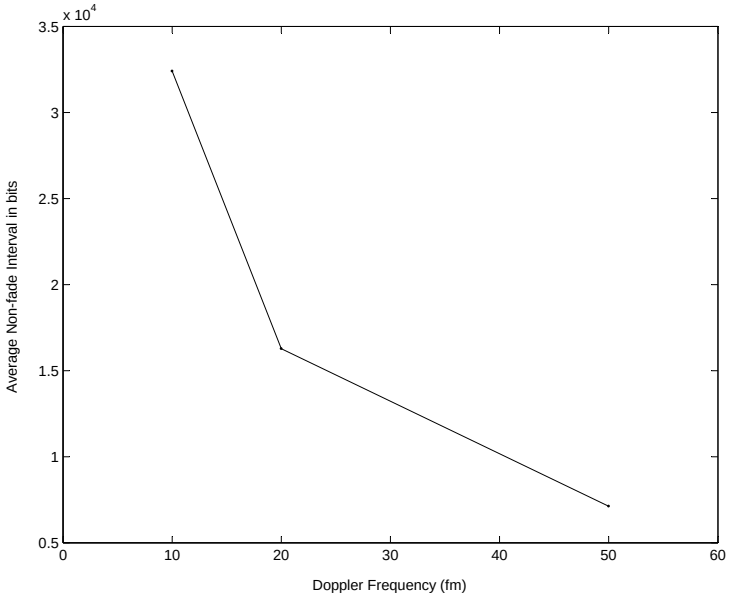

Figure 4.8: Average non-fade interval at SNR = 6 dB

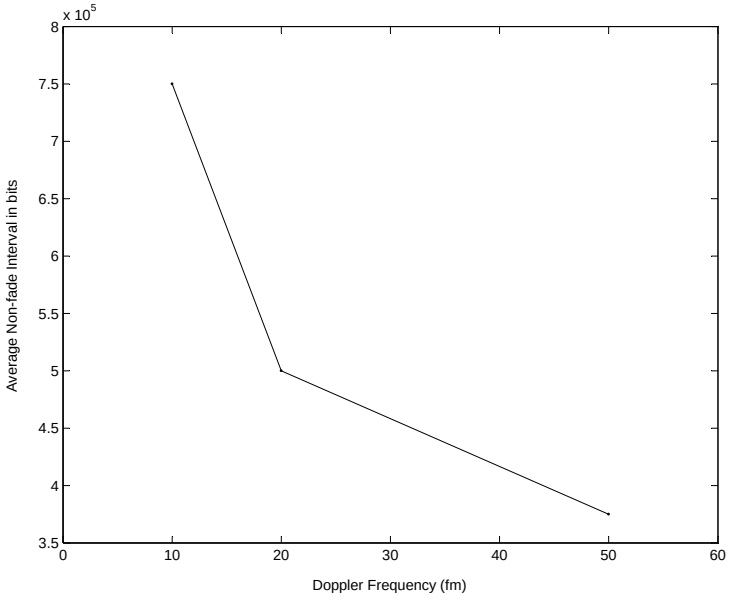

Figure 4.9: Average non-fade interval at SNR = 9 dB

4.3 Simulation Experiment Design

4.3.1 Error Process

The error process on a digital communication link can be viewed as a binary discrete-time stochastic process, i.e., a family of binary random variables $\{X_t, t \in I\}$ where I is the denumerable set of integers, and t denotes time. The sequence

$$x = \cdots x_{-1}, x_0, x_1, x_2, \cdots \tag{4.4}$$

Where x is representing a realization of error process and contain 0 and 1.

$$x_t = \begin{cases} 0, & \text{if there is no error} \\ 1, & \text{if there is an error} \end{cases}$$

The error process is thus a zero-one discrete-time stochastic process, as represented in [41].

4.4 Error Characterization and Modelling without Coding

4.4.1 Benchmark Example

A single transmitter and single receiver setup is made, which is used as benchmark for comparison with V-BLAST system. The comparison is done for parameters like error burst length, error free length, bit error rate. We also covered the impacts of Doppler on error statistics for V-BLAST in comparison to the benchmark system. In this arrangement single user transmits its data over a wireless channel. The phase of the received signal is compensated and then the signal is detected. Average error burst length, average error free length, and bit error rate parameters are simulated and shown in Fig. 4.10 to Fig. 4.12. The parameters are simulated over single path Rayleigh, Nakagami1.33, and Nakagami2.77 channels. Carrier frequency is 2.1 GHz with 10, 20, and 50 Hz Doppler frequencies. The error process length is taken 10^6 for every simulation. To make the analysis reliable, the numbers of errors achieved from the simulation are not less than 1000.

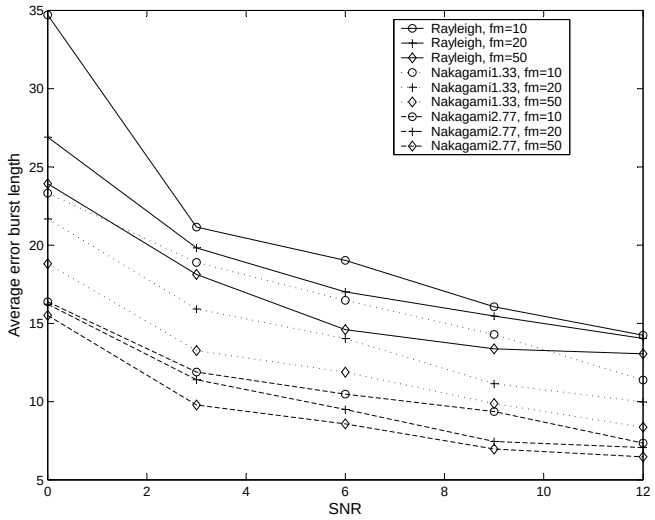

Figure 4.10: Average error burst length for Tx = 1, Rx = 1

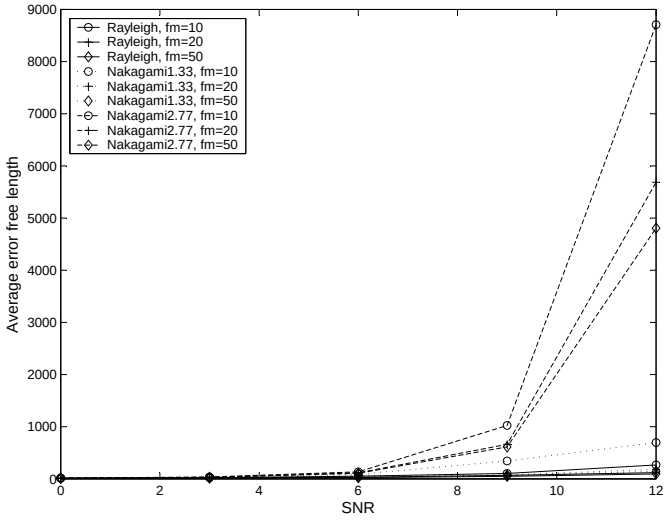

Figure 4.11: Average error free length for Tx = 1, Rx = 1

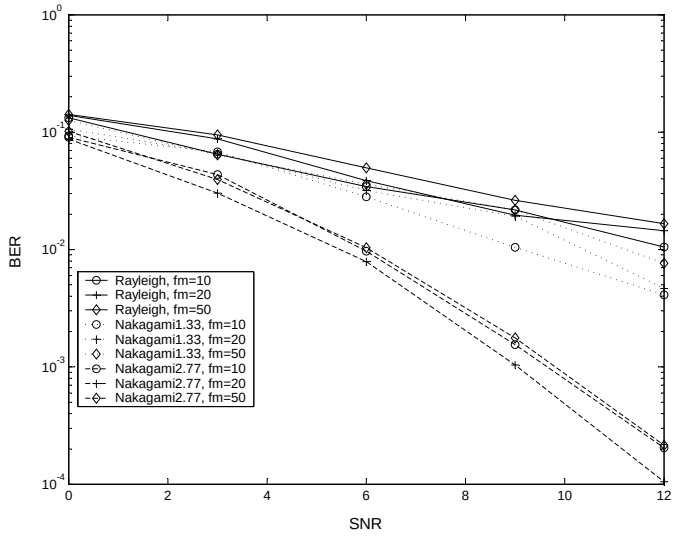

Figure 4.12: Bit error rate for Tx = 1, Rx = 1

Fig. 4.10 shows average error burst length for single transmitter single receiver system. Higher values of average error burst length occur at 0 dB and these values vary from 16 to 35. The average error burst length at 12 dB reduces to half of their corresponding 0 dB values. Increase in mobile speed reduces duration of fade. This reduction in fade duration results in shorter average error burst lengths as can be seen from figure. Introduction of correlation introduces line-of-sight (LOS) component. This LOS component reduces the depth of fade which in turn ensured reduction in average error burst lengths. The highest m channel (i.e. Nakagami2.77) resulted half the average error burst length than the lowest m channel (i.e. Rayleigh). Average error burst length for Rayleigh channel decreases from 28 to 14 while for Nakagami2.77 channel, it decreases from 16 to 7 at 20 Hz Doppler.

As increase in mobile velocity reduces duration of fades, it also reduces duration of

non fade intervals. Therefore average error free length for 10 Hz Doppler is higher than for 20 Hz, 50 Hz Doppler as seen in figure 4.11. At 10Hz Doppler, the highest value of average error free length for Rayleigh is 260, for Nakagami1.33 is 700, and for Nakagami2.77 is 8800. LOS reduces depth of fade and as a result average error free length (EFL) increased. At 9 dB and 10 Hz Doppler, Nakagami2.77 has twice the average EFL that of Nakagmai1.33, whereas Nakagami1.33 has twice the average EFL that of Rayleigh. At 12 dB and 10 Hz Doppler, average EFL of Nakagami2.77 is 10 times higher than Nakagmai1.33 whereas average EFL of Nakagami1.33 is 2.5 times higher than Rayleigh.

BER curves are shown in Fig. 4.12. Since increase in Doppler does not affect bit error rate, therefore the BER of single transmitter single receiver arrangement is unaffected from change in Doppler. Reduction in depth of fades due to addition of LOS component resulted lower BER. At approx. 10^{-2} BER, Nakagami2.77 showed 5 dB improvement over Nakagami1.33 while Nakagami1.33 showed around 2 dB improvement.

4.4.2 Average Error Burst Length of V-BLAST

V-BLAST is a *multiple input multiple output* system which require all the channel paths e.g. 3 channel paths in Tx = 3, Rx = 3, and 6 in Tx = 6, Rx = 6 for each substream. Although average fade and non-fade duration reduces with increase in Doppler but total fade duration are same for every Doppler at a specified signal to

noise ratio. Likewise non-fade durations are also same for every Doppler at a specific signal to noise ratio. This ensures that the probabilities that the signal magnitude lies below the threshold are same for all Doppler frequencies as well as the probabilities the signal magnitude l above the threshold are also same for all Doppler frequencies. Since all the channel paths are independent, therefore the probability that all three paths (in the case of Tx = 3, Rx = 3) be in fade simultaneously is the multiplication of probabilities of signal magnitude lies below the threshold. Since the probabilities (for all Dopplers) that the signal magnitude lies below the threshold are same. Likewise, the probabilities that the signal magnitude lies above the threshold are same at any Doppler. Therefore the probabilities of 1 or 2 or 3 channel paths be in fade are also same for all Dopplers. This phenomenon resulted in approximately same BER, average error burst length, and average error free length which can be seen in Figs. 4.13 to 4.21.

Figs. 4.13 to 4.15 shows the average error burst lengths for V-BLAST system for Doppler 10, 20, 50 Hz over single path Rayleigh, and two Nakagami channels. Simulations are performed for (3×3), and (6×6) transmitter receiver arrangements. Six transmitters six receivers setup utilizes 6×6 channels. For one data stream, six channels are utilized. In contrast with this, 3 transmitter 3 receiver setup utilizes 3×3 channels, and for one data stream there are 3 channels available only. Therefore, the power received in Tx = 6, Rx = 6, case is more stabilized i.e. the standard deviation of the received power is less than in Tx = 3, Rx = 3, setup. So

the arrangement with smaller standard deviation in the received power gives smaller average error burst lengths. As a result, Tx = 6, Rx = 6, arrangement has smaller average error burst lengths which can be seen from Fig. 4.13. Due to correlation in Nakagami channels, as the correlation increases the average error burst lengths increases.

VBLAST utilizes more than one channels (e.g. 9 in (3×3), and 36 in(6×6)), which resulted in shorter error burst length than Tx = 1, Rx = 1 system over Rayleigh channel. Over Rayleigh channel, error burst length for V-BLAST is 2 times shorter than Tx = 1, Rx = 1 system as shown in Fig. 4.10. BLAST uses independence of channel paths by the projection of received vector for detection process. Correlation in channel paths reduces independence and in turn degrade performance. This degradation in detection process produced more errors. Therefore, the average error burst length of V-BLAST system over Nakagami2.77 channels is higher than Tx = 1, Rx = 1, system and it is approx. 2-3 times than Tx = 1, Rx = 1, system. error burst length for Nakagami1.33 channel is 10-40 percent less than Tx = 1, Rx = 1 set for Doppler and approximately same for other Doppler frequencies.

4.4.3 Average Error Free Length of V-BLAST

Average error free lengths for 10, 20, 50 Hz Dopplers are shown in Figs. 4.16 to 4.18. Average error free length increases with the signal-to-noise ratio as shown in figures. These intervals are longer for Tx = 6, Rx = 6 setup due to larger number of utilized

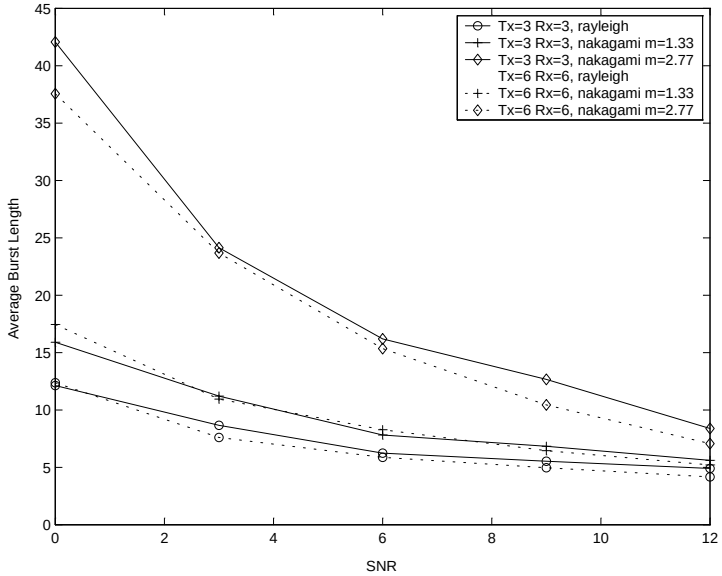

Figure 4.13: Average Error Burst Length of V-BLAST system for Doppler frequency 10 Hz

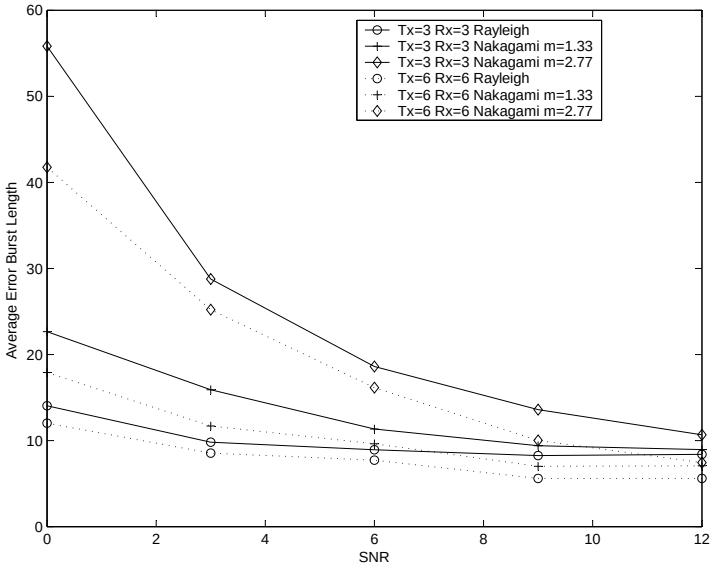

Figure 4.14: Average Error Burst Length of V-BLAST system for Doppler frequency 20 Hz

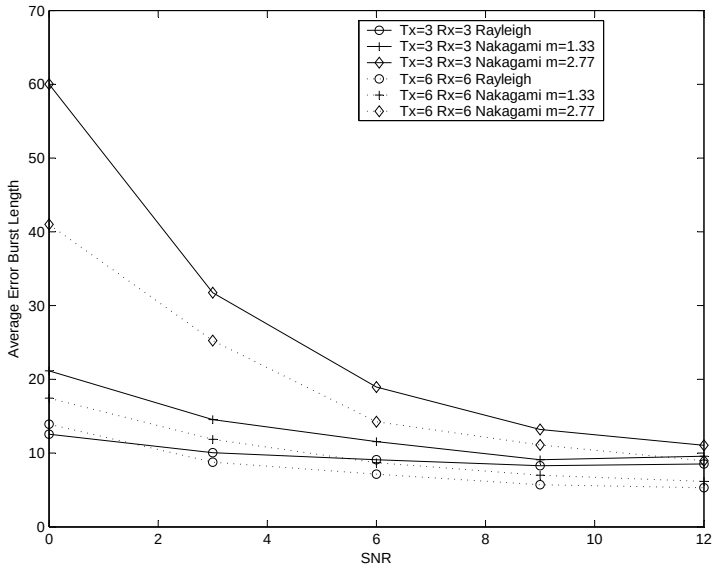

Figure 4.15: Average Error Burst Length of V-BLAST system for Doppler frequency 50 Hz

channels. This increased channel utilization aggrandizes the probability of correct detection of first symbol in the received vector set. Rayleigh distributed channel produces longer error free intervals because of independent paths. Average error free lengths for Rayleigh channel are 3 times higher than Tx = 1, Rx = 1. Increase in correlation resulted poor symbol detection and gave smaller error free intervals. Error free length of Nakagami1.33 is equal to Tx = 1, Rx = 1 and Nakagami2.77 resulted 100 times smaller average error free lengths as can be seen from figures.

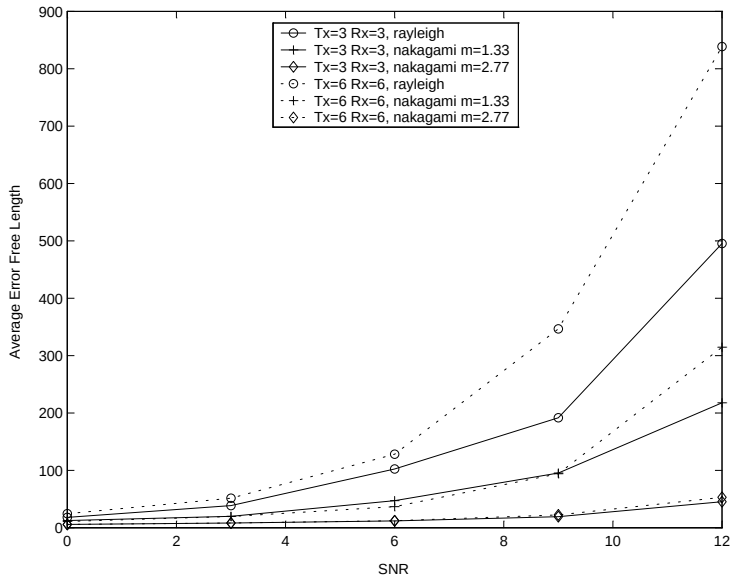

Figure 4.16: Average Error Free Length of V-BLAST system for Doppler frequency 10 Hz

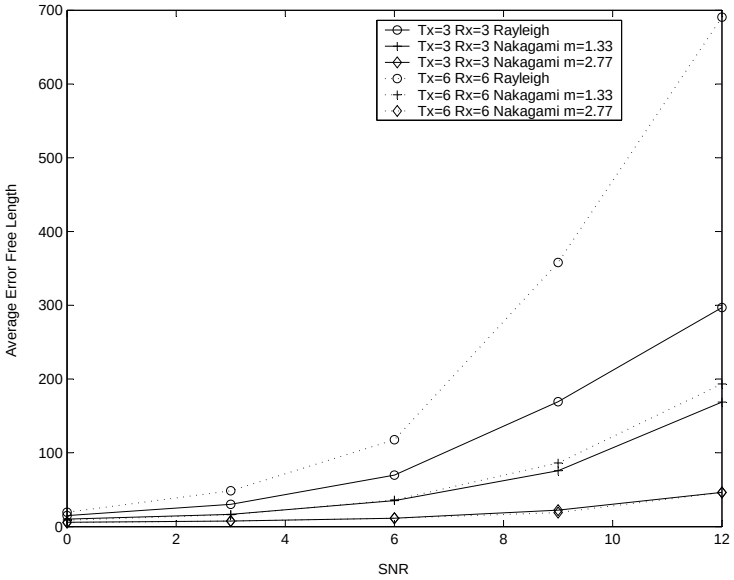

Figure 4.17: Average Error Free Length of V-BLAST system for Doppler frequency 20 Hz

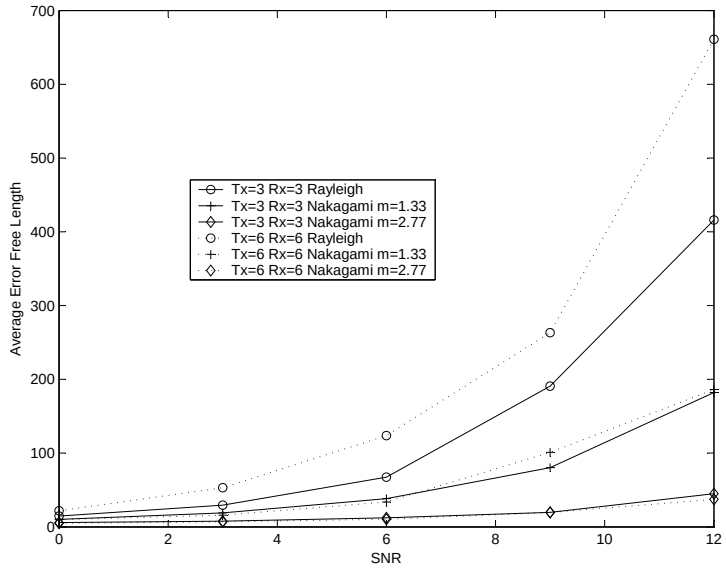

Figure 4.18: Average Error Free Length of V-BLAST system for Doppler frequency 50 Hz

4.4.4 Bit Error Rate of V-BLAST

The bit error rate (BER) performance of the system for 10, 20, 50 Hz Doppler frequencies are shown in Figs. 4.19 to 4.21. Arrangements with larger number of channels utilized (i.e. Tx = 6, Rx = 6) and uncorrelated paths (i.e. Rayleigh channel) give better performances. VBLAST utilizes more than one channels (e.g. 9 in (3×3), and 36 in(6×6)) that gave approx. 6 dB gain for Rayleigh channels at 10^{-2} BER. Correlation in channel paths reduces independence and in turn degrade performance. Therefore Nakagami2.77 channels resulted 10 dB loss at 4 $\times 10^{-1}$ BER. Nakagami1.33 is much closer to Rayleigh channel therefore its performance are not altered and it resulted same BER curves.

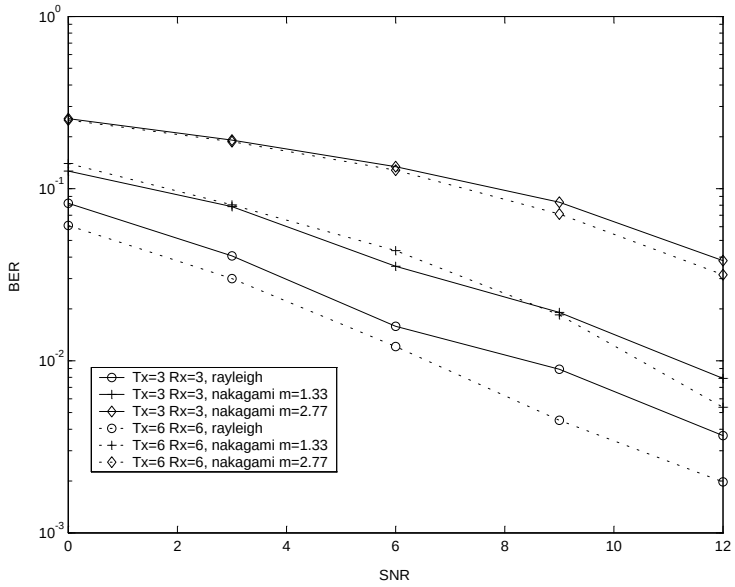

Figure 4.19: BER of V-BLAST system for Doppler frequency 10 Hz

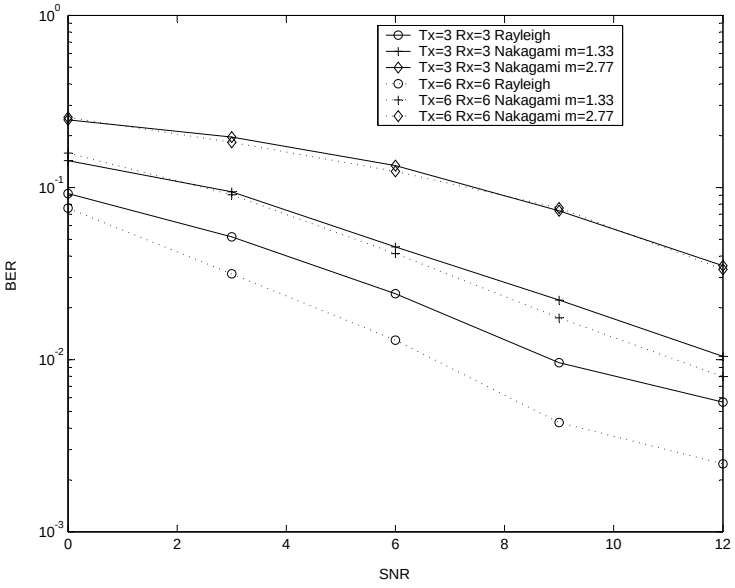

Figure 4.20: BER of V-BLAST system for Doppler frequency 20 Hz

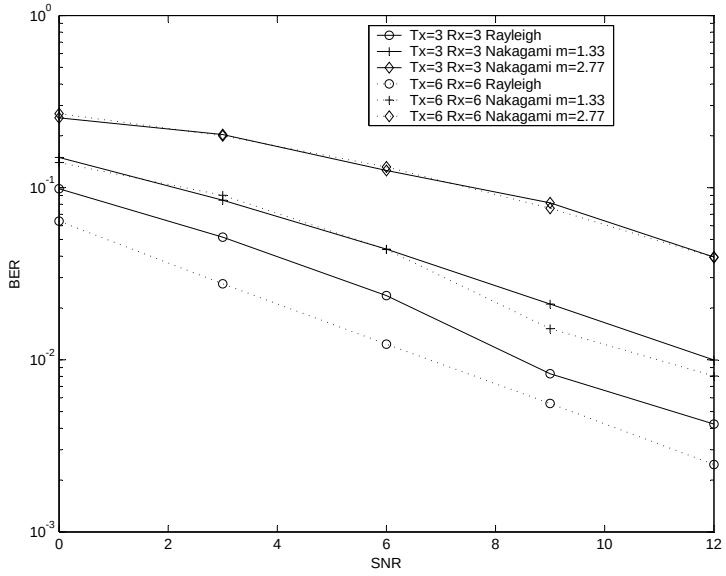

Figure 4.21: BER of V-BLAST system for Doppler frequency 50 Hz

Parallel utilization of sub-channels in V-BLAST system suppress the dependence of BER, average error burst length, and error free length on mobile speed. This independence of the V-BLAST system on mobile speed guarantees the validation of any result found with one mobile speed (say $10Hz$) over other mobile speeds (like $20Hz$, and $50Hz$). In accordance with the reason given rest of the simulations are performed for Doppler speed 10 Hz.

Error characteristics of V-BLAST system are also analyzed in detail by modelling error burst length distributions and error free length distributions. More than 25 functions are fitted on data to see which function describes distributions the best. The selection of the best fitted function is done by the criterion of correlation coeffi-

cients (cc). The quantity correlation coefficient (cc) is used to express the "goodness" of a particular curve fit. In general, the correlation coefficient will range from 0 to 1, with a correlation coefficient of 1 being the best. To explain the meaning of this measure, we must consider the data points and define the standard deviation, which quantifies the spread of the data around the mean:

$$S_t = \sum_{i=1}^{n} (\overline{y} - y_i)^2 \tag{4.5}$$

where n is the number of data points, y_i are data values, and $\overline{y}$ is mean of data. The average of the data points $\overline{y}$ is simply given by

$$y = \frac{1}{n} \sum_{i=1}^{n} y_i \tag{4.6}$$

The quantity S_t considers the spread around a constant line (the mean) as opposed to the spread around the regression model. This is the uncertainty of the dependent variable prior to regression. We also define the deviation from the fitting curve as

$$S_r = \sum_{i=1}^{n} (y_i - f(x_i))^2 \tag{4.7}$$

This quantity measures the spread of the points around the fitting function. Thus, the improvement (or error reduction) due to describing the data in terms of a regression model can be quantified by subtracting the two quantities. Because the

magnitude of the quantity is dependent on the scale of the data, this difference is normalized to yield

$$cc = \sqrt{\frac{S_t - S_r}{S_t}} \tag{4.8}$$

where 'cc' is defined as the correlation coefficient. As the regression model better describes the data, the correlation coefficient will approach unity. For a perfect fit, the correlation coefficient will approach cc=1.

For some simulation parameters, data is so random that no function modelled the data with good correlation. When data have less than 0.8 correlation coefficient with all functions than it is not modelled e.g. for Rayleigh and Nakagami1.33 channels for $Tx = 3, Rx = 3$ setup.

4.4.5 Error Burst Length

Error burst length distributions of the V-BLAST system are plotted in Figs. 4.22, to 4.27. The error process length is taken 10^6 for each simulation. This makes the result of the occurrences of the bursts directly comparable. To make the analysis reliable, the numbers of errors achieved from the simulation are not less than 1000. The system is analyzed on single path Rayleigh, Nakagami1.33, and Nakagami2.77 channels. A number of functions are fitted on the data to see the characteristics of error burst lengths. The best fitted curves are shown in the figures. This selection is done by the maximizing correlation coefficients (cc), which are also shown in plots.

Modelling can give intermediate values for error burst length distributions with the accuracy found from correlation coefficients. It can also be used in future to get error burst lengths without simulations. The most representative function for the error burst length distribution is Rational Function, and that is:

$$y = \frac{a + bx}{1 + cx + dx^2} \tag{4.9}$$

The other functions that approximate the distributions are MMF Model, Harris Model, and 3^{rd} degree polynomial. Equation 4.10 gives the MMF Model, while Harris Model is given in (4.11), and the 3^{rd} degree polynomial model is given in (4.12).

$$y = \frac{ab + cx^d}{b + x^d} \tag{4.10}$$

$$y = \frac{1}{a + bx^c} \tag{4.11}$$

$$y = a + bx + cx^2 + dx^3 \tag{4.12}$$

The frequency of occurrences of error bursts decreases exponentially as the length increases. For Rayleigh channel, when the channel has rich scattering results in less error propagation, therefore less number of errors are produced. Over Rayleigh channels, the frequency of longer bursts increases up to a certain length and then exponentially decreases. With the increase in signal-to-noise ratio, the burst frequency is reduced. Also, the burst length is reduced. This is due to increase in

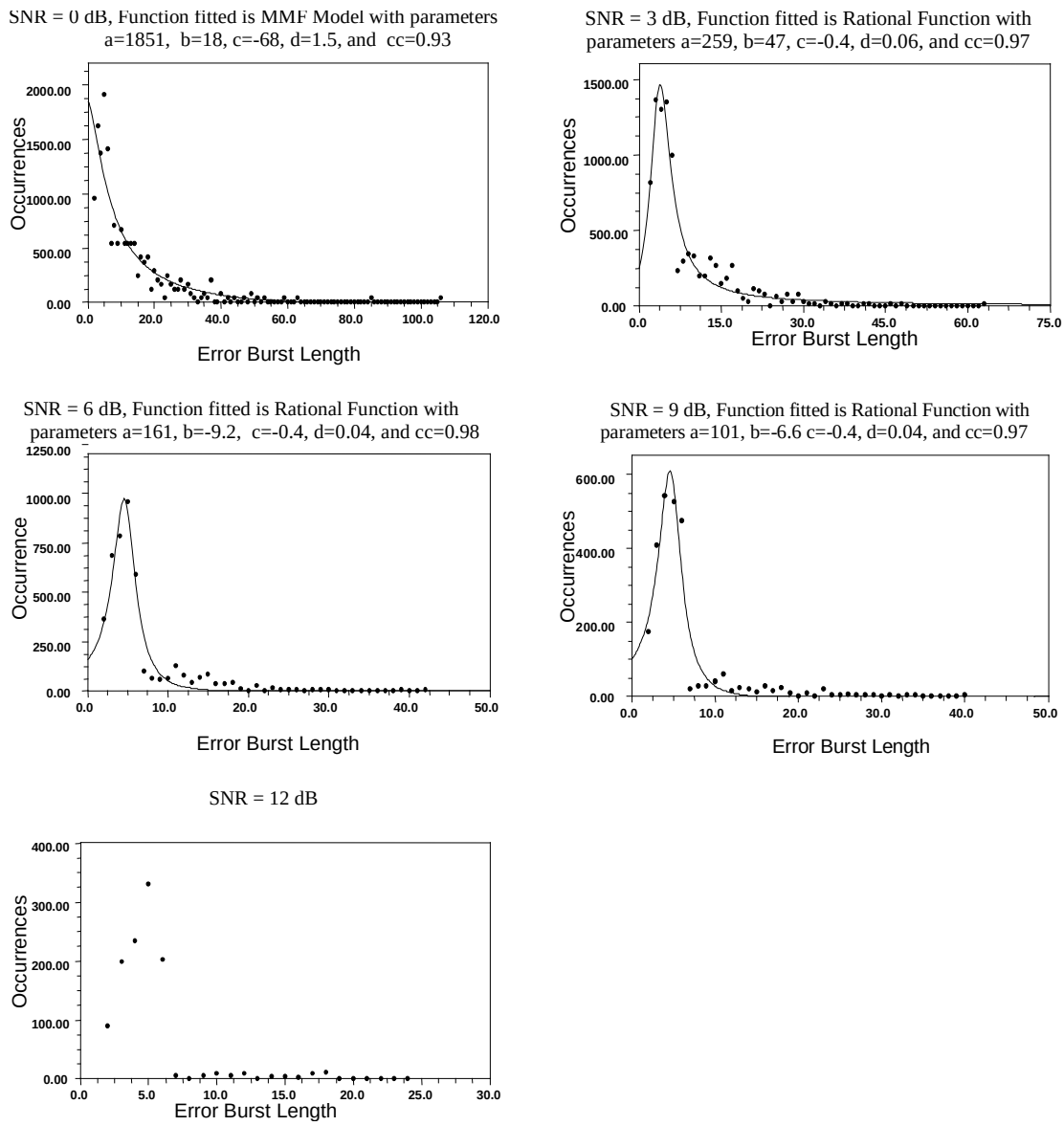

Figure 4.22: Error Burst Length Histogram for Rayleigh channel, and Tx =3, Rx = 3

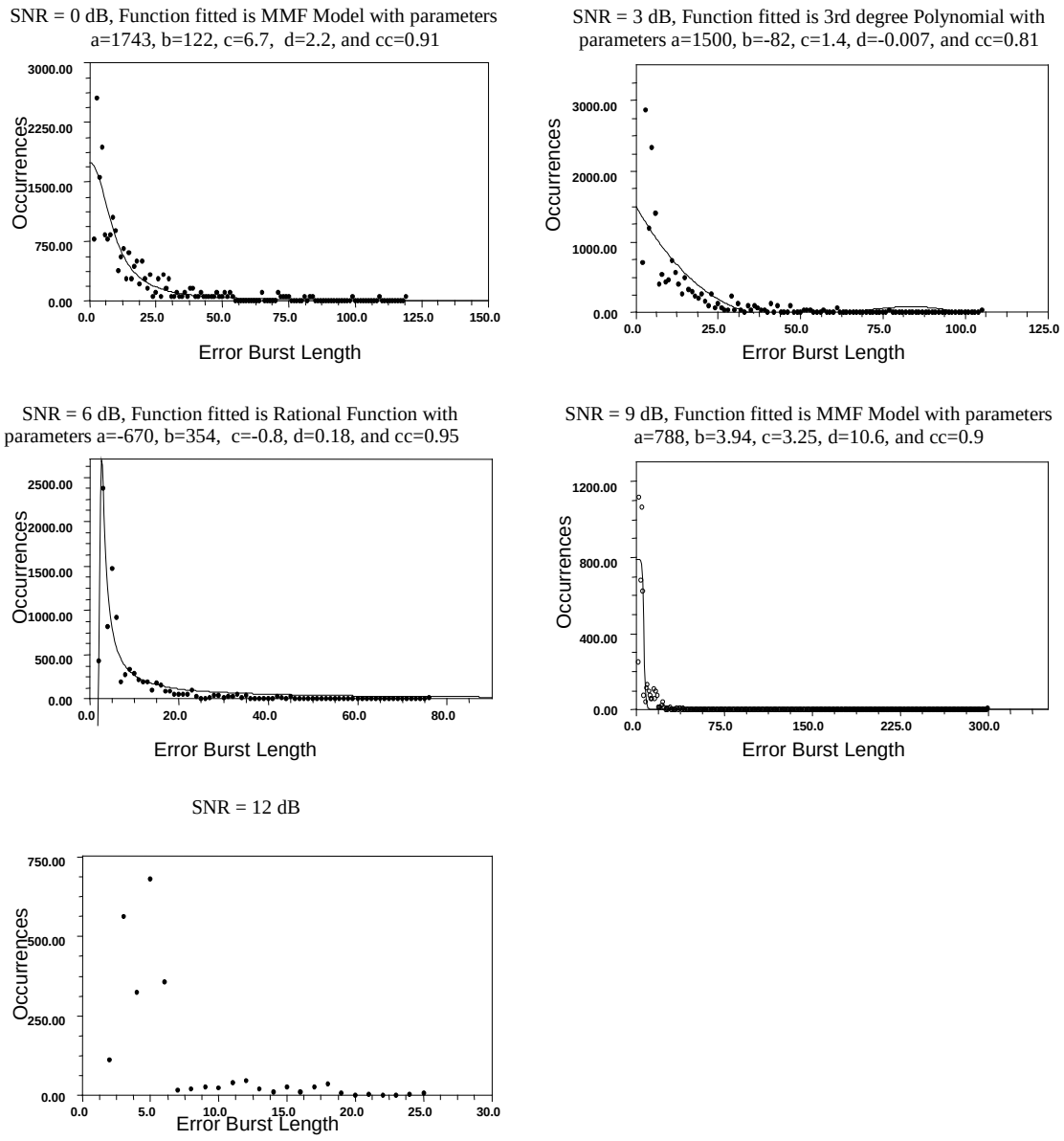

Figure 4.23: Error Burst Length Histogram for Nakagami1.33 channel, and Tx =3, Rx = 3

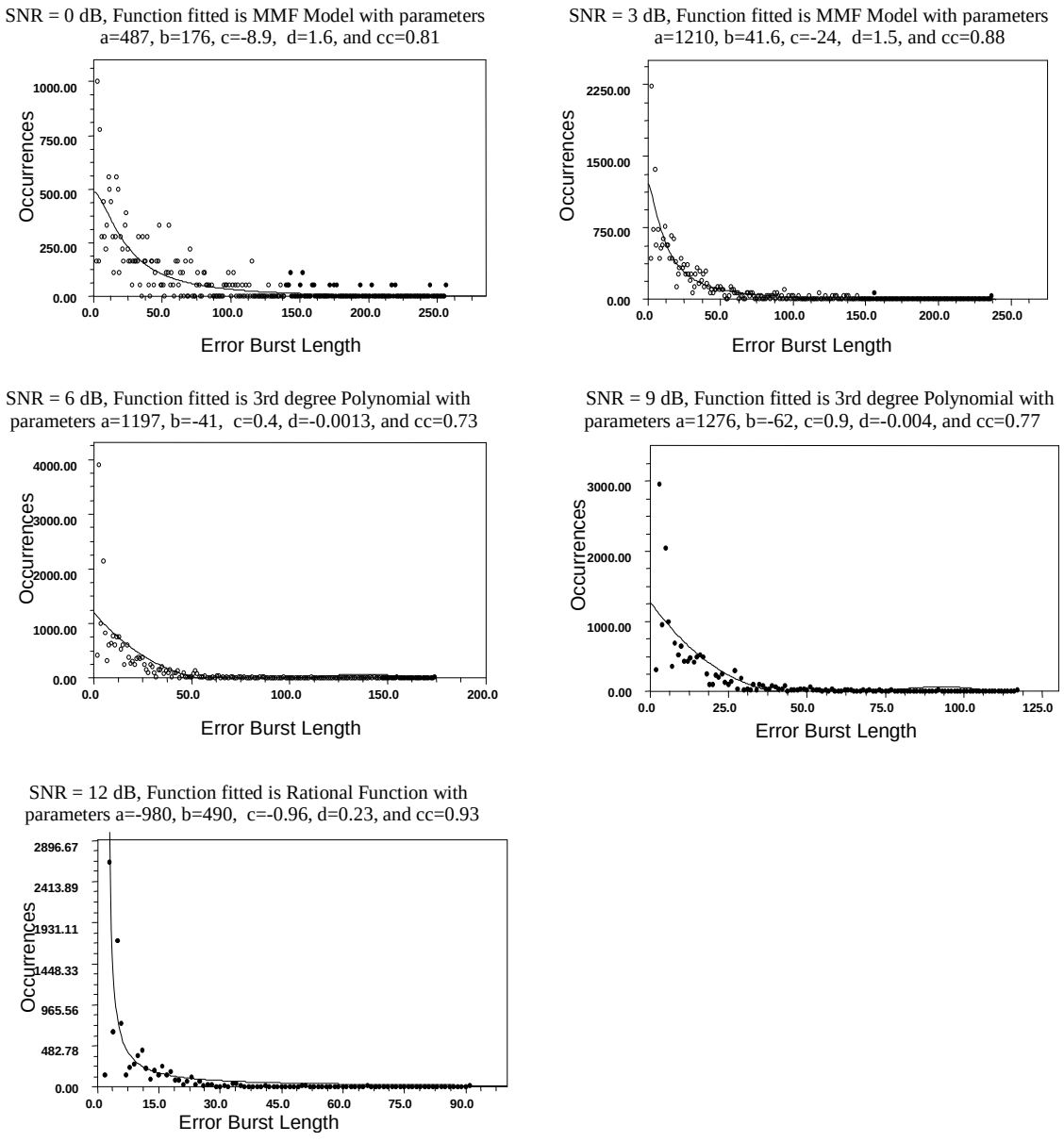

Figure 4.24: Error Burst Length Histogram for Nakagami2.77 channel, and Tx =3, Rx = 3

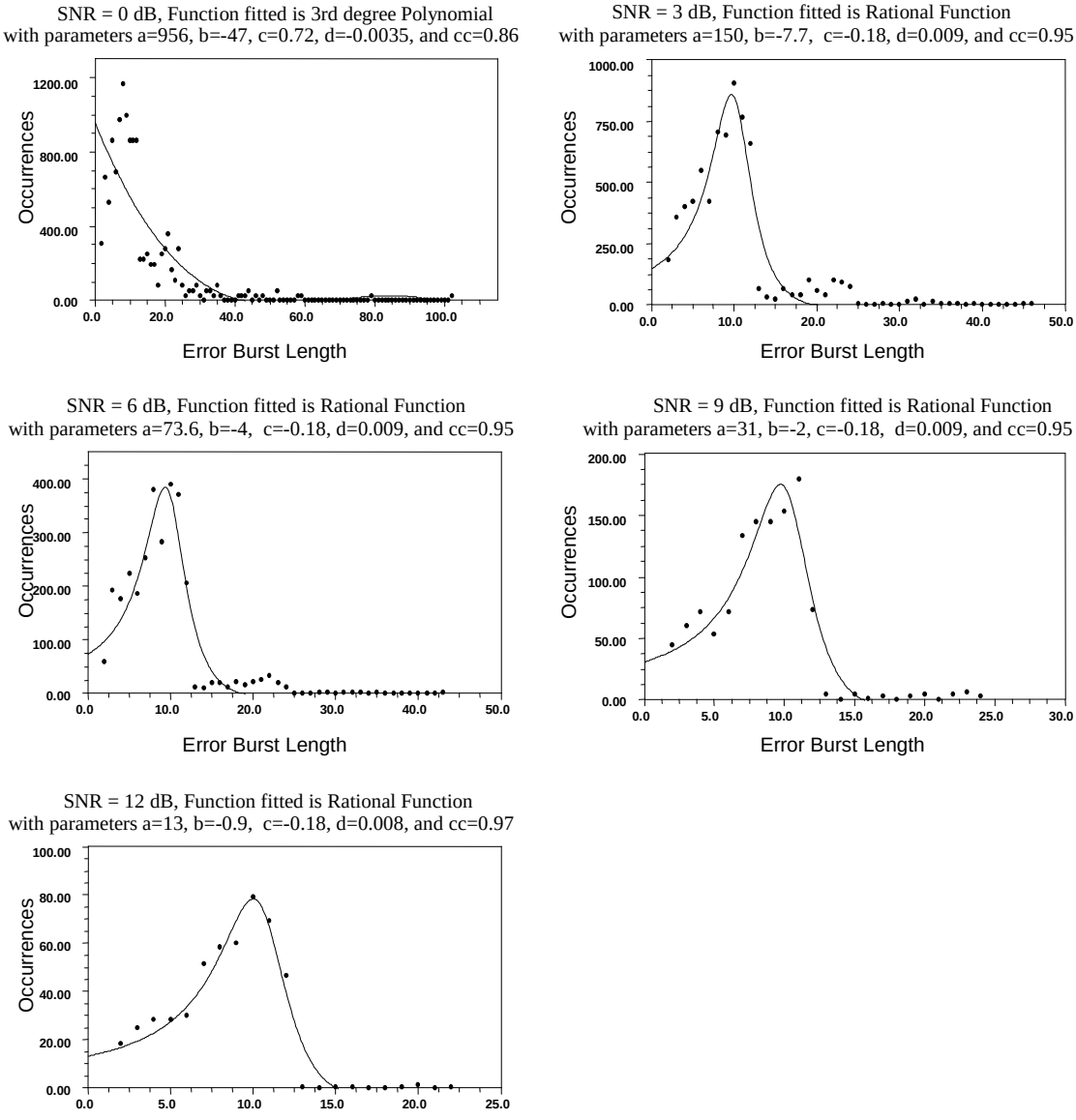

Figure 4.25: Error Burst Length Histogram for Rayleigh channel, and Tx =6, Rx = 6

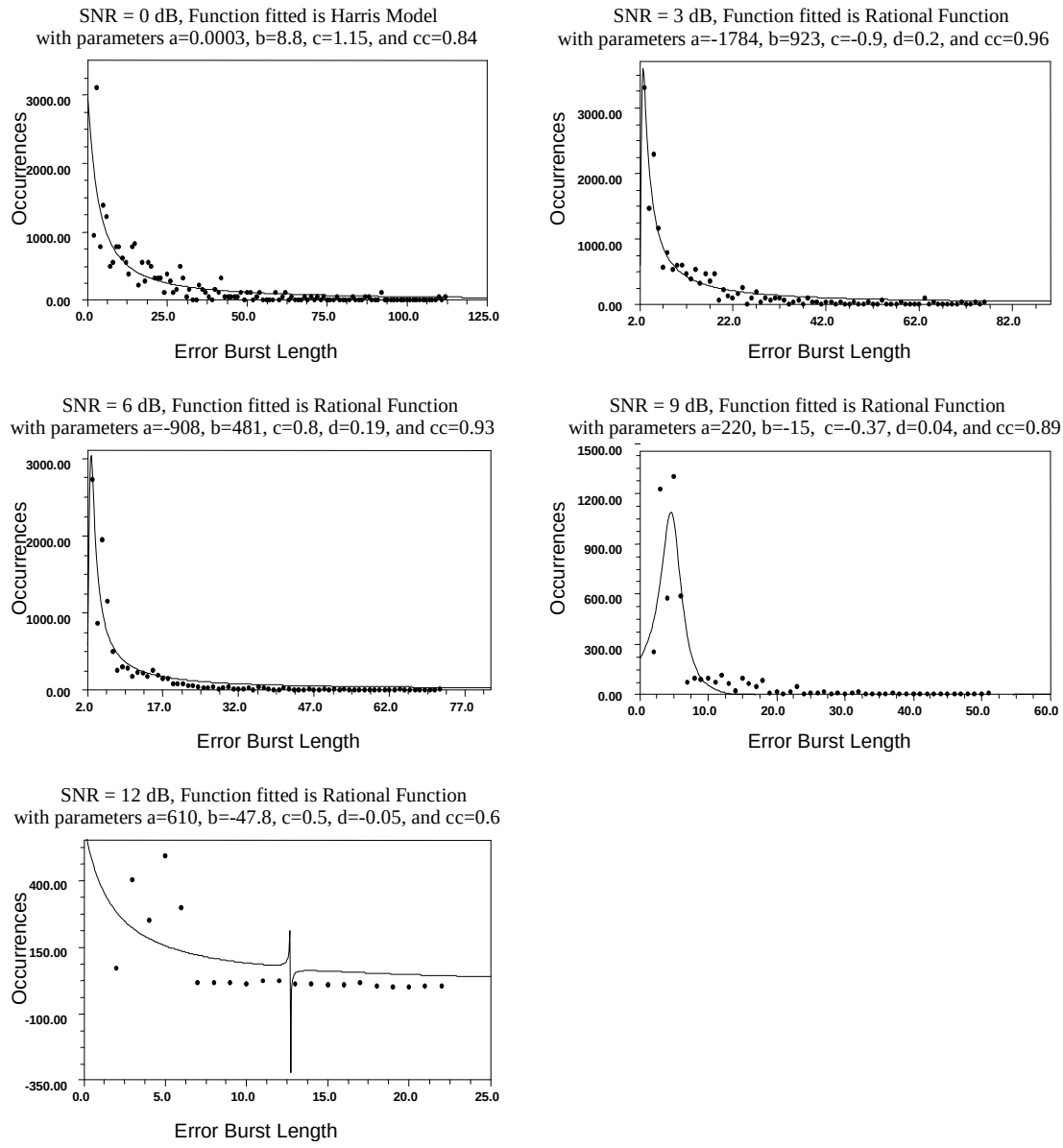

Figure 4.26: Error Burst Length Histogram for Nakagami1.33 channel, and Tx =6, Rx = 6

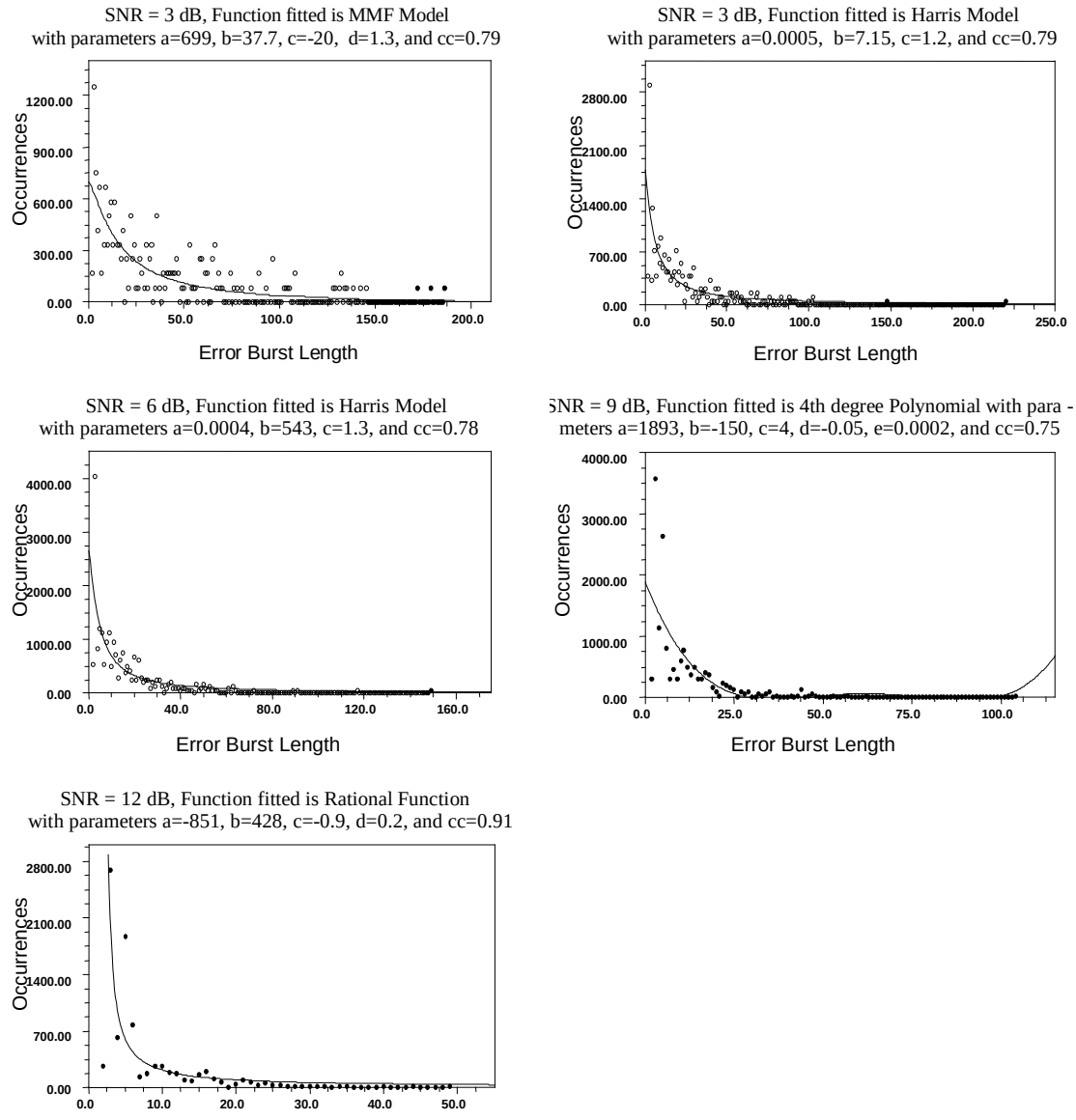

Figure 4.27: Error Burst Length Histogram for Nakagami2.77 channel, and Tx =6, Rx = 6

the mean signal level in Rayleigh fading envelope of the channel and increase in the probability of detecting the first symbol in the received vector. BLAST system utilizes the multiple paths of the wireless channel. If the paths are uncorrelated the performance will be better. As the Nakagami channels paths are correlated (higher m), the performance is worse. As m increases performance degrades. Occurrences of error bursts are increased with m. Even more longer bursts occur in the system with the increase in inter-path correlations.

To give a calculative eye, occurrences of error burst lengths for different lengths are shown in Tables: 4.2 to 4.7. Tables: 4.2 to 4.7 clearly shows that Rayleigh channel has least number of longer error bursts while Nakagami2.77 has the most. EBLOs for $10<\text{BL}\leq 20$ increases with increase in SNR in some point for Nakagami2.77 channel e.g. at 3 dB in Tx = 3, Rx = 3 case, and 6 dB in Tx = 6, Rx = 6 case. This phenomenon can be explained by examining the Table: 4.1. Average error burst length is continuously decreasing while total number of error bursts is increasing from 0 dB to 6 dB then it starts decreasing. Due to higher signal power, long error bursts are transformed into small error bursts. That resulted in higher number of error bursts but shorter in length. Ratio of longer BLs to smaller BLs is 0.47 for Rayleigh, 0.6 for Nakagami1.33, 1.65 for Nakagami2.77 at 3 dB and Tx = 3, Rx = 3. Ratio of longer BLs to shorter BLs is 0.233 for Rayleigh, 0.56 for Nakagami1.33, 1.8 for Nakagami2.77 at 3 dB and Tx = 6, Rx = 6. This ratio decreases exponentially (having 0.9 to 1 cross correlation) from Rayleigh to Nakagami2.77 channel.

Table 4.1: Total error statistics of Nakagami2.77, without Turbo Coding, error process length = 10^6

Tx = 3, Rx = 3

SNR in dB	0	3	6	9	12
Total Error Bursts	17000	21500	21389	16146	9384
Average Error Burst Lengths	42	24	16	13	9

Tx = 6, Rx = 6

Total Error Bursts	18500	21722	21667	15700	8694
Average Error Burst Lengths	37	24	15	10	7

Table 4.2: EBLOs for 2<BL≤10, Tx = 3 Rx = 3,without Turbo Coding, error process length = 10^6

SNR	Burst Length Occurrences		
in dB	Rayleigh	Nakagami1.33	Nakagami2.77
0	9750	11222	3667
3	7050	10333	7600
6	3687	7111	10639
9	2250	4108	9479
12	1081	2129	6917

Table 4.3: EBLOs for 10< BL ≤20, Tx = 3 Rx = 3,without Turbo Coding, error process length = 10^6

SNR	Burst Length Occurrences		
in dB	Rayleigh	Nakagami1.33	Nakagami2.77
0	4042	4444	3611
3	1767	3800	5233
6	533	1319	5083
9	213	667	3750
12	47	237	1850

Table 4.4: EBLOs for BL>20, Tx = 3 Rx = 3,without Turbo Coding, error process length = 10^6

SNR	Burst Length Occurrences		
in dB	Rayleigh	Nakagami1.33	Nakagami2.77
0	2625	4722	9722
3	833	2267	8667
6	100	597	5667
9	67	175	2917
12	2	17	617

Table 4.5: EBLOs for 2<BL≤10, Tx = 6 Rx = 6,without Turbo Coding, error process length = 10^6

SNR	Burst Length Occurrences		
in dB	Rayleigh	Nakagami1.33	Nakagami2.77
0	7056	10056	4750
3	4650	11333	8222
6	2147	8617	10875
9	878	4317	10100
12	379	1575	7083

Table 4.6: EBLOs for 10< BL ≤20, Tx = 6 Rx = 6,without Turbo Coding, error process length = 10^6

SNR	Burst Length Occurrences		
in dB	Rayleigh	Nakagami1.33	Nakagami2.77
0	3417	5278	3583
3	1858	3933	4833
6	717	1750	5542
9	277	608	3767
12	121	113	1153

Table 4.7: EBLOs for BL>20, Tx = 6 Rx = 6,without Turbo Coding, error process length = 10^6

SNR in dB	Burst Length Occurrences		
	Rayleigh	Nakagami1.33	Nakagami2.77
0	1861	6056	10167
3	433	2200	8667
6	117	817	5250
9	15	150	1833
12	1	8	458

4.4.6 Error Free Interval

Error free length distributions of V-BLAST system are shown in Figs. 4.28, to 4.33. Error process length is again taken to be 10^6. Simulations are performed over single path Rayleigh, Nakagami m = 1.33, Nakagami m = 2.77 channels. Best fitted curves are also drawn on the data with their correlation coefficients. The mostly fitted curve is Hyperbolic Fit that is shown in 4.13.

$$y = a + \frac{b}{x} \tag{4.13}$$

An interesting observation is found that the parameter 'a' of Hyperbolic fit is exponentially increases while parameter 'b' is exponentially decreases with SNR. The exponential functions that represent these parameters show around 0.98 to 0.999

correlation coefficients with these parameters. This ensures the finding of error free intervals at any SNR other than these given with a good approximation.

The frequency of occurrences of error free gaps decreases with increase in length. With increase in SNR, longer error free intervals occur. In comparison with Nakagami channels, Rayleigh channels results in longer error free intervals because the paths are independents. Independent paths improve symbol detection.

Turbo coding is applied on V-BLAST system as an example to evaluate its effectiveness and how the parameters error burst length, error free length, and bit error rate change. We analyzed the parameters with different interleaver lengths. The length of interleavers are chosen so that the delay produced is small. Data as well as voice can be transmitted at this delay.

4.5 Error Characterization and Modelling with Turbo Coding

A good trade-off between coding gain and complexity can be achieved by serial concatenated codes proposed by Forney [42]. A serial concatenated code is one that applies two levels of coding, an inner and an outer code linked by an interleaver. The primary reason for using a concatenated code is to achieve a low error rate with an overall decoding complexity lower than that required for a single code of the corresponding performance. *Turbo Codes* exploit a similar idea of connecting two

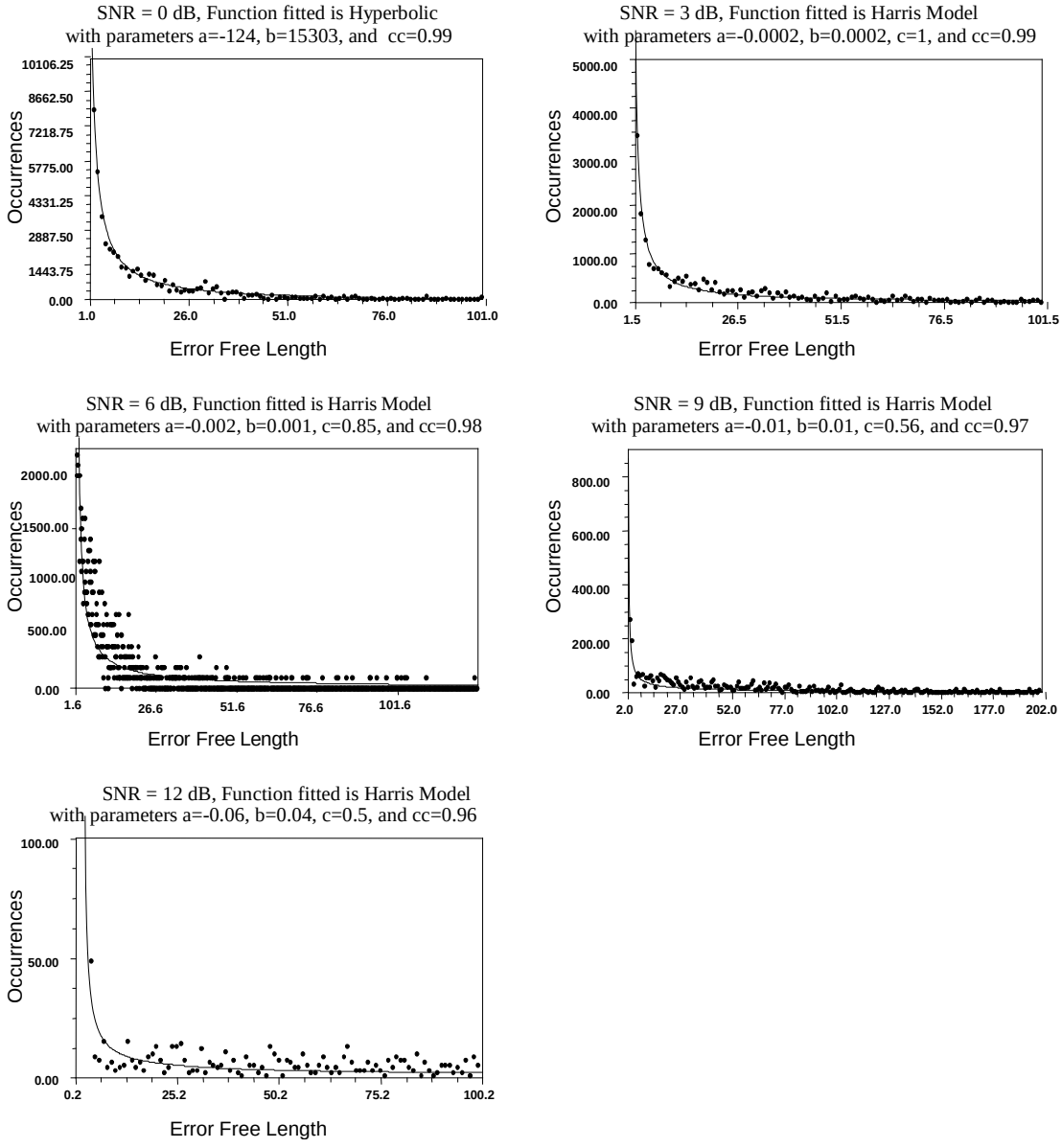

Figure 4.28: Error Free Length Histogram for Rayleigh channel, and Tx =3, Rx = 3

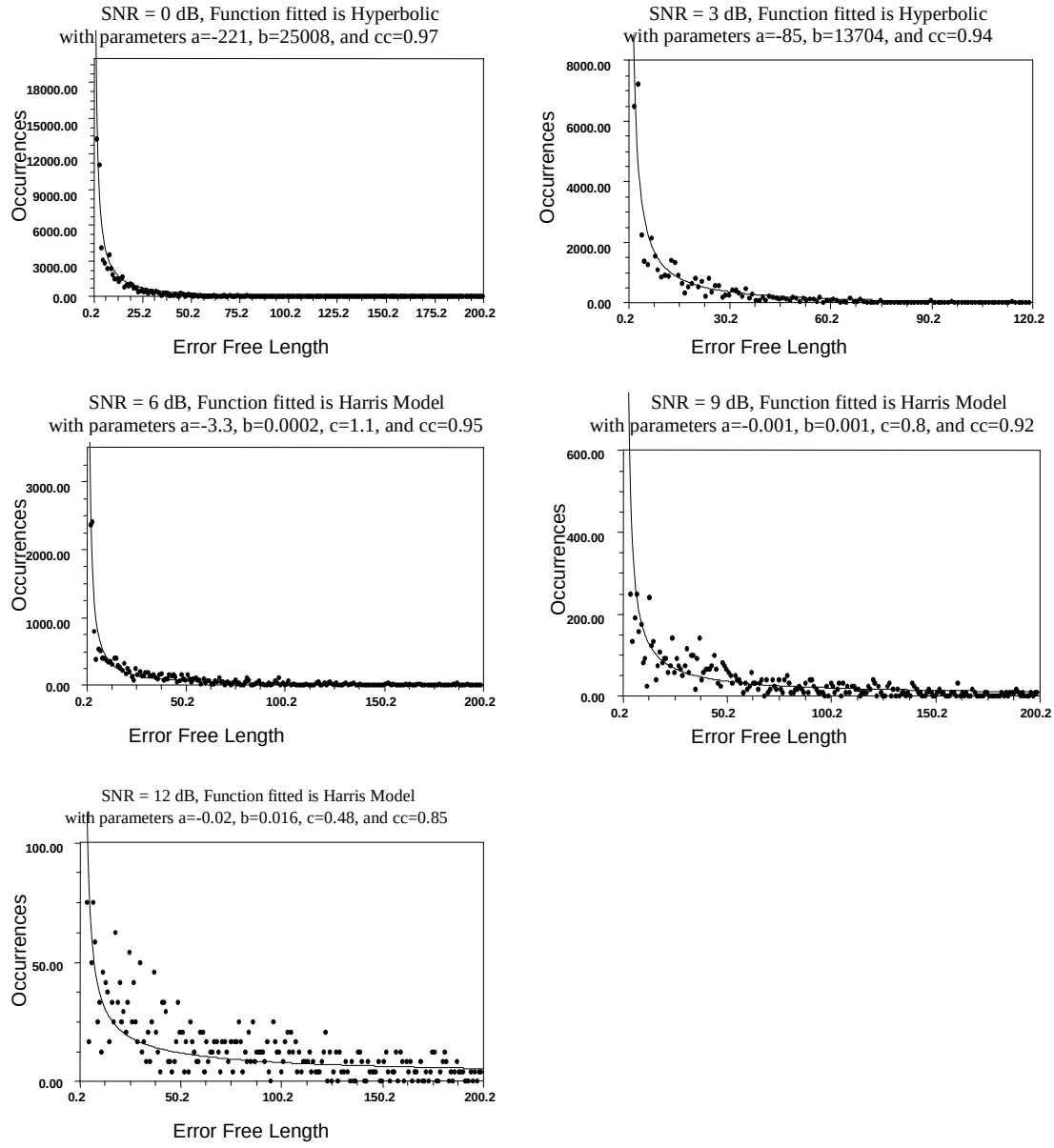

Figure 4.29: Error Free Length Histogram for Nakagami1.33 channel, and Tx =3, Rx = 3

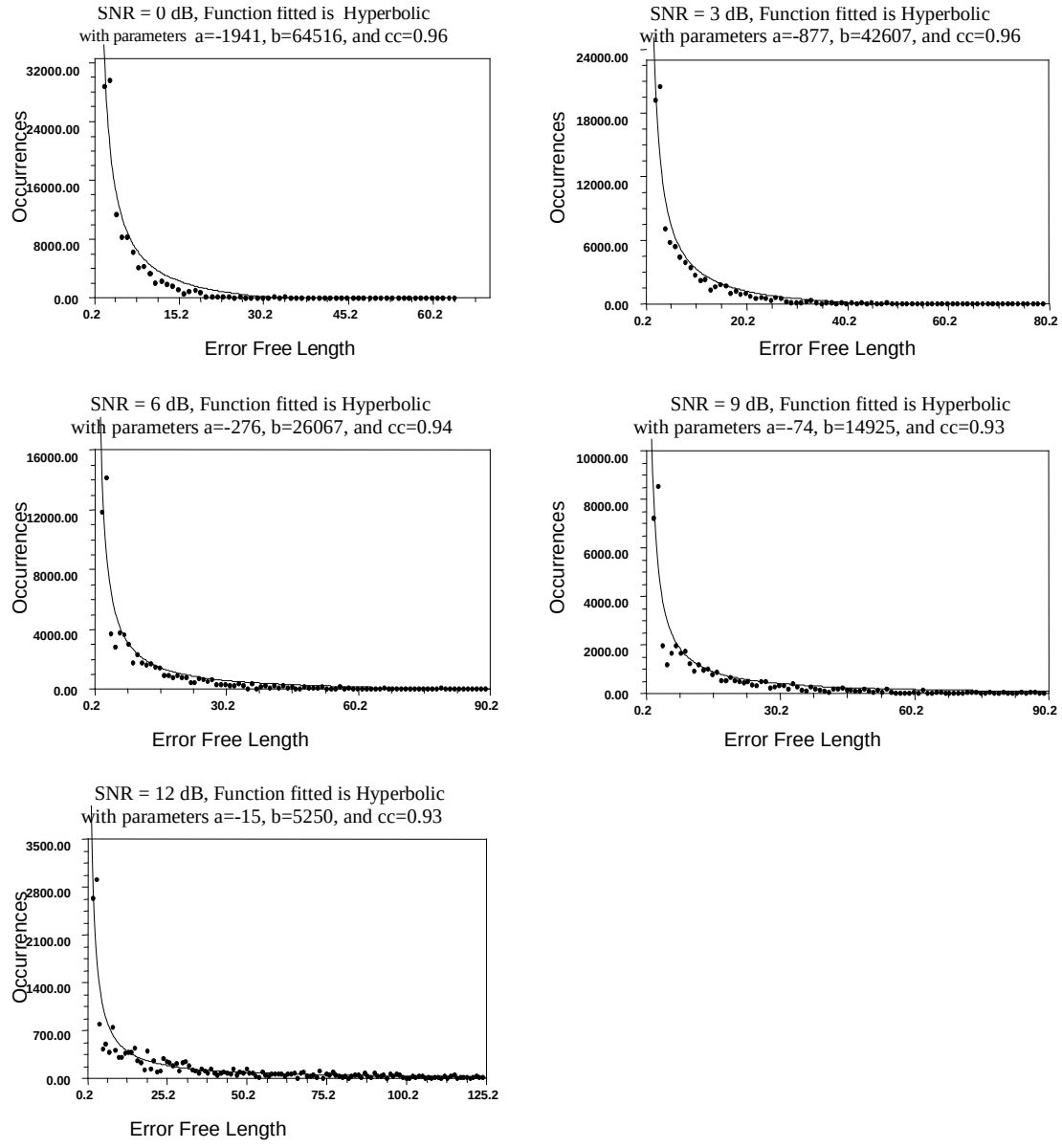

Figure 4.30: Error Free Length Histogram for Nakagami2.77 channel, and Tx =3, Rx = 3

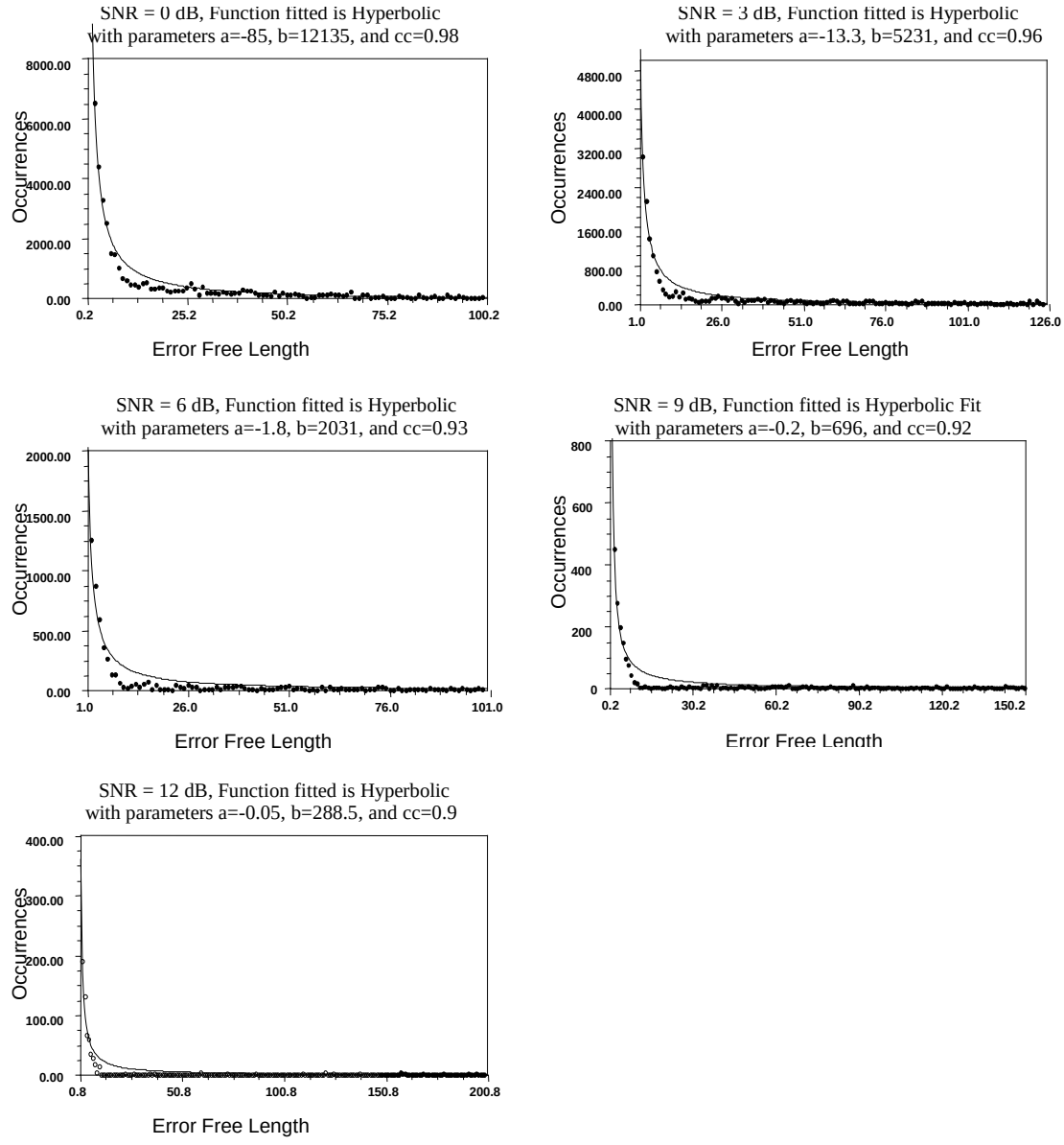

Figure 4.31: Error Free Length Histogram for Rayleigh channel, and Tx =6, Rx = 6

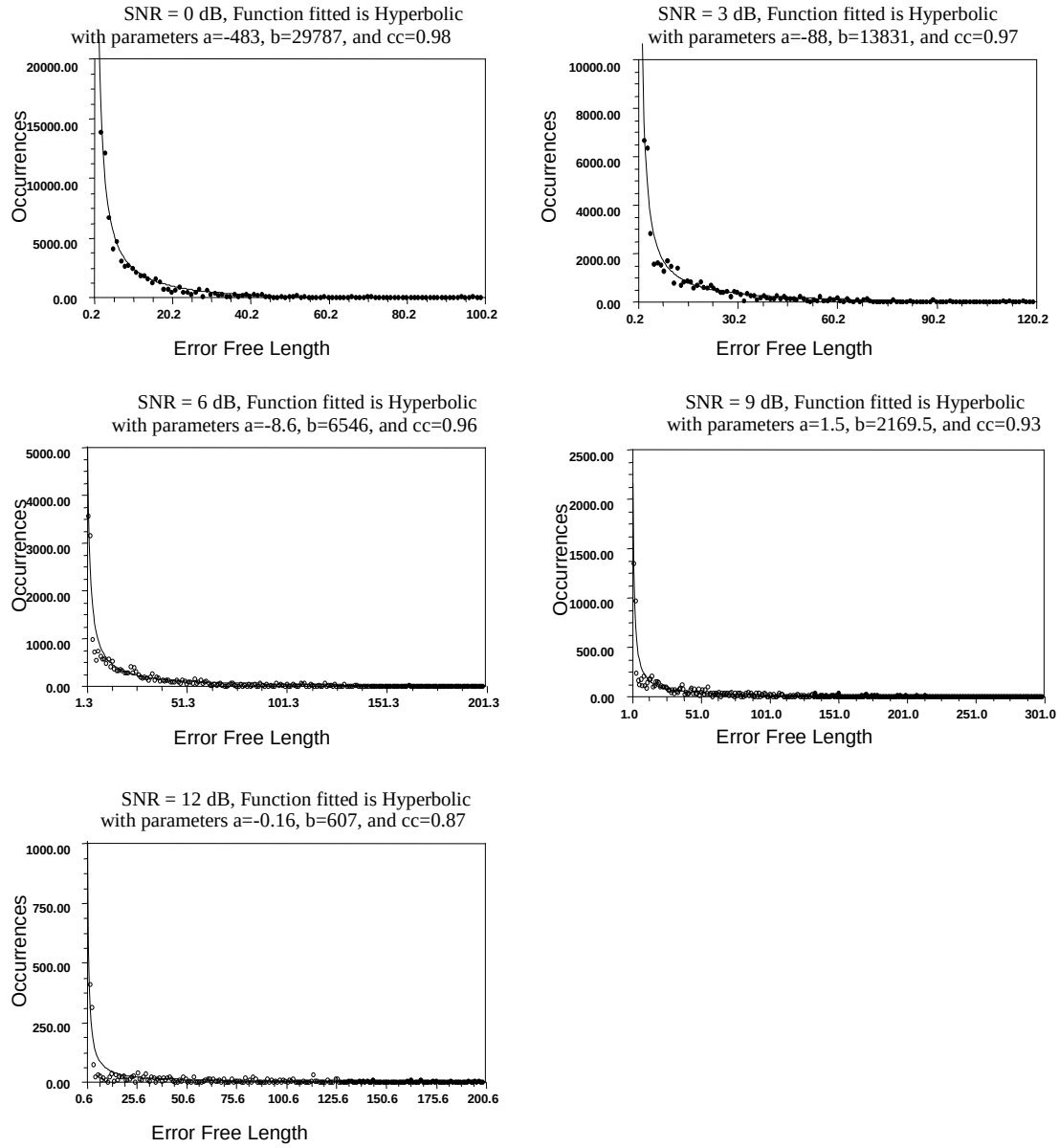

Figure 4.32: Error Free Length Histogram for Nakagami1.33 channel, and Tx =6, Rx = 6

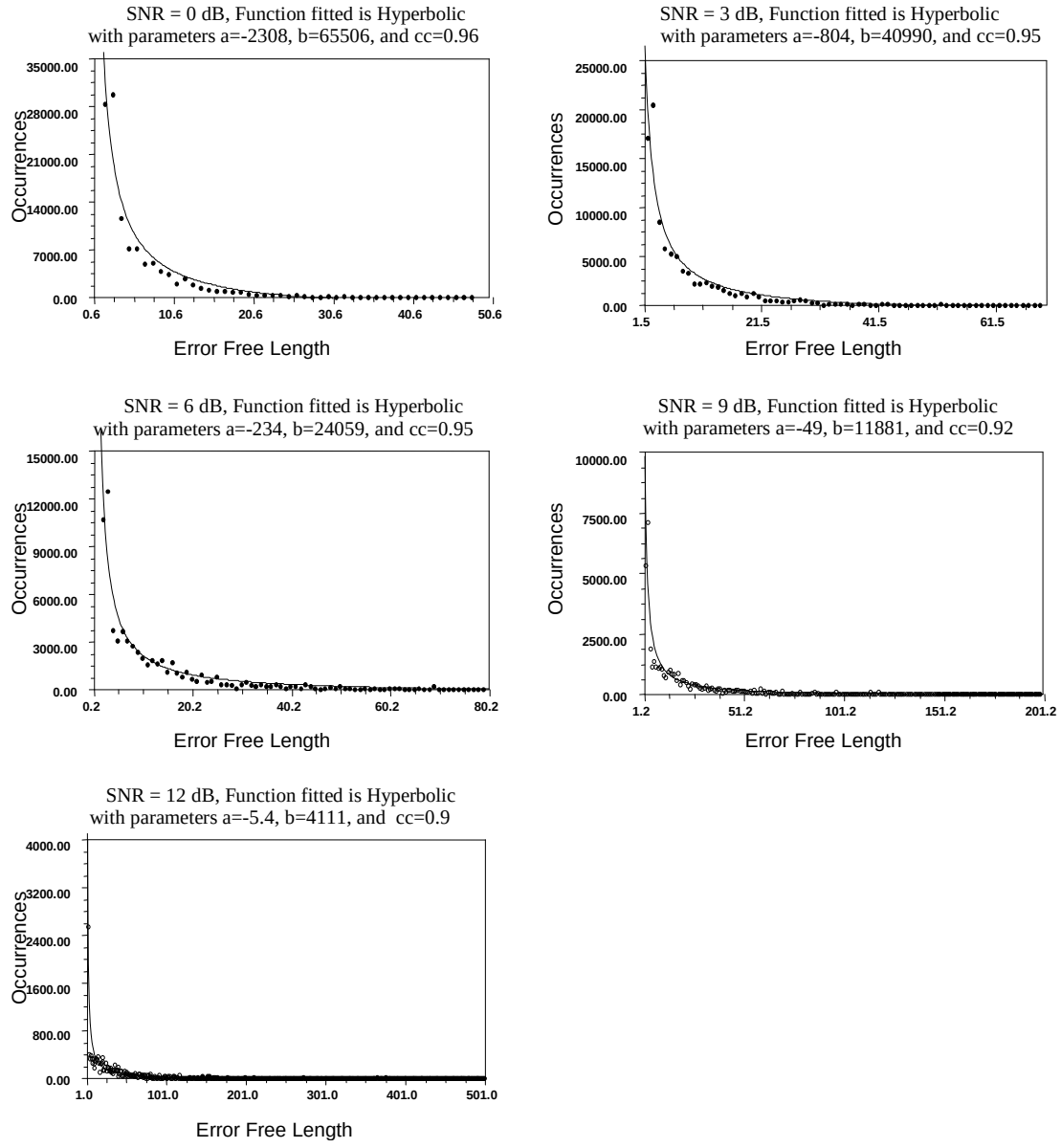

Figure 4.33: Error Free Length Histogram for Nakagami2.77 channel, and Tx =6, Rx = 6

codes and separating them by an interleaver [43]. The difference between turbo and serial concatenated codes is that in turbo codes two identical systematic component codes are connected in parallel. V-BLAST system performance is analyzed when Turbo Coding is applied. This exercise is taken up to evaluate the effectiveness of Turbo Coding in V-BLAST. The parameters like error burst lengths, error free lengths, and BER, which are calculated without coding in the previous section, are computed with turbo coding. Encoder used has a rate $R = 1/3$ and memory ν=4. Generator polynomials for the two constituent codes are $G_1 = 37$ and $G_2 = 33$ (in octal form). Each component decoder uses maximum a posteriori probability (MAP) algorithm. An iterative decoding with number of iteration = 6 is used. Iterative process performs information exchange between the two component decoders. Cyclic shift type interleavers with three different lengths (64, 512, 1024) are used. For a matrix of m rows and n columns to generate interleaver mapping, the m and n of the interleavers are: $m = 4, n = 16$, for interleaver depth 64; $m = 8, n = 64$, for interleaver depth 512; $m = 16, n = 64$, for interleaver depth 1024.

4.5.1 Error Burst Lengths

Error burst length distributions of V-BLAST are shown in Figs. 4.34 to 4.51, when turbo coding is applied. The error process length is 10^6. This ensures direct comparison for frequency of error burst lengths for cases with or without coding. Error burst lengths are statistically modelled. Correlation coefficient measure is used for

modelling. When data have correlation coefficient less than 0.8 with all functions then it is not modelled. Model parameters and correlation coefficients are shown in figures. Functions that are used to model error burst lengths are Harris Model, Rational Function, and MMF Model. Best fit models that approximate closely are Harris Model and Rational Function. Correlation coefficient increases with increase in signal power in Nakagami2.77. Nakagami2.77 channel has the highest correlation among all channel paths under consideration. This correlation in channel paths gives worse detection performance for V-BLAST . It resulted in very long error bursts that can be seen in figures. For stronger signals, not only error burst lengths become shorter also their occurrences reduced that in turn resulted in shaping the distributions as well as good approximation of models.

Error burst length histograms show that the arrival rate of error burst lengths (EBLs) decreases exponentially with increase in length of error bursts. Rayleigh channel ($m = 1$) has strong scattering which results in no correlation in channel paths. Rich scattering results in increased probability of signal to be detected correctly. Which reduced propagation in error. Figs. 4.34 to 4.51 clearly shows that Rayleigh channel has smallest error burst lengths while Nakagami2.77 has the longest error burst lengths. For higher signal powers compared to noise variance, occurrences of EBL are reduced with increase in SNRs. This is due to increase the mean signal level in Rayleigh fading envelope of the channel as well as the probability of detecting the first symbol in the received vector is increased. Interleavers

are used to decorrelate the received symbols affected by burst errors as well as to produce long codes. Interleaver size affected the occurrences of error burst. Larger interleaver size produce longer code lengths [34] and separate errors in close proximity to far enough so that they can be corrected. With the increase in interleaver size, error burst lengths and their occurrences reduced. V-BLAST detection technique is affected severely with correlation in channel paths. Correlation in channel paths increases errors. Therefore, EBLs and their occurrences increase with the increase in m i.e these are least in Rayleigh, and most in Nakagami 2.77 channels.

Six transmitter six receiver setup utilizes 6×6 channels. For one data stream, there are 6 channels utilized. In contrast with this, 3 transmitter 3 receiver setup utilizes 3×3 channels, and for one data stream only 3 channels are available. Therefore, the power received in Tx = 6, Rx = 6, case is improved i.e. the standard deviation of the received power is less than in Tx = 3, Rx = 3, setup. So the arrangement with smaller standard deviation in the received power gives smaller error burst lengths. As a result, Tx = 6, Rx = 6, arrangement has smaller error burst lengths. Frequency of occurrences of error burst lengths is reduced to 70-50 percent when comparing with distributions of error burst length of V-BLAST system without any coding shown in Figs. 4.22 to 4.27. Increasing interleaver size from 64 to 1024 reduced the frequency of error burst lengths to further 10-20 percent. Which illustrates the correction capability of turbo coding.

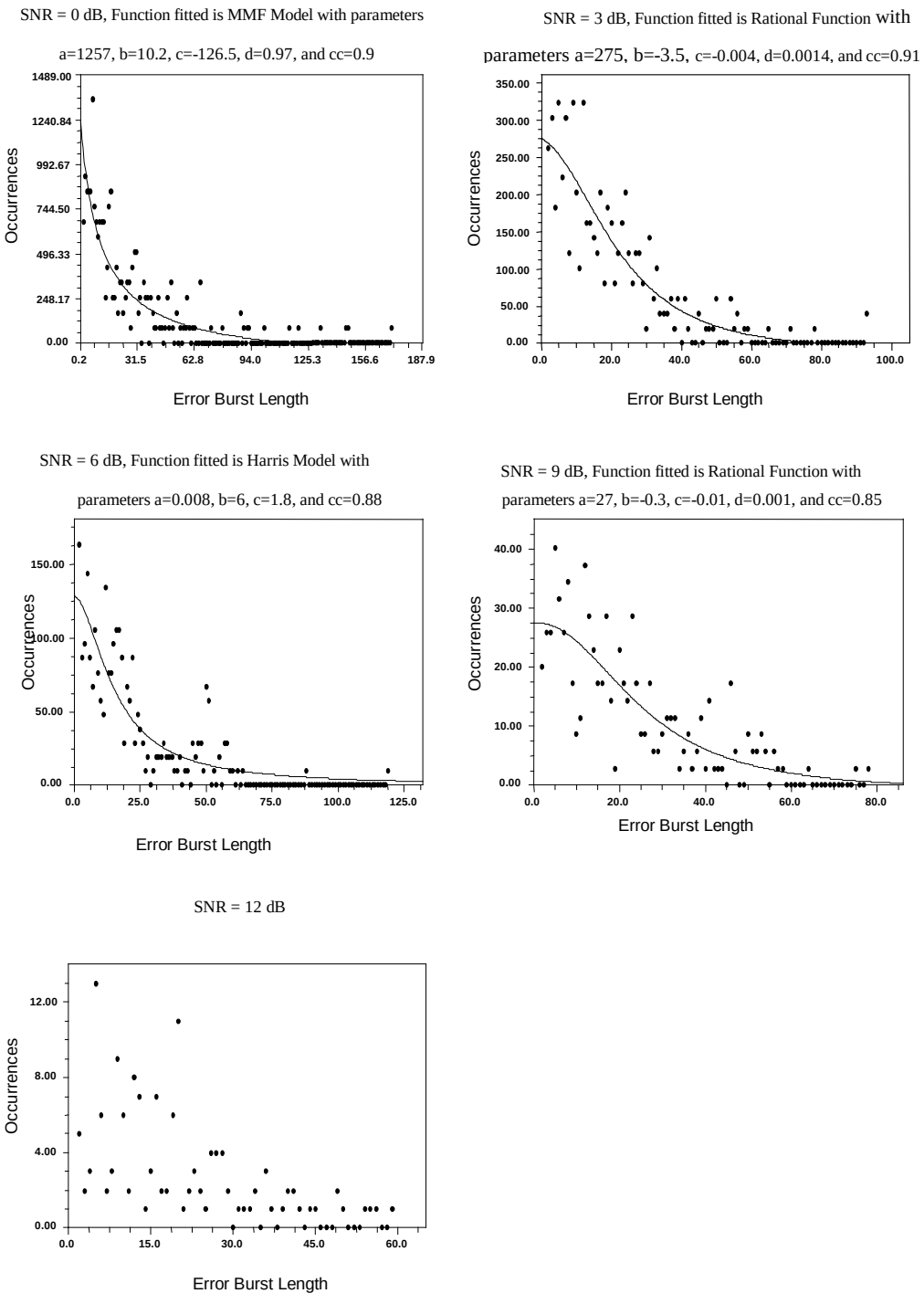

Figure 4.34: Error Burst Length Histogram for Rayleigh channel, interleaver size = 64, and Tx =3, Rx = 3

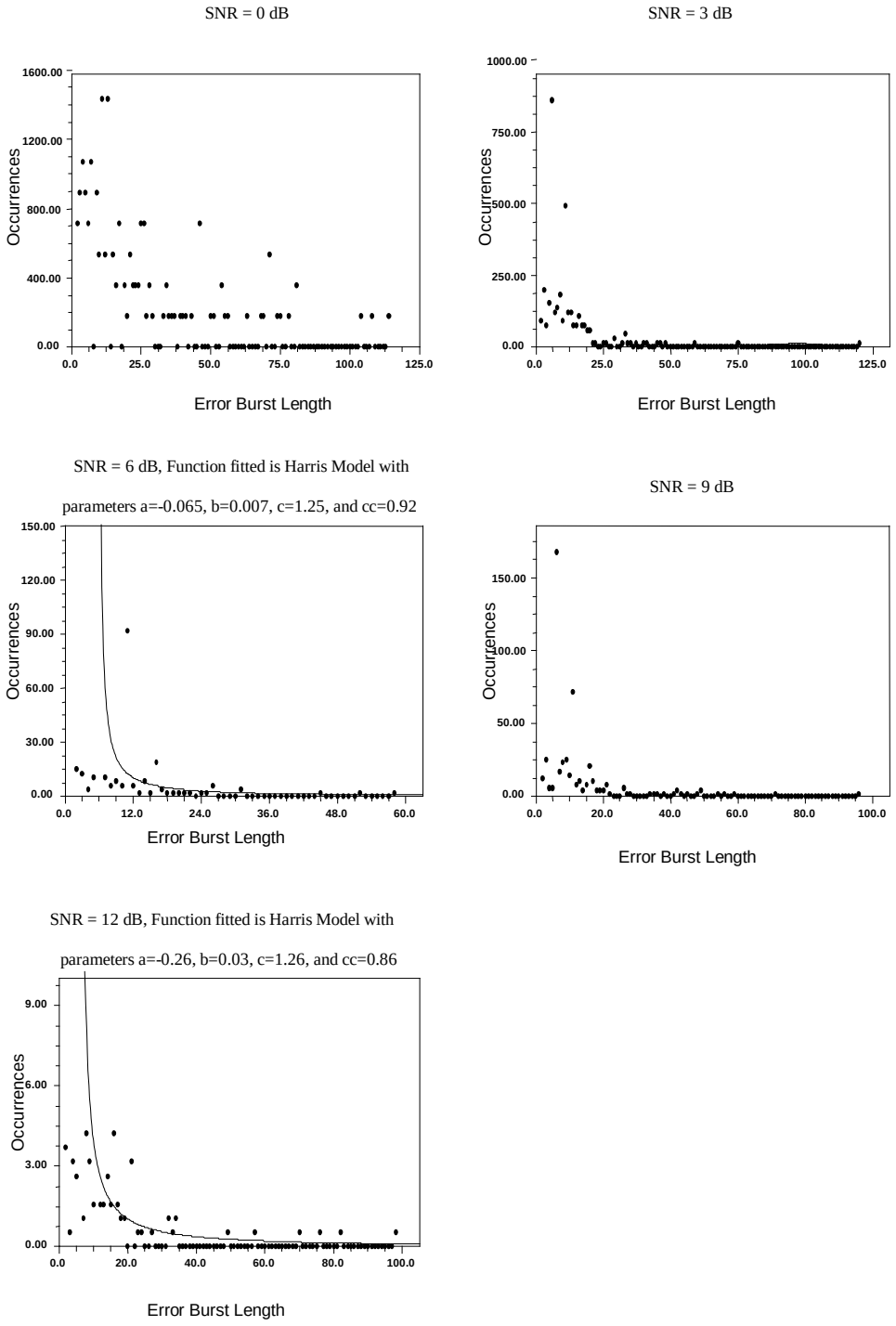

Figure 4.35: Error Burst Length Histogram for Rayleigh channel, interleaver size = 512, and Tx =3, Rx = 3

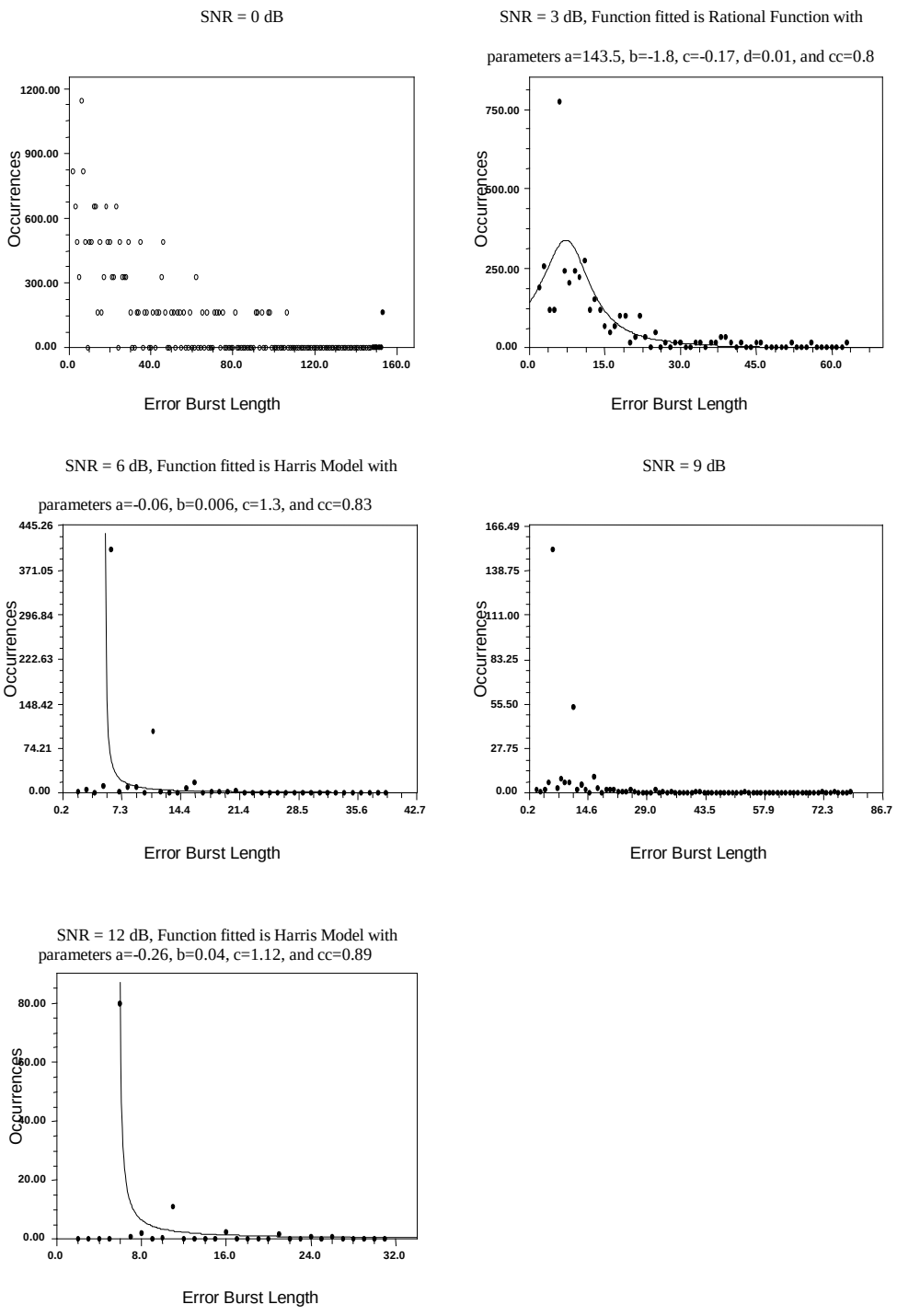

Figure 4.36: Error Burst Length Histogram for Rayleigh channel, interleaver size = 1024, and Tx = 3, Rx = 3

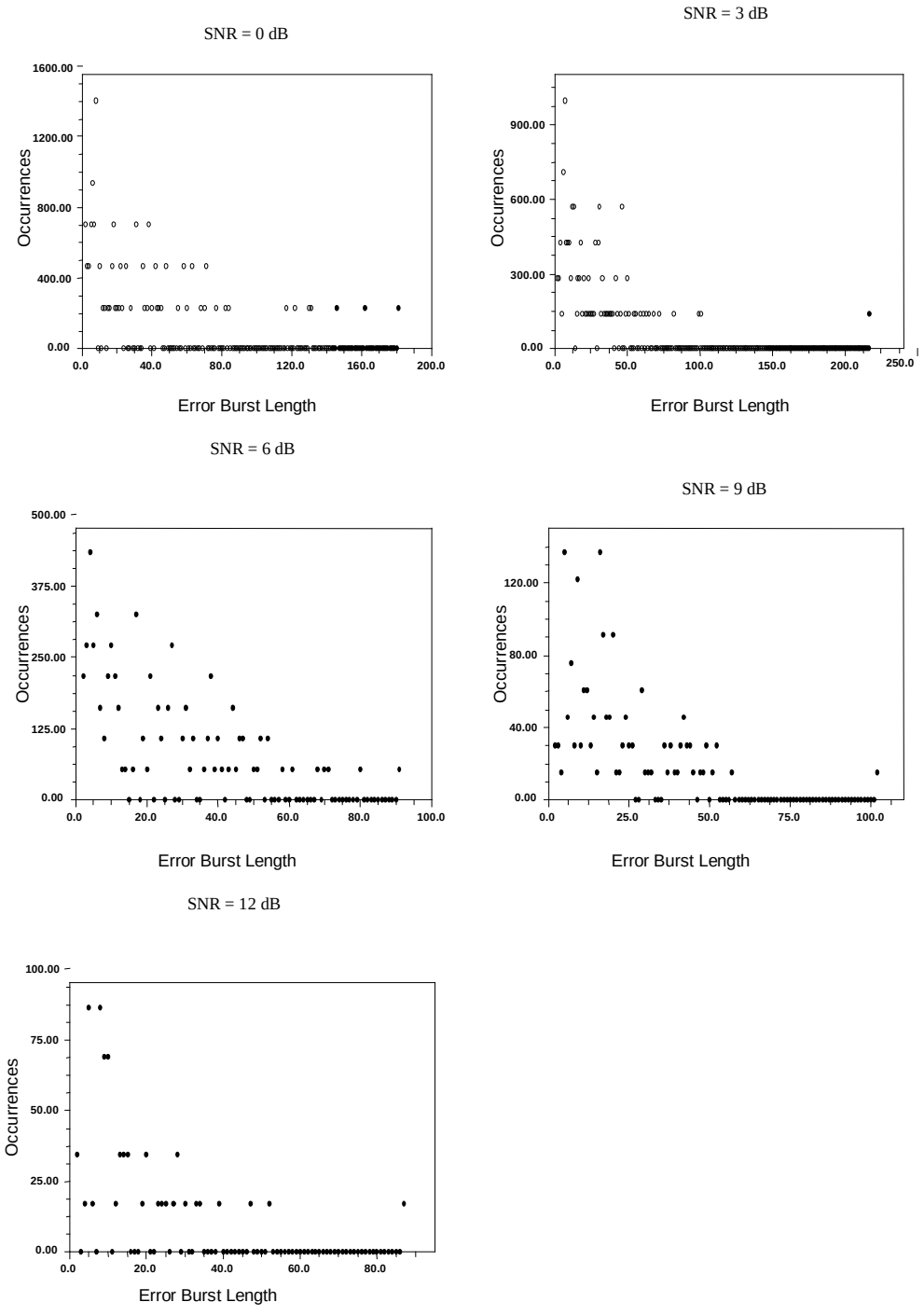

Figure 4.37: Error Burst Length Histogram for Nakagami1.33 channel, interleaver size = 64, and Tx = 3, Rx = 3

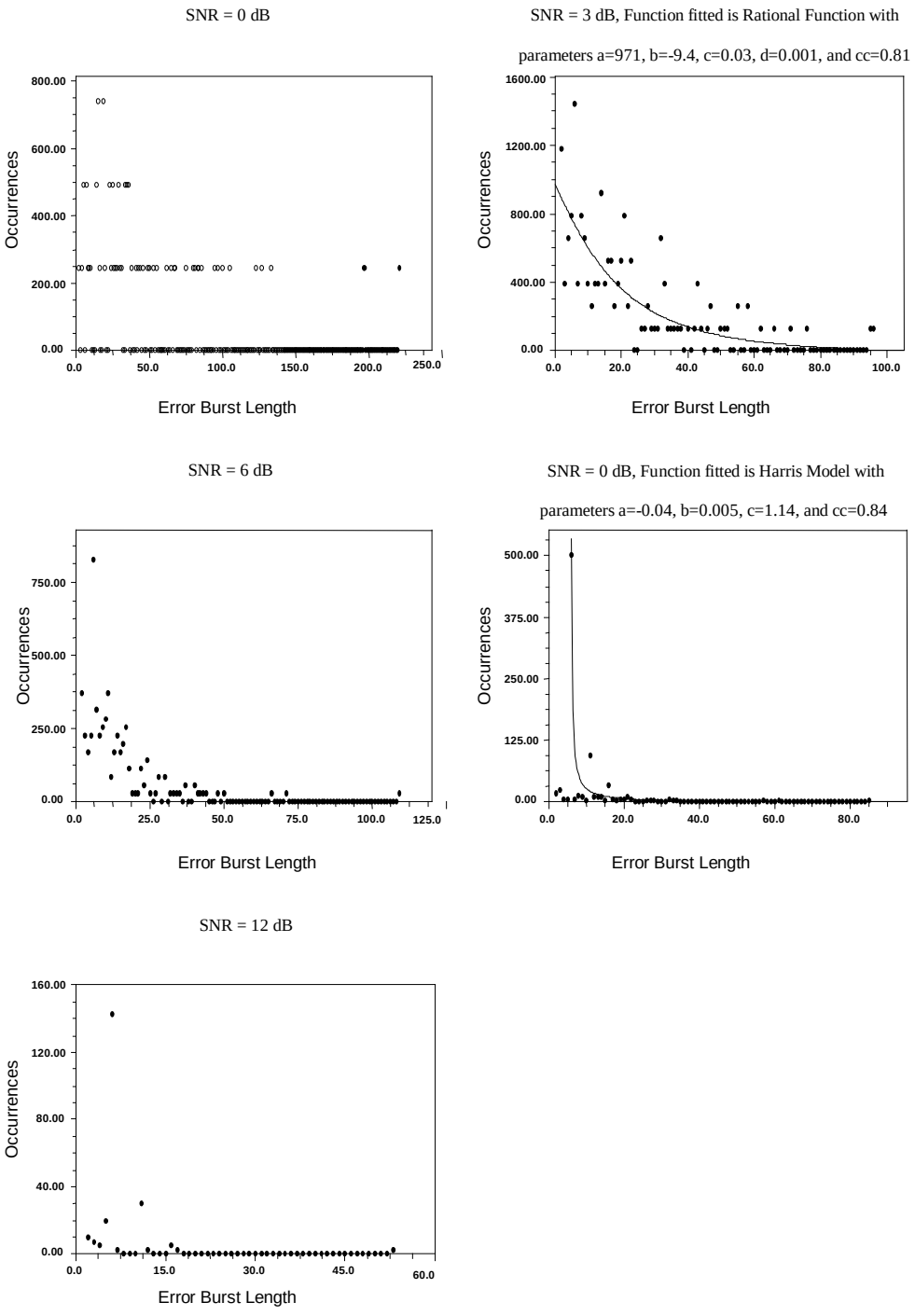

Figure 4.38: Error Burst Length Histogram for Nakagami1.33 channel, interleaver size = 512, and Tx = 3, Rx = 3

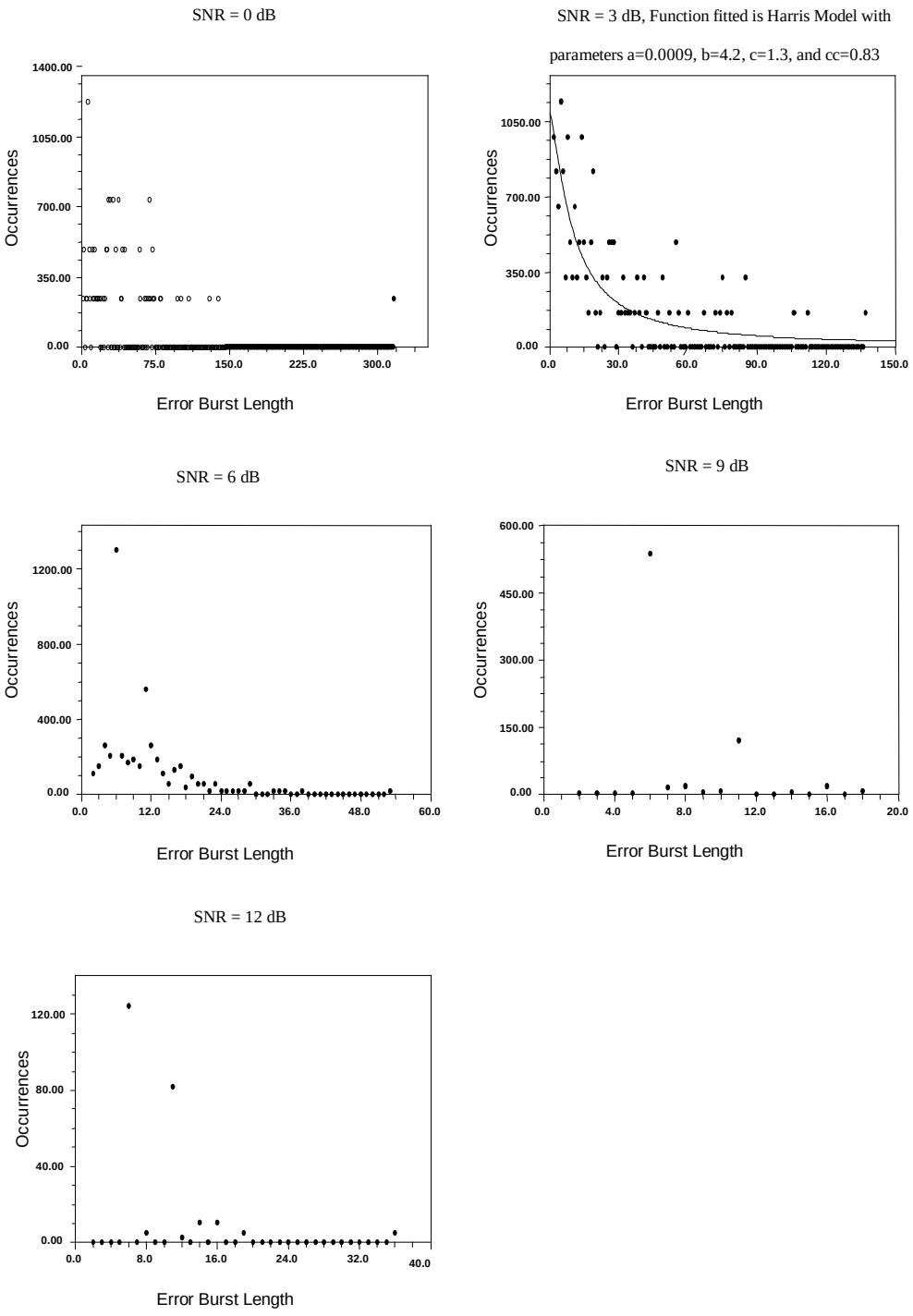

Figure 4.39: Error Burst Length Histogram for Nakagami1.33 channel, interleaver size = 1024, and Tx = 3, Rx = 3

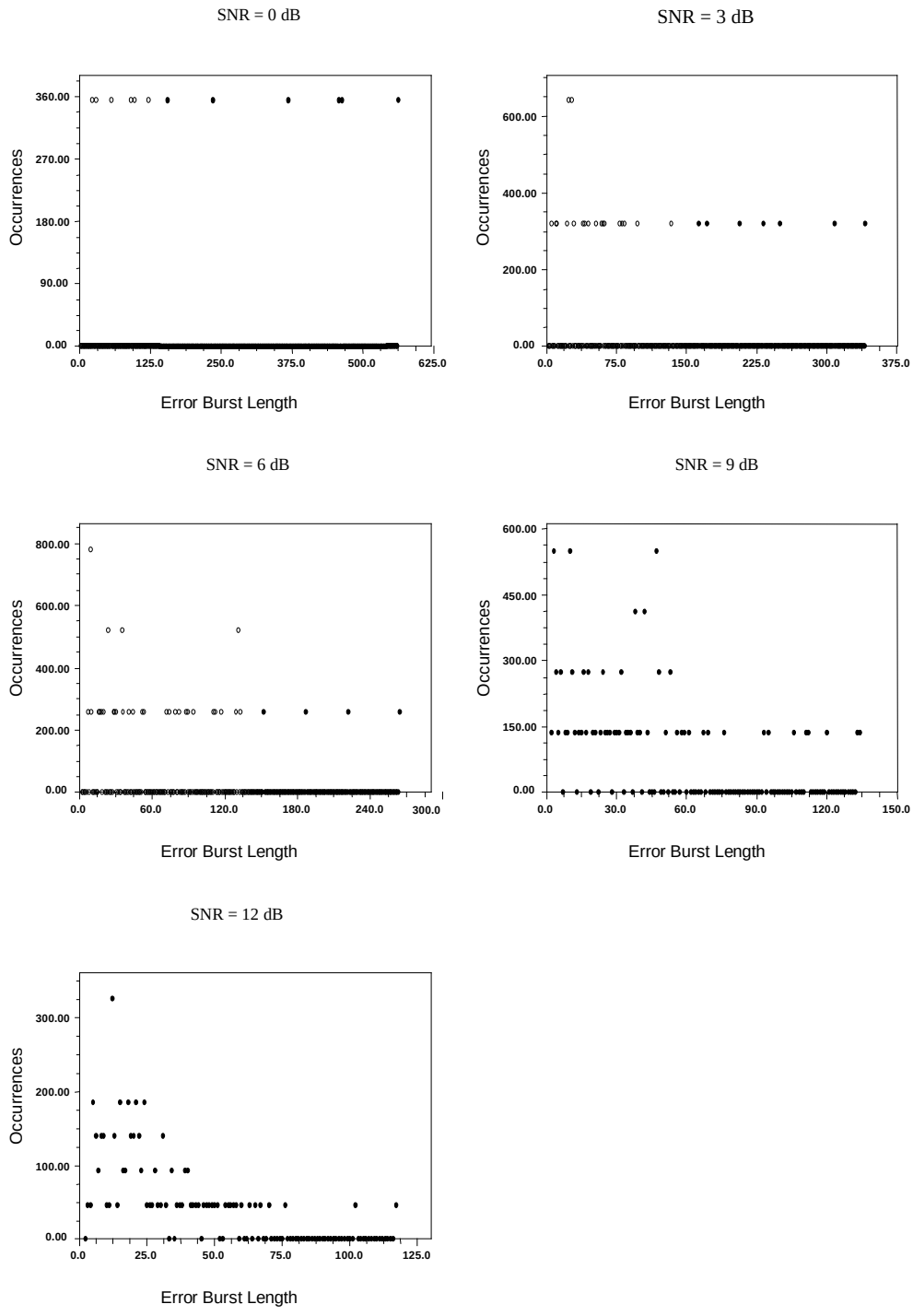

Figure 4.40: Error Burst Length Histogram for Nakagami2.77 channel, interleaver size = 64, and Tx = 3, Rx = 3

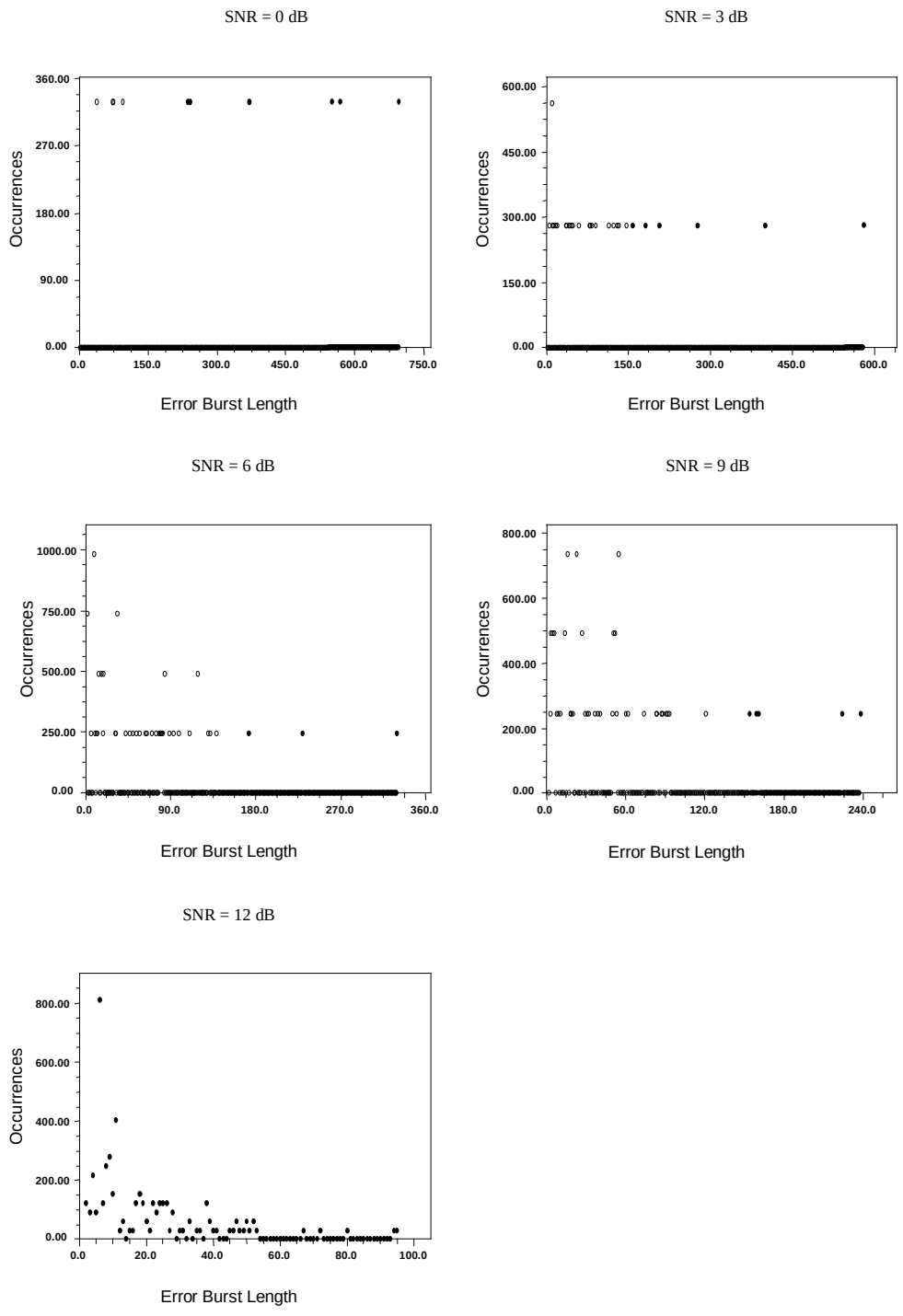

Figure 4.41: Error Burst Length Histogram for Nakagami2.77 channel, interleaver size = 512, and Tx = 3, Rx = 3

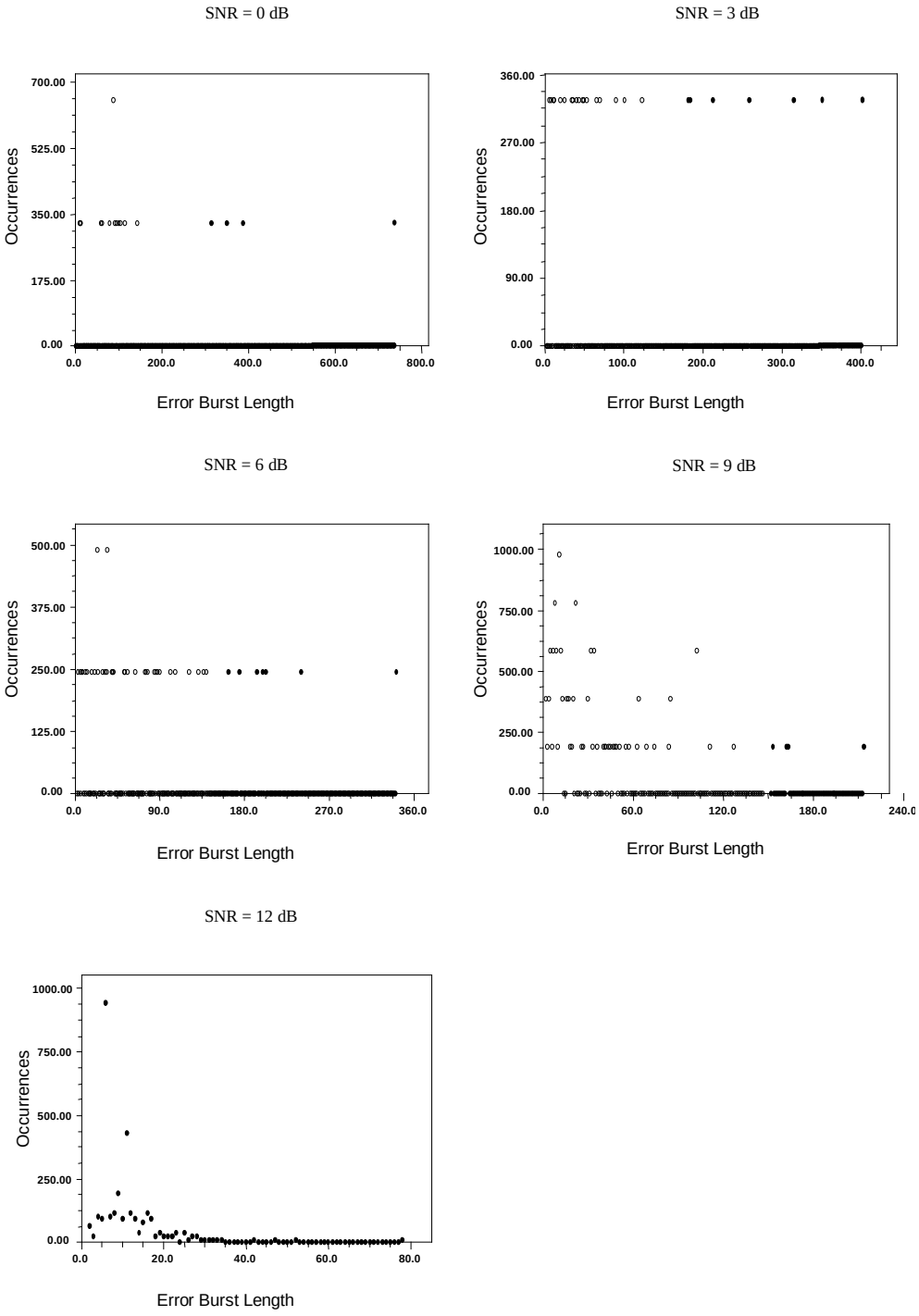

Figure 4.42: Error Burst Length Histogram for Nakagami2.77 channel, interleaver size = 1024, and Tx = 3, Rx = 3

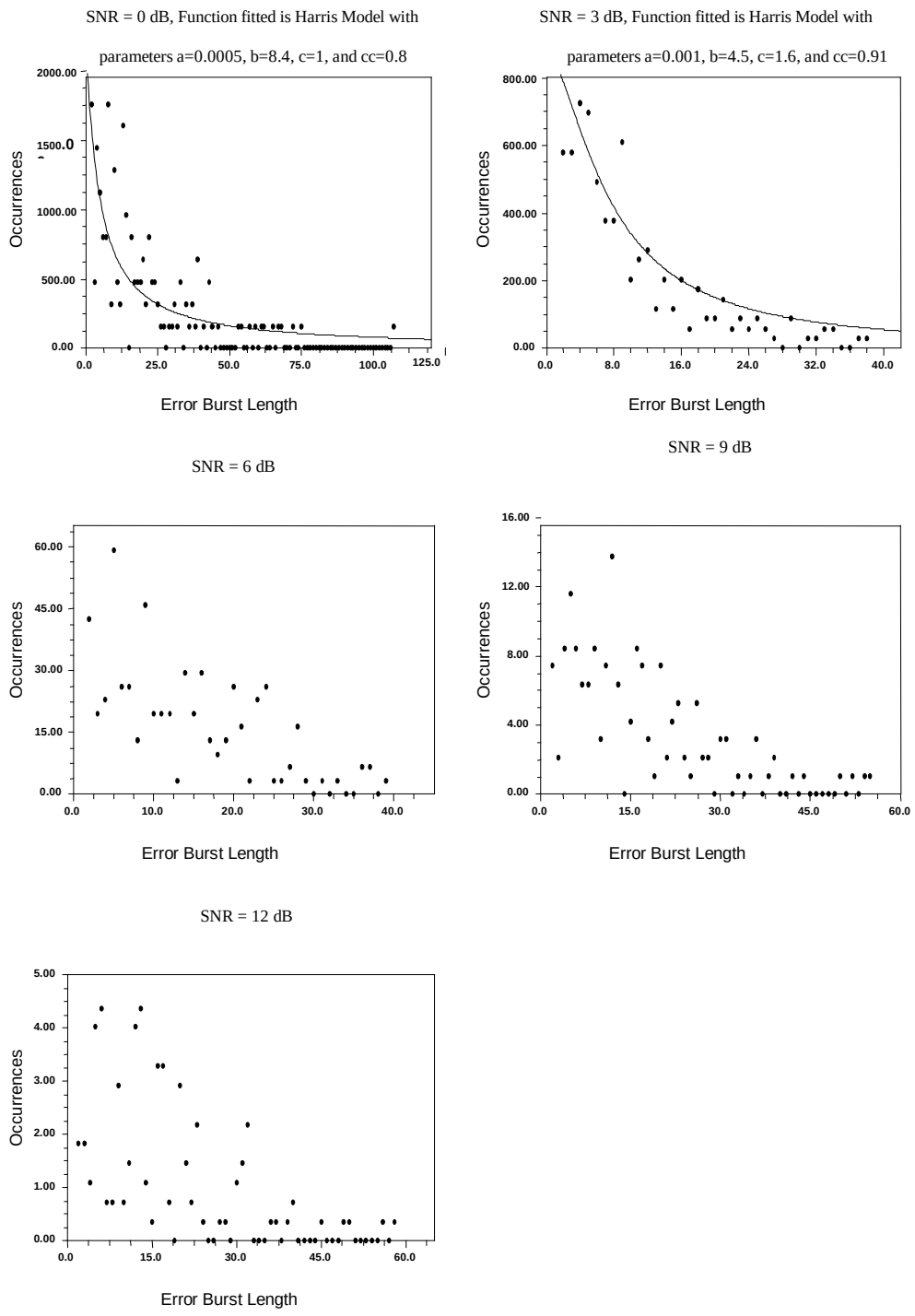

Figure 4.43: Error Burst Length Histogram for Rayleigh channel, interleaver size = 64, and Tx = 6, Rx = 6

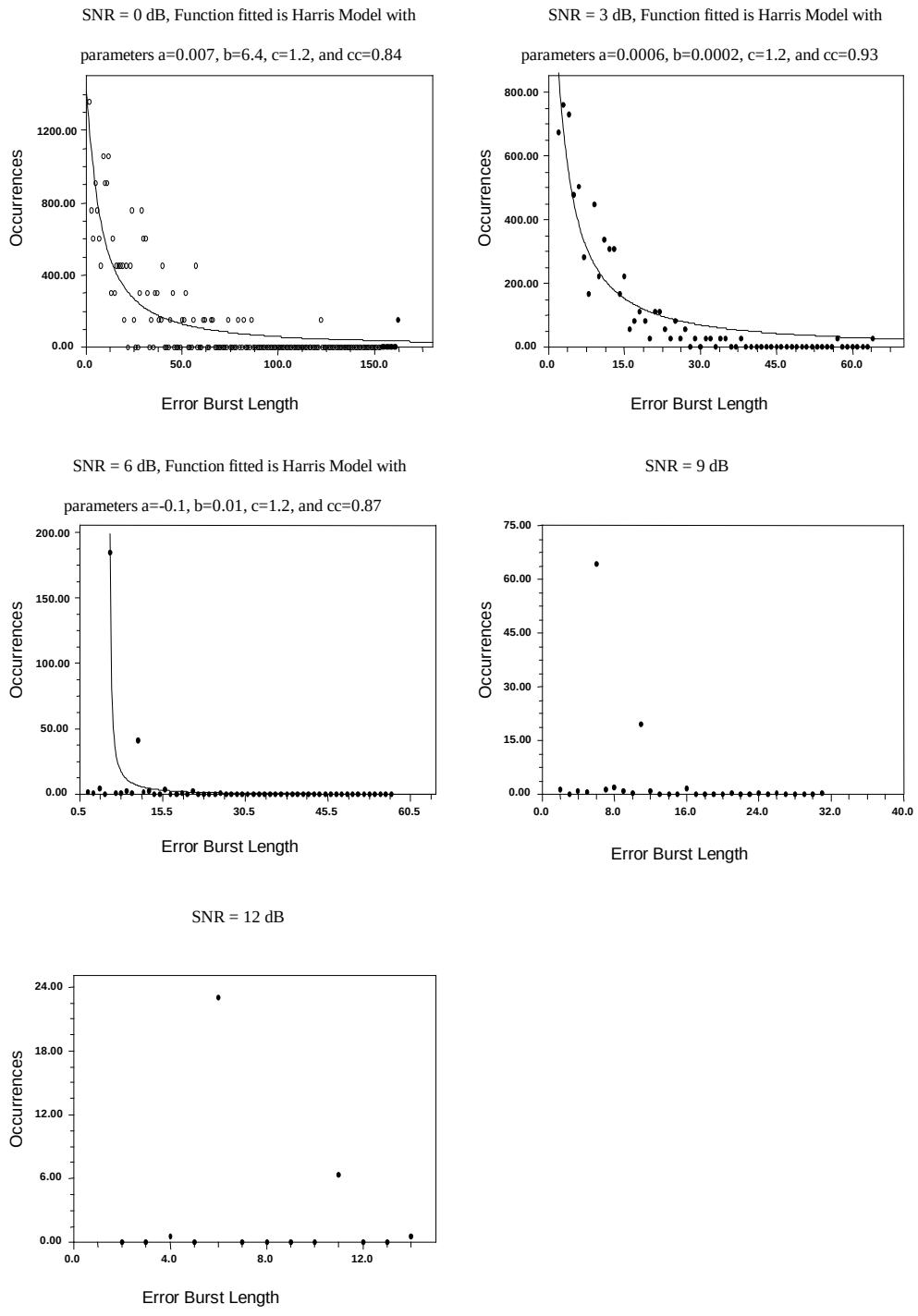

Figure 4.44: Error Burst Length Histogram for Rayleigh channel, interleaver size = 512, and Tx = 6, Rx = 6

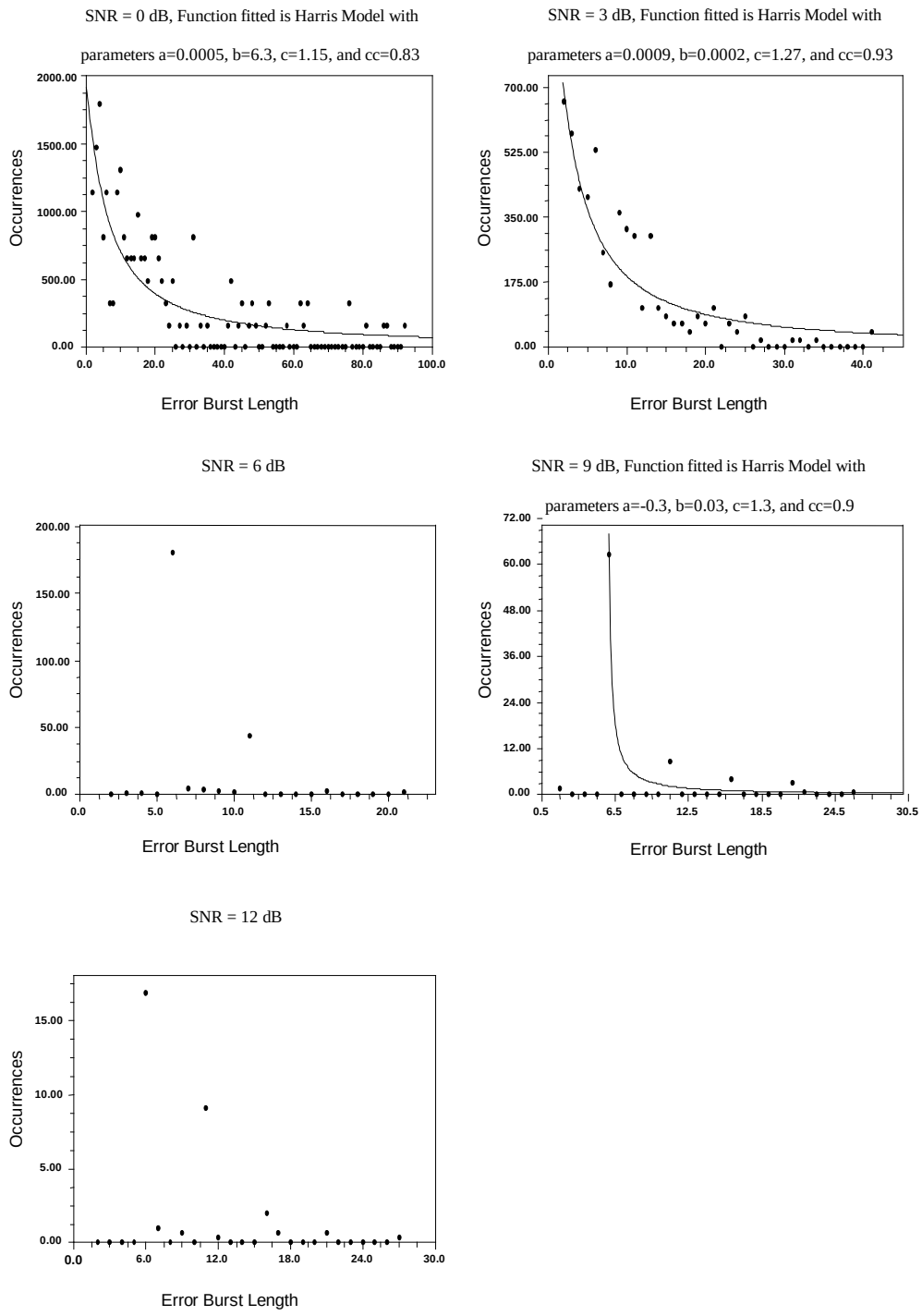

Figure 4.45: Error Burst Length Histogram for Rayleigh channel, interleaver size = 1024, and Tx = 6, Rx = 6

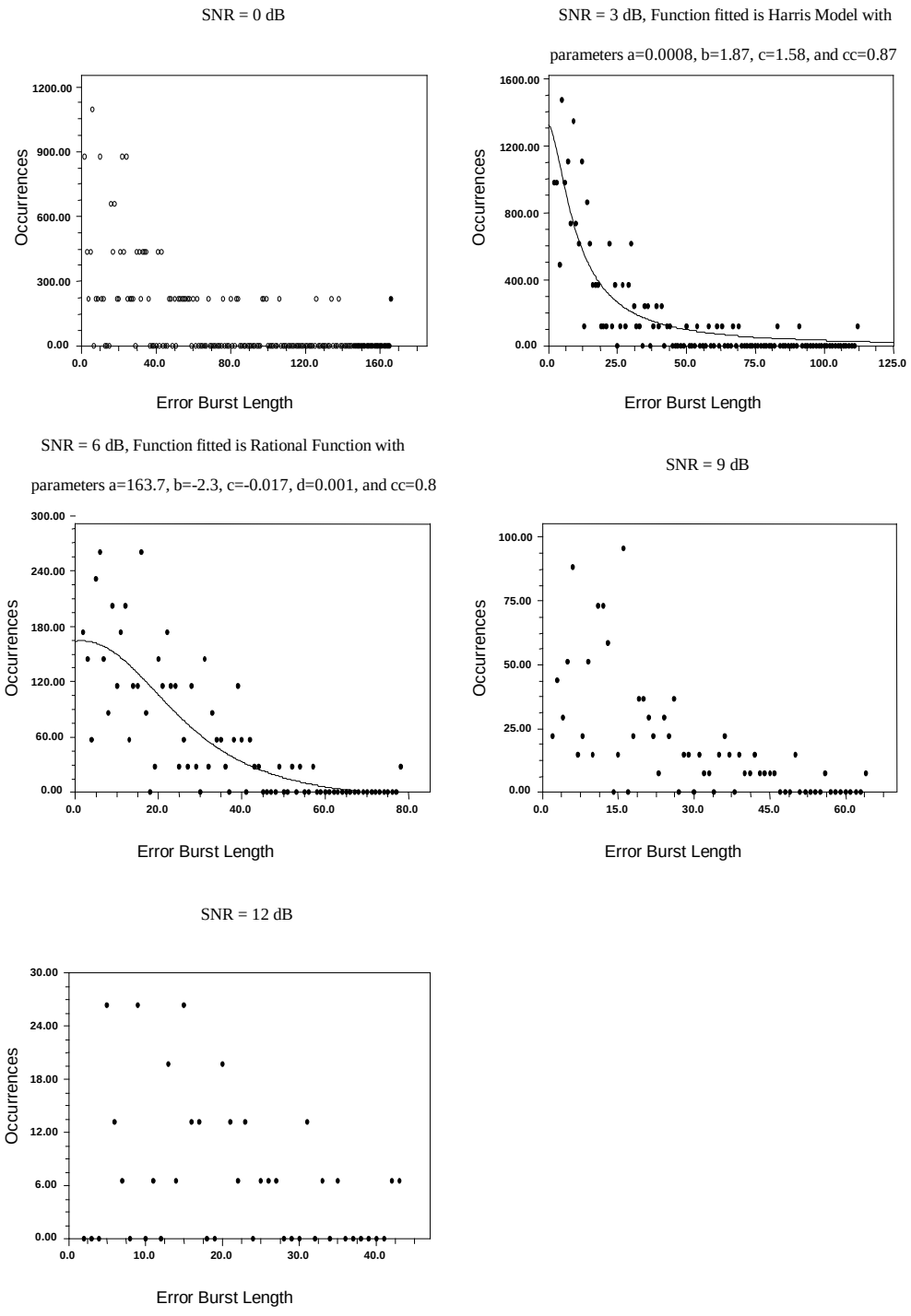

Figure 4.46: Error Burst Length Histogram for Nakagami1.33 channel, interleaver size = 64, and Tx = 6, Rx = 6

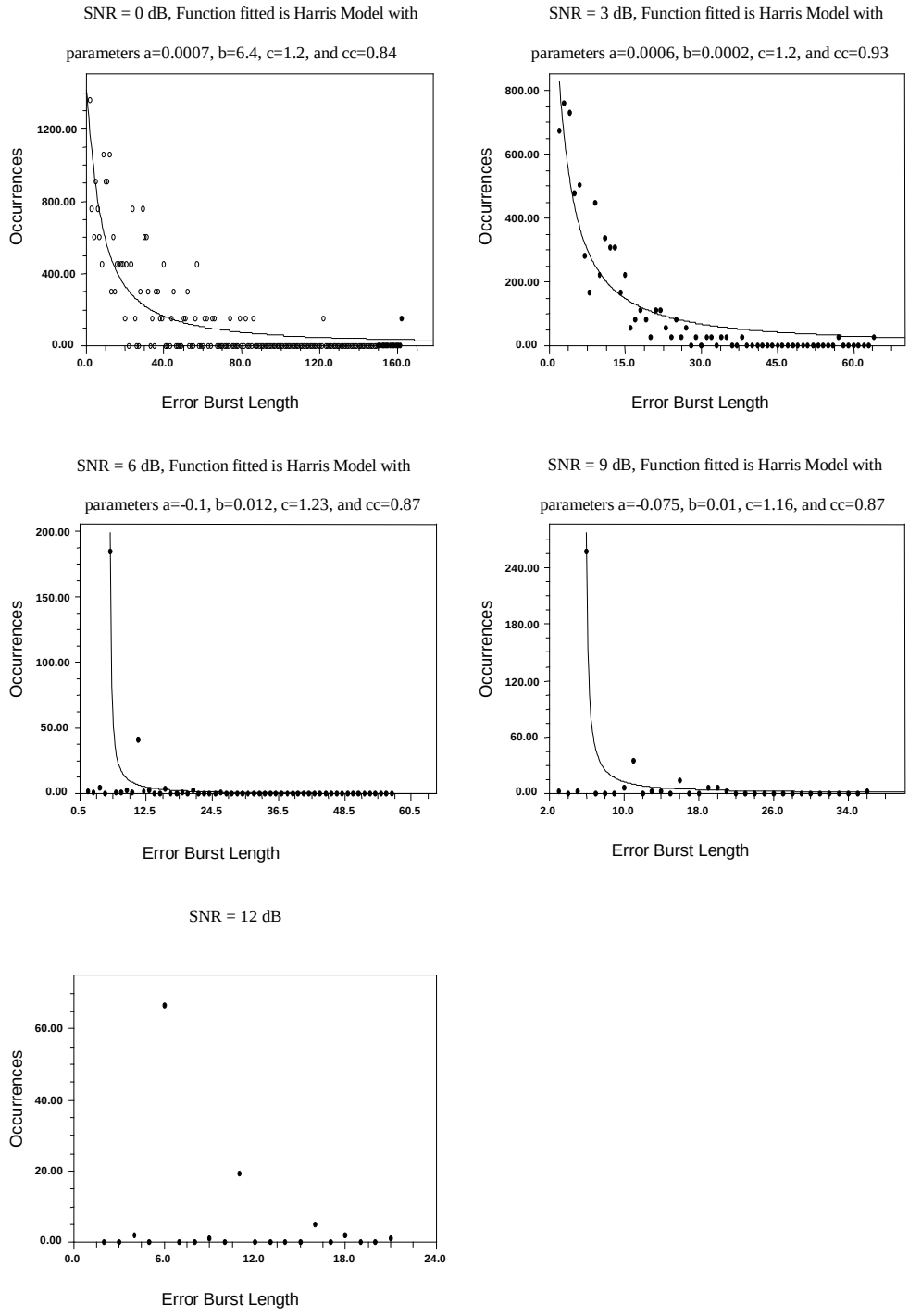

Figure 4.47: Error Burst Length Histogram for Nakagami1.33 channel, interleaver size = 512, and Tx = 6, Rx = 6

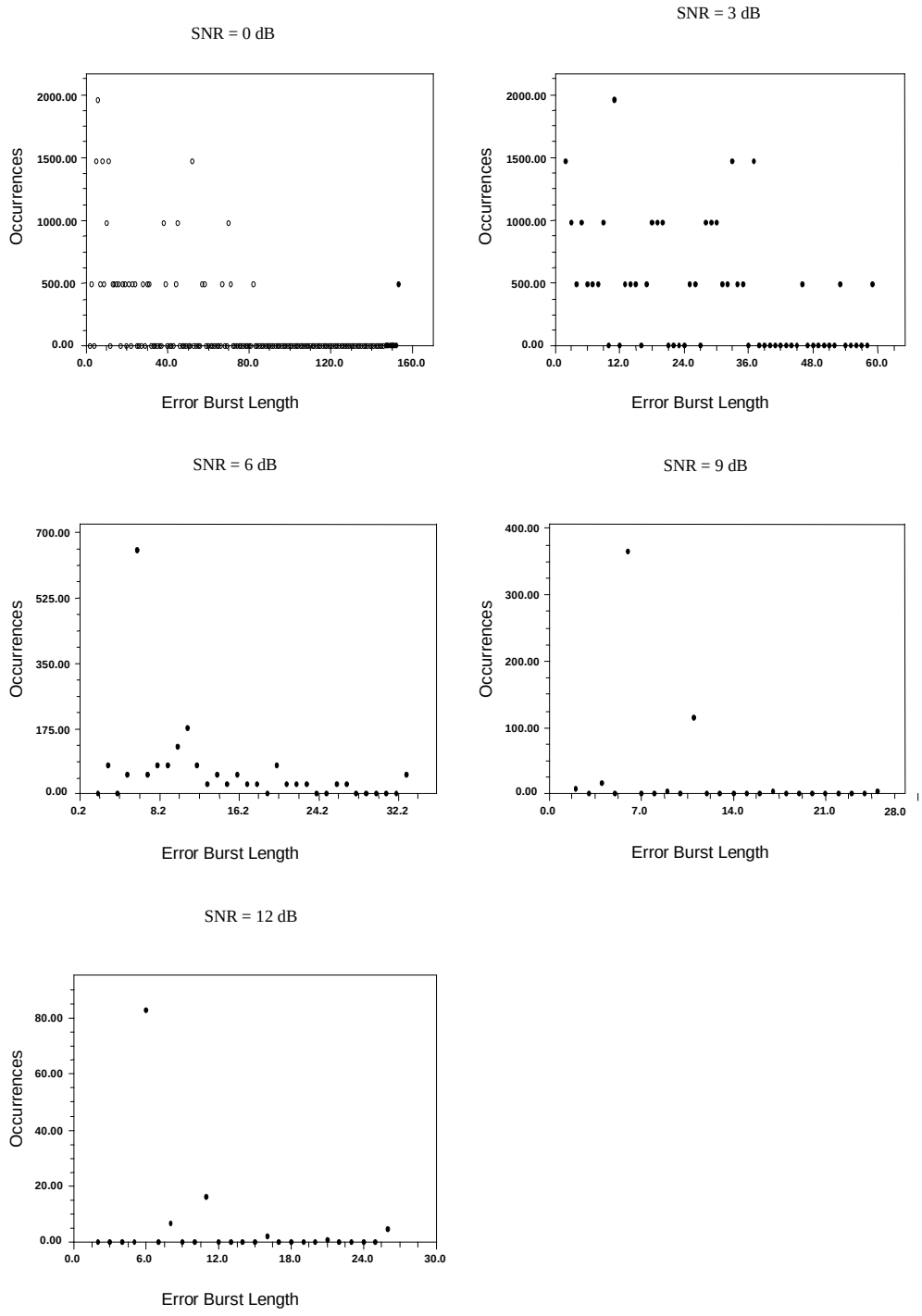

Figure 4.48: Error Burst Length Histogram for Nakagami1.33 channel, interleaver size = 1024, and Tx = 6, Rx = 6

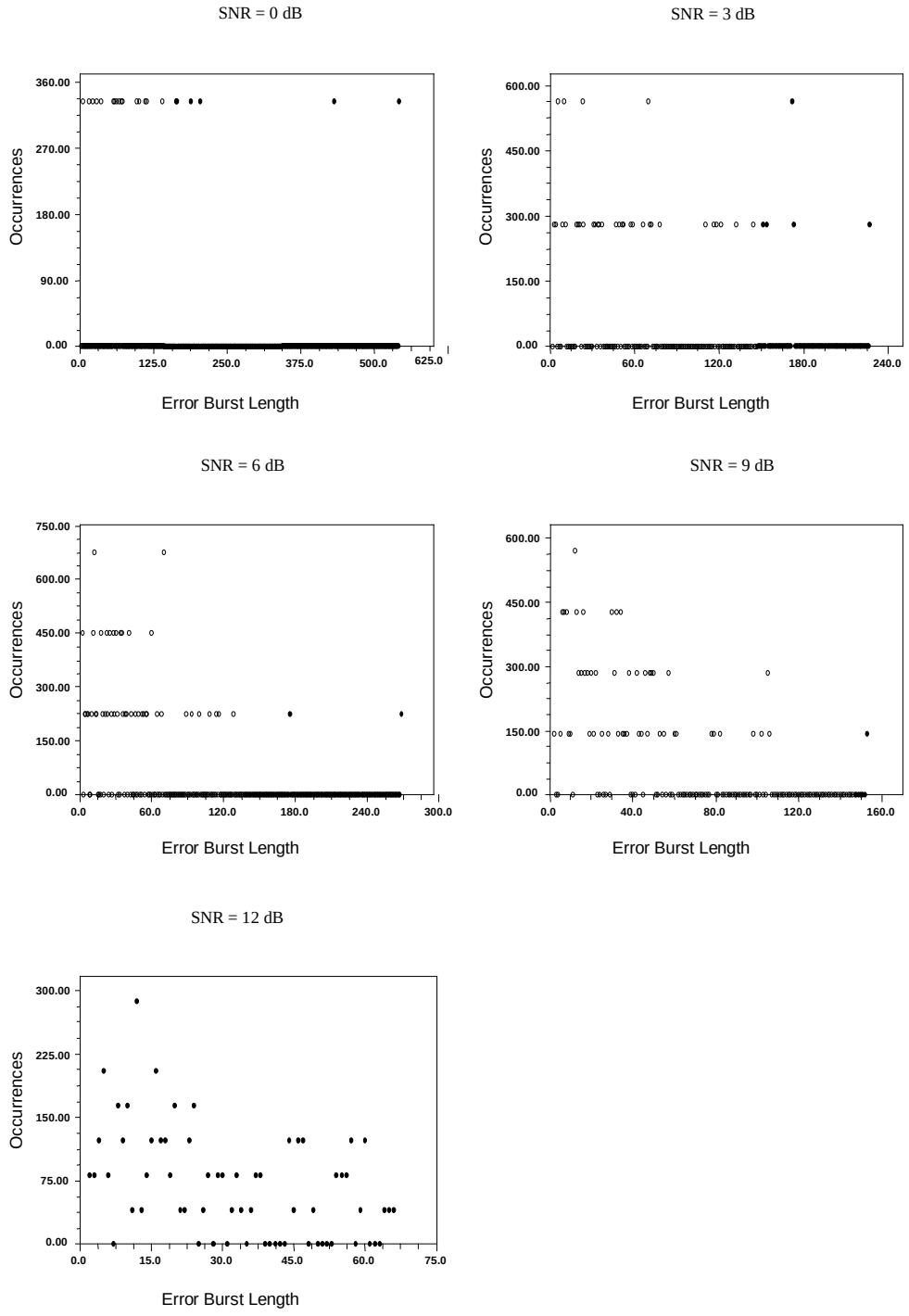

Figure 4.49: Error Burst Length Histogram for Nakagami2.77 channel, interleaver size = 64, and Tx = 6, Rx = 6

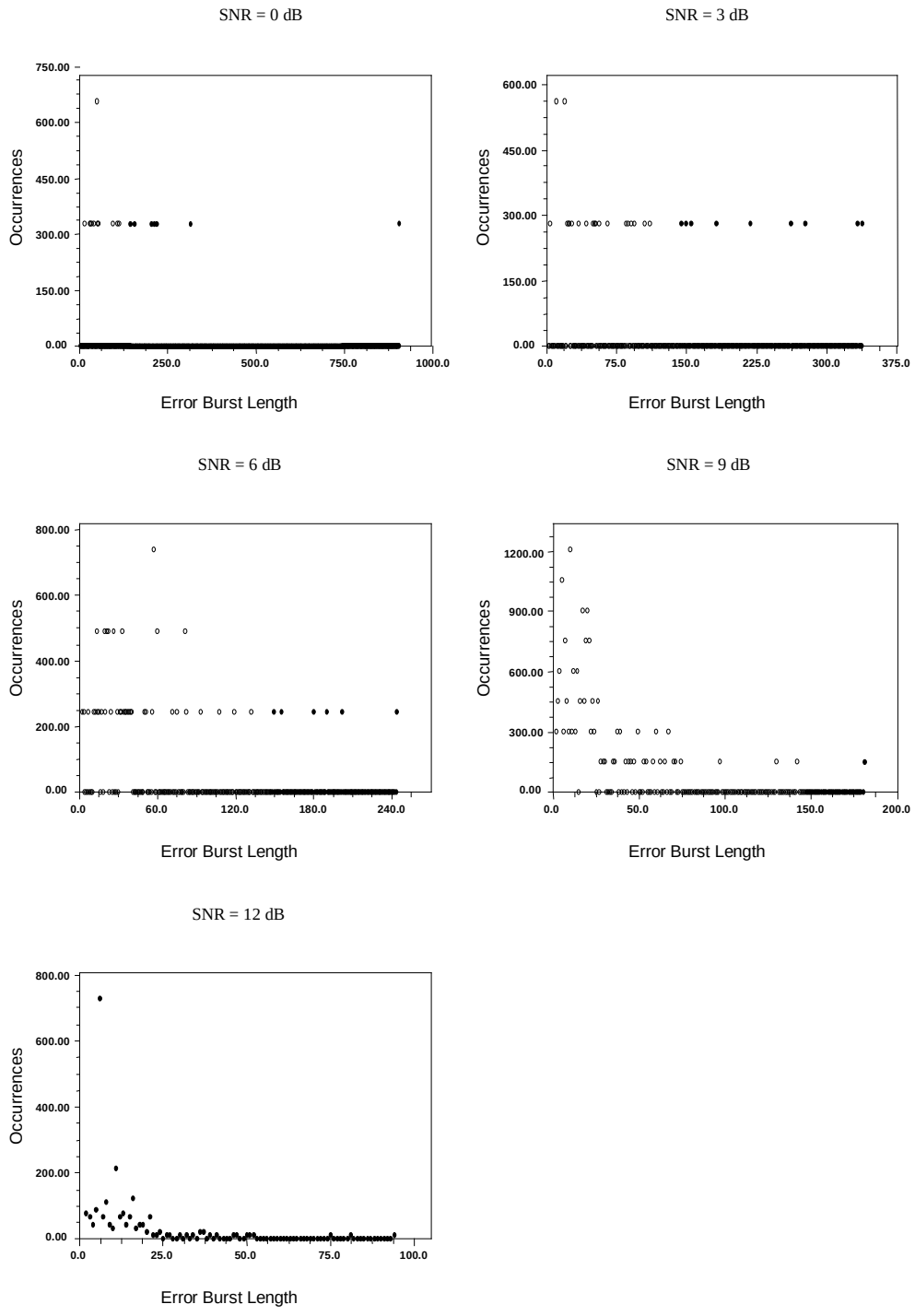

Figure 4.50: Error Burst Length Histogram for Nakagami2.77 channel, interleaver size = 512, and Tx = 6, Rx = 6

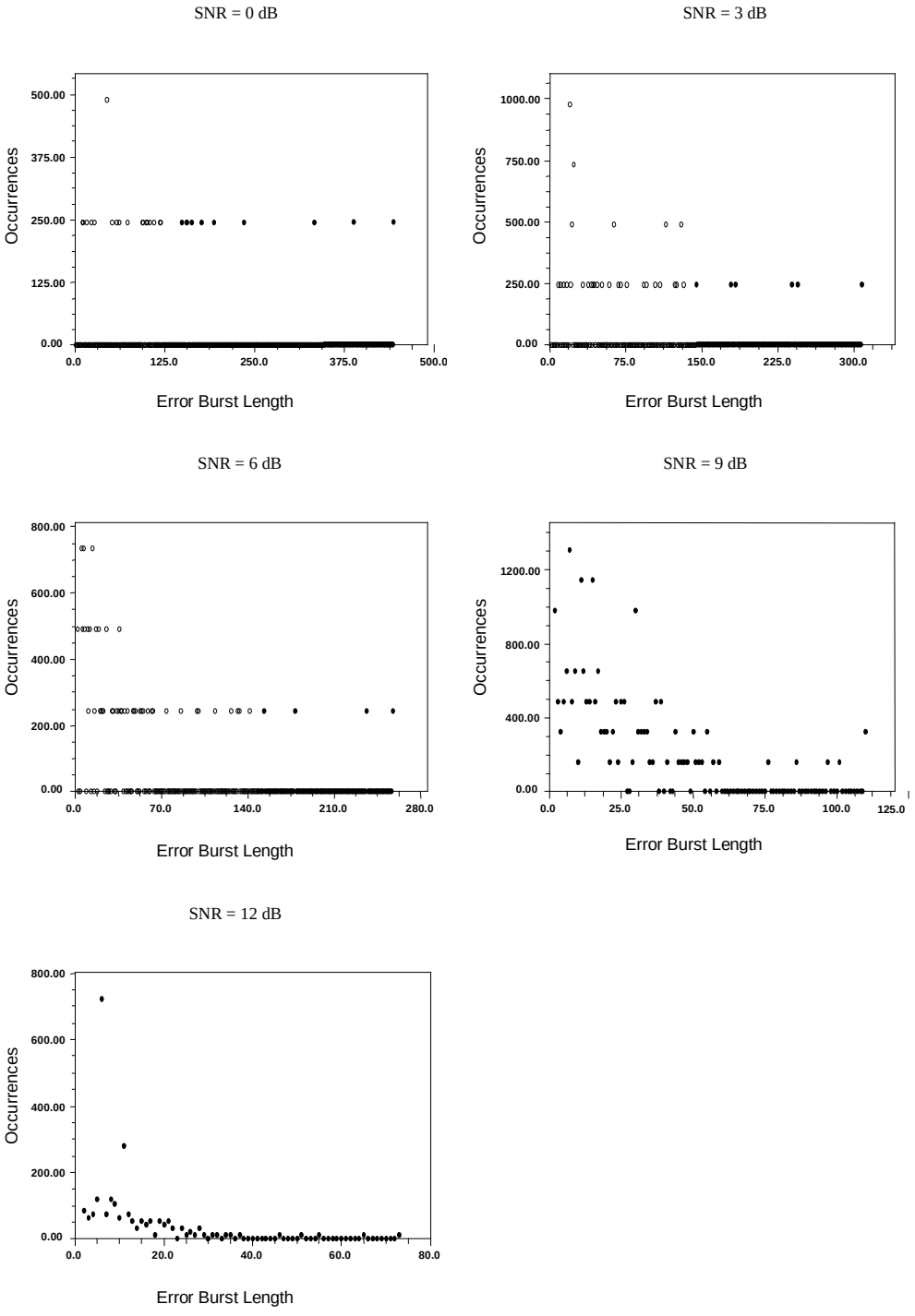

Figure 4.51: Error Burst Length Histogram for Nakagami2.77 channel, interleaver size = 1024, and Tx = 6, Rx = 6

Tables: 4.8, to 4.13 shows error burst length occurrences (EBLOs) when burst length (BL) is in between 2 and 10, 11 and 20, and greater than 20 for Rayleigh, Nakagami 1.33, and Nakagami 2.77 channels, while the interleaver sizes (IS) are 64, 512, 1024. Fields of the tables represent the number of occurrences of error burst lengths (EBLs) in the range specified.

Tables: 4.8 to 4.13 clearly shows that Rayleigh channel has the least number of longer error bursts while Nakagami2.77 has the most. Error burst length occurrence frequency reduces as signal to noise ratio increases. Increase in interleaver depth improves the performance of turbo coding [44] by decorrelating large burst of errors and reduced the effects of memory in the channel. Comparing Tables: 4.8 to 4.13 with the Tables: 4.2 to 4.7, having EBLO without coding, the EBLOs are reduced with coding.

V-BLAST exploits the random nature of radio propagation by finding independent (or at least highly uncorrelated) signal paths for communication. If one radio path undergoes a deep fade, another independent path may have a strong signal. By having more paths, both the instantaneous and average SNRs, at the receiver may be improved. This phenomenon resulted in higher rate of decrease of EBLOs (for IS=64, 512, 1024, and Rayleigh, Nakagami1.33 channels) *w.r.t.* SNR in the setup (6× 6) than in the setup (3×3) as shown in Tables: 4.8 to 4.13. Setup (6×6) utilizes 6 channel paths for each substream while (3×3) utilizes only 3 channel paths. For example, in Rayleigh (3,3) BLOs are reduced from 5229, 4575, and 9641 to 84, 14,

Table 4.8: EBLOs for 2<BL≤10 , Tx = 3 Rx = 3, with Turbo Coding, error process length = 10^6

SNR in dB	Error Burst Length Occurrences								
	Rayleigh			Nakagami 1.33			Nakagami 2.77		
	IS=64	IS=512	IS=1024	IS=64	IS=512	IS=1024	IS=64	IS=512	IS=1024
0	7530	6800	5229	5869	2215	3186	0	0	327
3	2245	1922	2374	4131	6693	6536	641	844	654
6	881	481	455	2280	2910	2753	1302	2215	980
9	230	299	190	518	591	609	2204	2215	3922
12	107	98	84	382	189	129	838	2156	1739

Table 4.9: EBLOs for 10 <BL≤ 20 , Tx = 3 Rx = 3, with Turbo Coding, error process length = 10^6

SNR in dB	Error Burst Length Occurrences								
	Rayleigh			Nakagami 1.33			Nakagami 2.77		
	IS=64	IS=512	IS=1024	IS=64	IS=512	IS=1024	IS=64	IS=512	IS=1024
0	5245	5547	4575	2582	2461	2696	0	0	654
3	1638	1277	1084	2992	4593	4902	321	844	980
6	824	142	150	1032	1655	1659	1042	2215	735
9	204	149	83	625	185	158	1515	2215	3529
12	89	40	14	173	40	111	1397	1030	1059

Table 4.10: EBLOs for BL> 20 , $Tx = 3Rx = 3$, with Turbo Coding, error process length = 10^6

SNR in dB	Error Burst Length Occurrences								
	Rayleigh			Nakagami 1.33			Nakagami 2.77		
	IS=64	IS=512	IS=1024	IS=64	IS=512	IS=1024	IS=64	IS=512	IS=1024
0	9053	9843	9641	10563	11319	11765	4255	3280	4902
3	2185	323	533	7407	7087	801	8013	6468	6536
6	910	26	11	3149	1056	377	7813	8120	8824
9	307	57	21	671	46	0	6612	8858	8628
12	68	11	4	225	3	5	2607	1719	327

Table 4.11: EBLOs for 2<BL≤10 , Tx = 6 Rx = 6,with Turbo Coding, error process length = 10^6

SNR in dB	Error Burst Length Occurrences								
	Rayleigh			Nakagami 1.33			Nakagami 2.77		
	IS=64	IS=512	IS=1024	IS=64	IS=512	IS=1024	IS=64	IS=512	IS=1024
0	9776	7420	9477	4386	7420	7353	333	0	245
3	4646	4275	3708	8824	4275	6373	1977	844	245
6	276	202	197	1420	202	1103	1577	738	431
9	62	73	64	338	271	396	1852	5451	5556
12	18	23	18	73	70	90	1026	1271	1433

Table 4.12: EBLOs for 10 <BL≤ 20 , Tx = 6 Rx = 6, with Turbo Coding, error process length = 10^6

SNR in dB	Error Burst Length Occurrences								
	Rayleigh			Nakagami 1.33			Nakagami 2.77		
	IS=64	IS=512	IS=1024	IS=64	IS=512	IS=1024	IS=64	IS=512	IS=1024
0	6250	5148	7190	2632	5148	4412	333	328	490
3	1597	1715	1215	4657	1715	6863	847	562	1716
6	184	52	48	1188	52	528	2252	2461	2941
9	59	23	13	411	70	120	2992	5300	6046
12	22	7	7	103	27	18	1273	742	700

Table 4.13: EBLOs for BL> 20 , Tx = 6 Rx = 6,with Turbo Coding, error process length = 10^6

SNR in dB	Error Burst Length Occurrences								
	Rayleigh			Nakagami 1.33			Nakagami 2.77		
	IS=64	IS=512	IS=1024	IS=64	IS=512	IS=1024	IS=64	IS=512	IS=1024
0	8494	9085	7843	12500	9085	11275	6667	5906	6373
3	820	703	426	6005	703	10294	9322	7312	8824
6	125	5	2	1681	5	176	10135	10335	9069
9	46	2	5	360	7	4	7123	6966	9477
12	14	0	1	92	1	6	2135	326	312

and 4 respectively. While in Rayleigh (6,6) these are reduced from 9447, 7190, and 7843 to 18, 7, and 1.

Nakagami2.77 channel needs more attention to be explained for the phenomenon of why occurrences of error burst lengths are increasing with increase in signal power. Table: 4.14, shows average error burst length decreases with SNR. While total number of error bursts increases up to 9 dB then decreases with SNR. This indicate that increase in signal power increases the correct detection of symbols which also improve correcting power of the code. In turn long error bursts are transformed into small error bursts i.e. some of errors in long bursts are corrected and transform the long bursts into more shorter bursts. For example, if some errors that lies in a long burst of errors are detected correctly or corrected by the code can make error free interval greater than error free threshold. It results larger number of error bursts but shorter in length. Comparing this table with Table: 4.1, without applying turbo coding, average error burst length are more but less in numbers. For example, at 12 dB, average error burst lengths are 28, 19, 11 for (3×3) and interleaver sizes 64, 512, 1024 while this was 9 for the without coding case. This means that error burst lengths are of longer length. Another observation can be seen that the occurrences of error bursts are lesser when turbo coding is applied. For example, at 12 dB, occurrences of error burst lengths are 4842, 4906, 3125 for (3×3) and interleaver sizes 64, 512, 1024 while this was 9384 for the without coding case. Reduction in the occurrence and increment in average error burst length is due to correction of

shorter error bursts by coding which resulted in lesser but longer error bursts than the without coding case. Coding give a legitimate code word for a block of input symbols. If number of errors are more than the correcting capability of a coding scheme then it may produce more errors. In Nakagami2.77 channels, errors are in clusters therefore coding is unable to correct burst errors. This phenomenon of error increment in Nakagami2.77 is a serious impediment to good over all performance of V-BLAST system.

The average error burst length (EBL) for interleaver depths 64, 512, 1024, shown in Figs. 4.52, 4.53, and 4.54, decreases exponentially with increase in signal to noise ratio. Average error burst lengths increased with the increase in m. Average EBLs are the smallest for least m (i.e. Rayleigh channel) while the highest for the biggest m due to the effects of correlation in channel paths that severely degrades the V-BLAST performance. Higher utilization of space diversity in the arrangement (6×6) improved the average EBLs over the arrangement (3×3). For any type of channel, (6×6) gave less average EBLs than (3×3). Average error burst length reduced with increased interleaver depth. This effect is prominent for Nakagami2.77 channels. Comparing Figs: 4.52, 4.53, and 4.54 with the case of without coding shown in Fig. 4.13, the average EBL increased because of the correction of shorter error bursts. This increased the average EBL for the cases of coding.

Table 4.14: Total error statistics of Nakagami2.77, with Turbo Coding, error process length = 10^6

Tx = 3, Rx = 3

SNR in dB	0	3	6	9	12
Total Error Bursts (IS=64)	4255	8975	10157	10391	4842
Average Error Burst Lengths (IS=64)	222	96	72	38	28
Total Error Bursts (IS=512)	3280	8156	12550	13288	4906
Average Error Burst Lengths (IS=512)	204	103	63	43	19
Total Error Bursts (IS=1024)	5883	8170	10539	16079	3125
Average Error Burst Lengths (IS=1024)	159	110	81	39	11

Tx = 6, Rx = 6

Total Error Bursts (IS=64)	7333	12146	13964	11967	4434
Average Error Burst Lengths (IS=64)	125	67	46	35	25
Total Error Bursts (IS=512)	6434	8718	13540	17717	2339
Average Error Burst Lengths (IS=512)	123	64	47	26	13
Total Error Bursts (IS=1024)	7108	10785	12441	21079	2445
Average Error Burst Lengths (IS=1024)	126	80	49	25	12

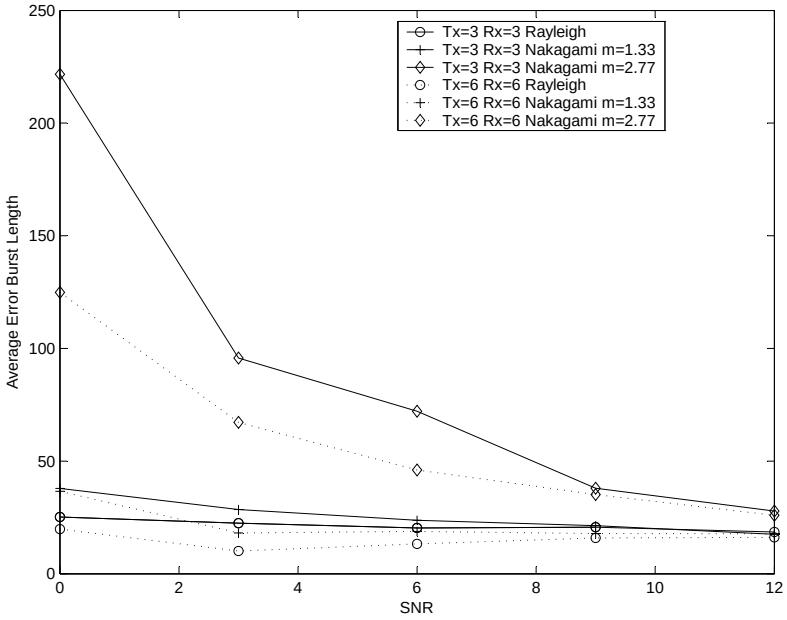

Figure 4.52: Average Error Burst Length for interleaver depth = 64

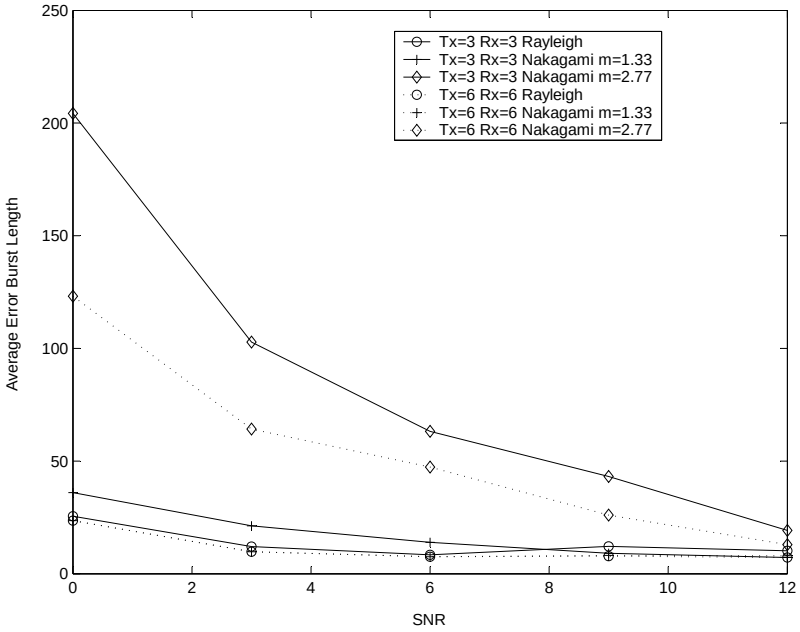

Figure 4.53: Average Error Burst Length for interleaver depth = 512

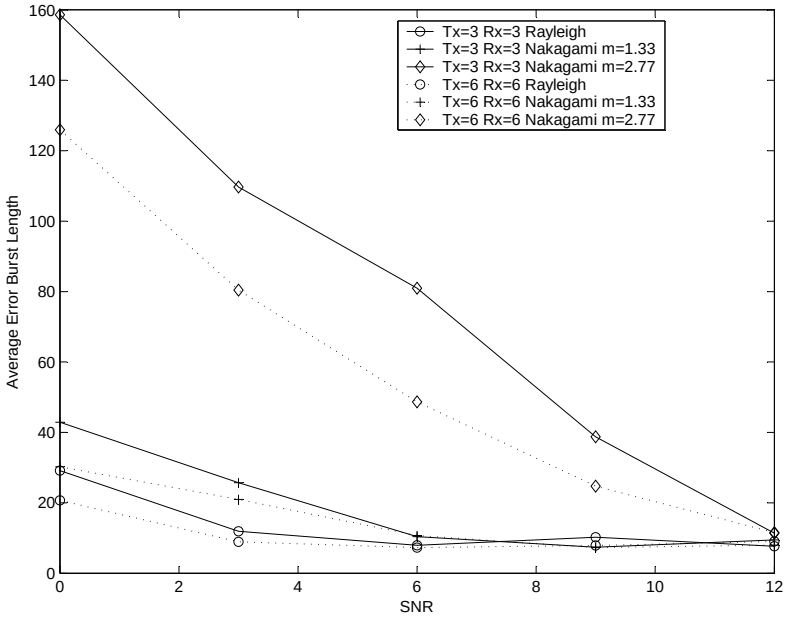

Figure 4.54: Average Error Burst Length for interleaver depth = 1024

4.5.2 Error Free Lengths

Error free length (EFL) distributions of V-BLAST system are shown in Figs. 4.55 to 4.72. Error process length is again taken to be 10^6. Simulations are performed over Rayleigh, Nakagami m = 1.33, Nakagami m = 2.77 channels. EFL distributions are shown after applying turbo coding. Modelling of distributions of error free lengths is performed. The criterion for a model to be selected is still correlation coefficient. Parameters of models and correlation coefficients are shown in figures. The best fit functions are Hyperbolic Fit and Harris Model. The most precise representative model for any error free length distribution is hyperbolic function.

Error free gaps are increased with increase in signal to noise ratio. The frequency of occurrences of error free lengths is reduced hyperbolically with increase in length of error free gaps. Interleaver is used to generate a long code from small memory convolutional codes and to decorrelate the inputs of the two decoders so that an iterative suboptimum decoding algorithm based on information exchange between the two component decoders can be applied [34]. Long interleavers scramble large block and that can decorrelate long error bursts. If the input sequences to the two component decoders are decorrelated there is a high probability that after correction of some of the errors in one decoder some of the remaining errors should become correctable in the second decoder. This gives longer error free intervals for longer interleaver depths. The performance is improved with increase in interleave size.

When adding more transmitter receiver elements to a system, the additional channels can be used to improve performance simply because of augmenting the degrees of freedom of the chi-squared variates appearing on the right hand side of Eq: 3.5. This improves the performance for the system which utilizes higher number of transmitters and receivers. Arrangement Tx = 6, Rx = 6 has longer error free gaps than arrangement Tx = 3, Rx = 3. For all three channels and for every SNR, error free length increases when Turbo Coding is applied. This can be seen when compared with the cases of without coding.

Occurrences of error free lengths decrease with increase in m(correlation) in channel paths. Rayleigh channel results in longer error free intervals while Nakagami2.77 channel in the smallest. Although direct line-of-sight reduces fading but inherent system property of being severely degraded by correlation in channel paths and degraded the overall performance for higher m channels.

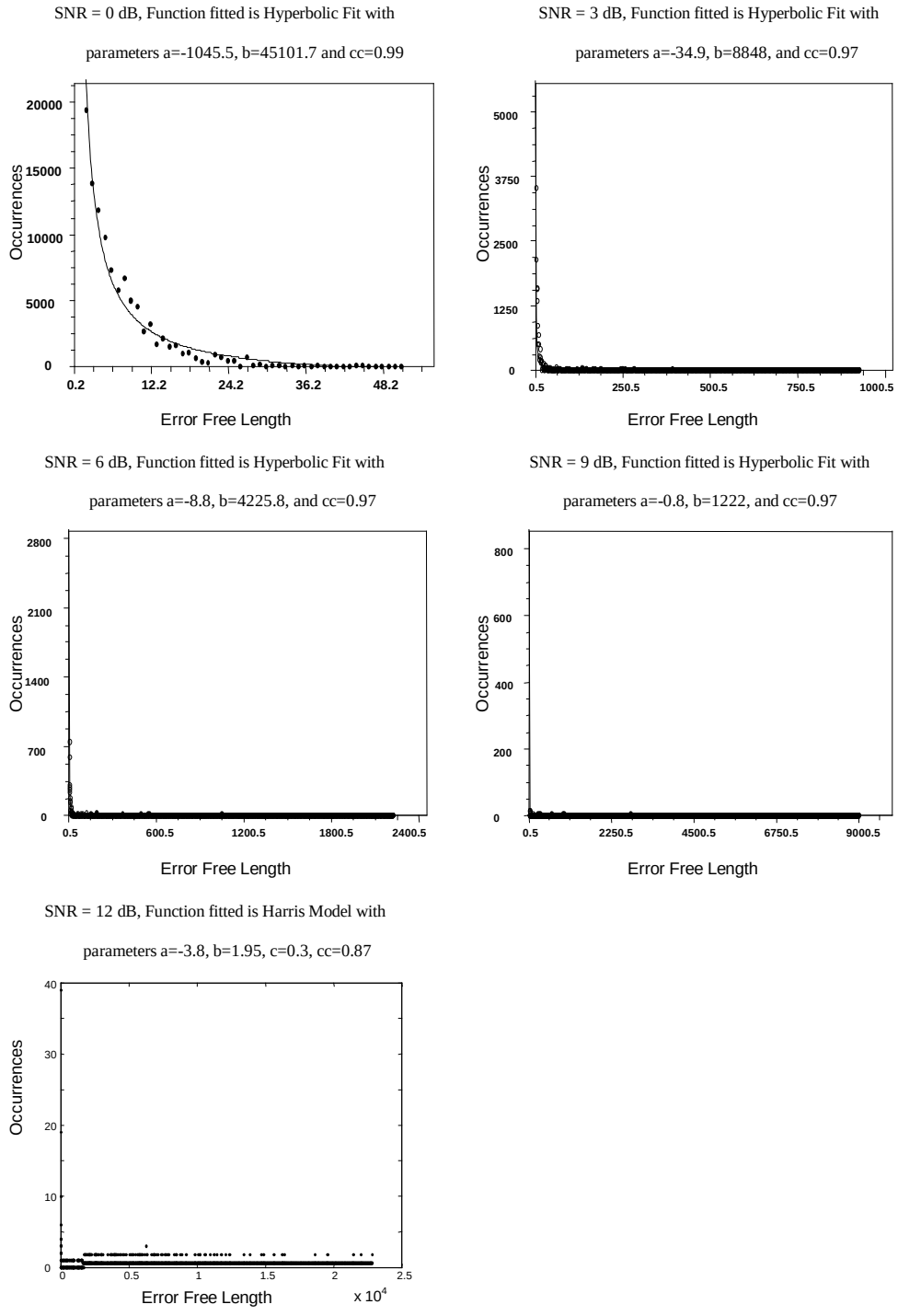

Figure 4.55: Error Free Length Histogram for Rayleigh channel, interleaver size = 64, and Tx = 3, Rx = 3

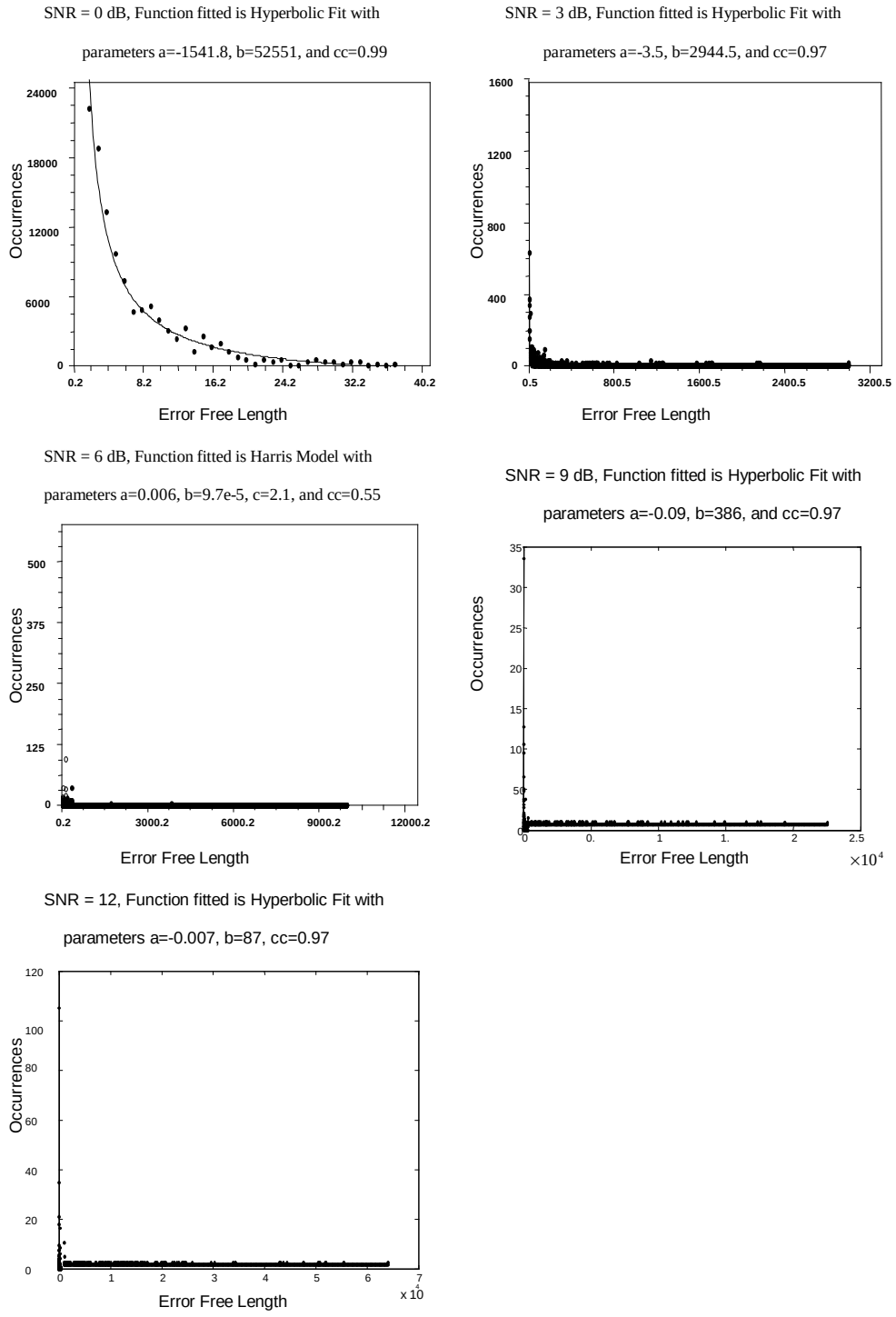

Figure 4.56: Error Free Length Histogram for Rayleigh channel, interleaver size = 512, and Tx = 3, Rx = 3

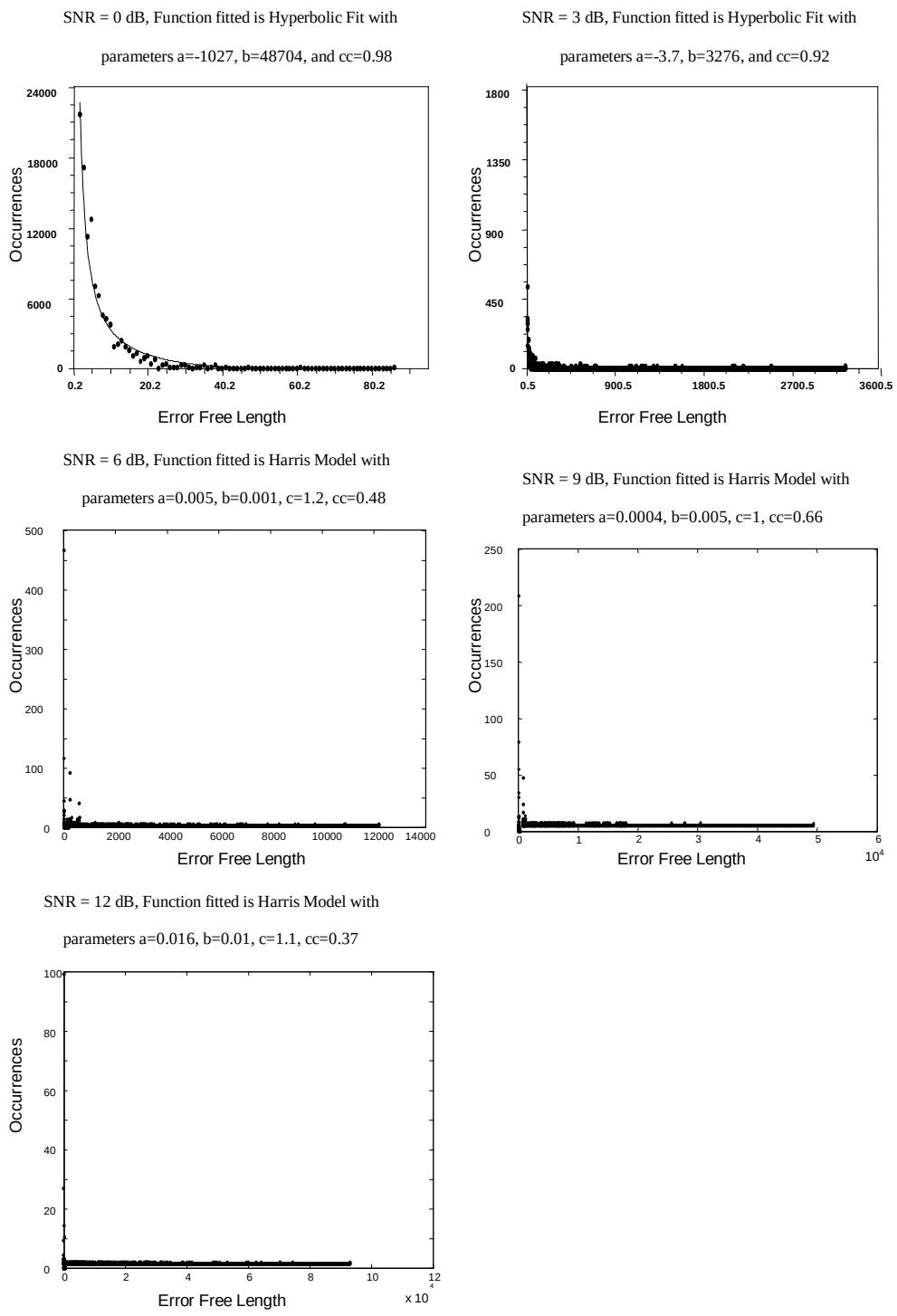

Figure 4.57: Error Free Length Histogram for Rayleigh channel, interleaver size = 1024, and Tx = 3, Rx = 3

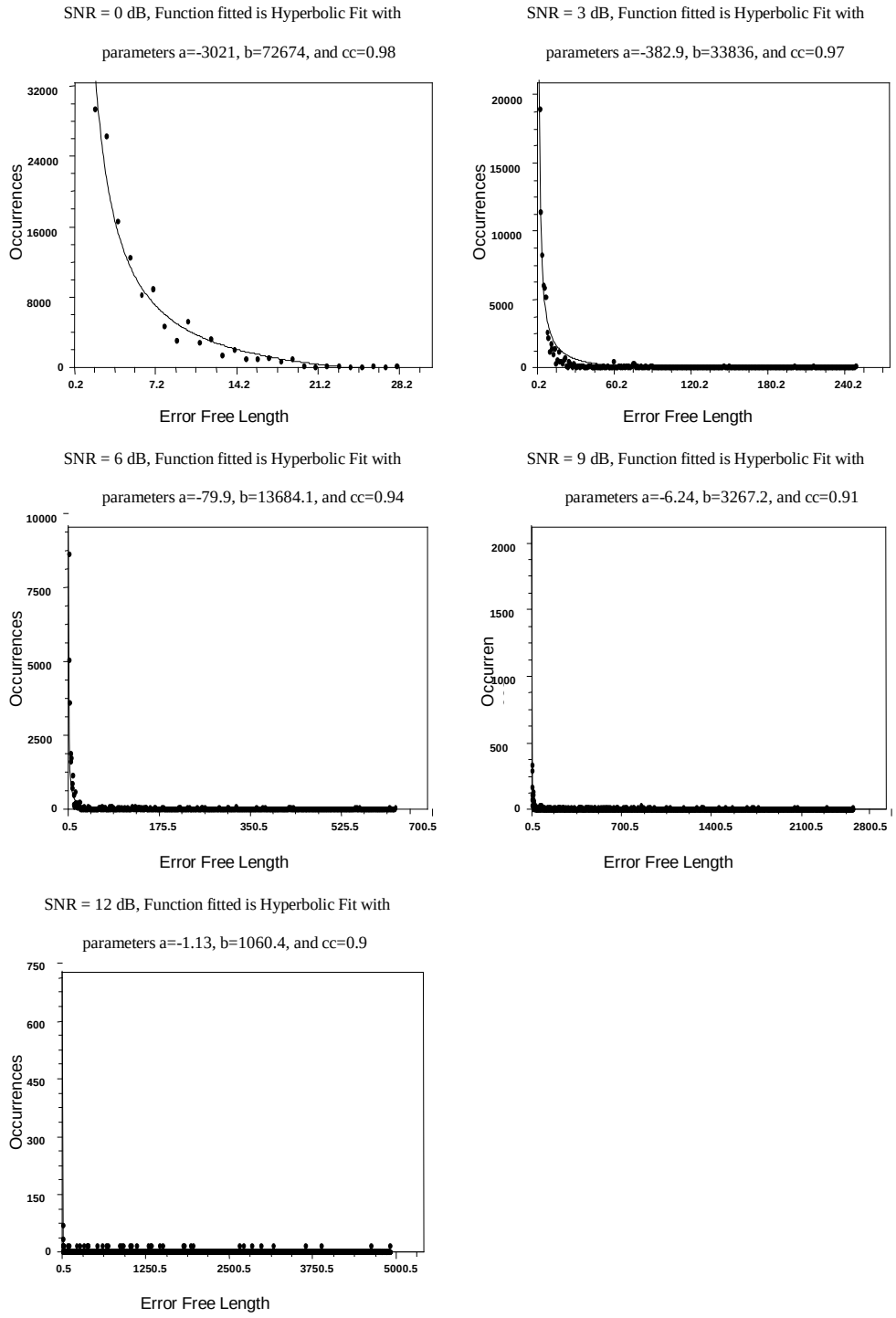

Figure 4.58: Error Free Length Histogram for Nakagami1.33 channel, interleaver size = 64, and Tx = 3, Rx = 3

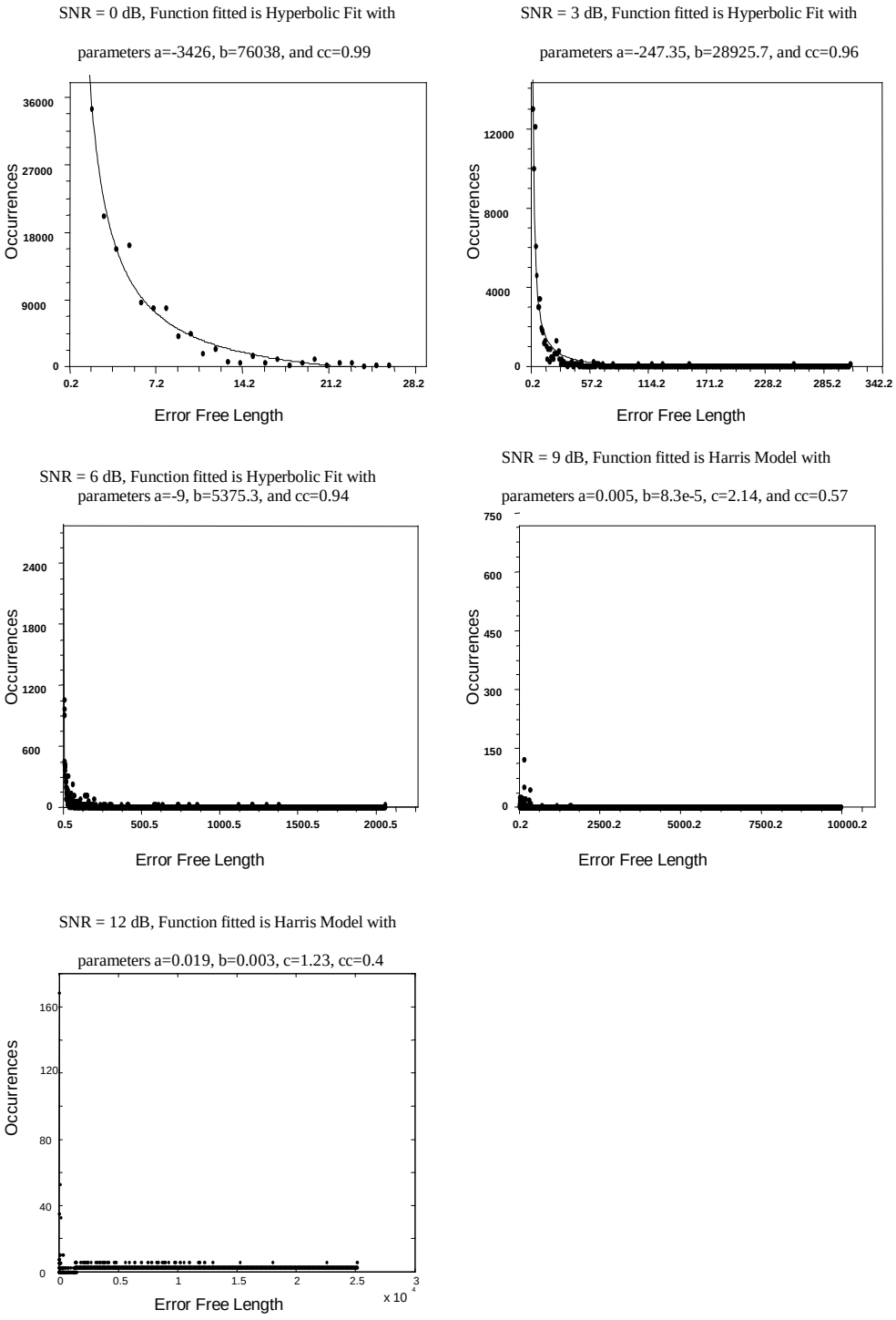

Figure 4.59: Error Free Length Histogram for Nakagami1.33 channel, interleaver size = 512, and Tx = 3, Rx = 3

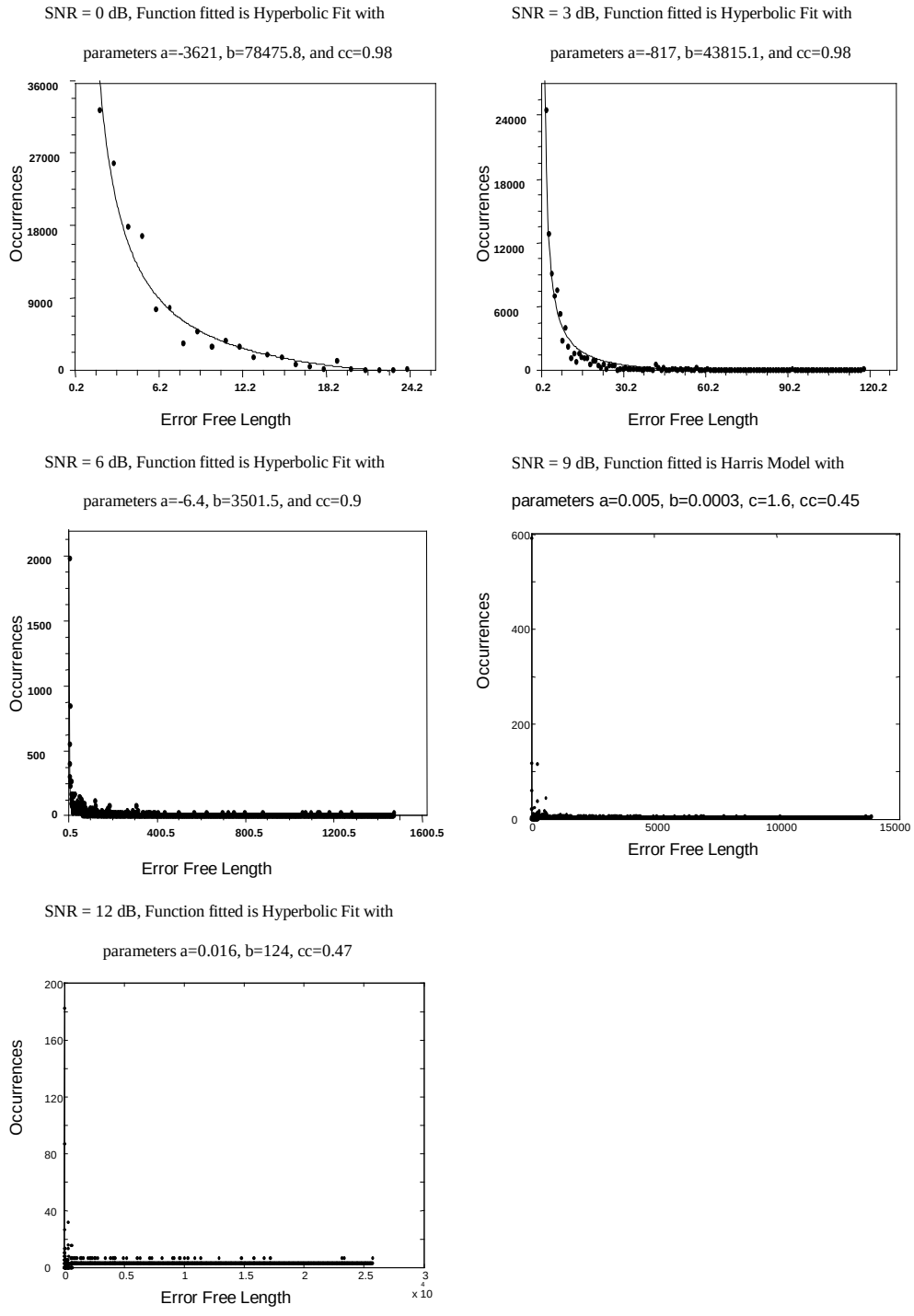

Figure 4.60: Error Free Length Histogram for Nakagami1.33 channel, interleaver size = 1024, and Tx = 3, Rx = 3

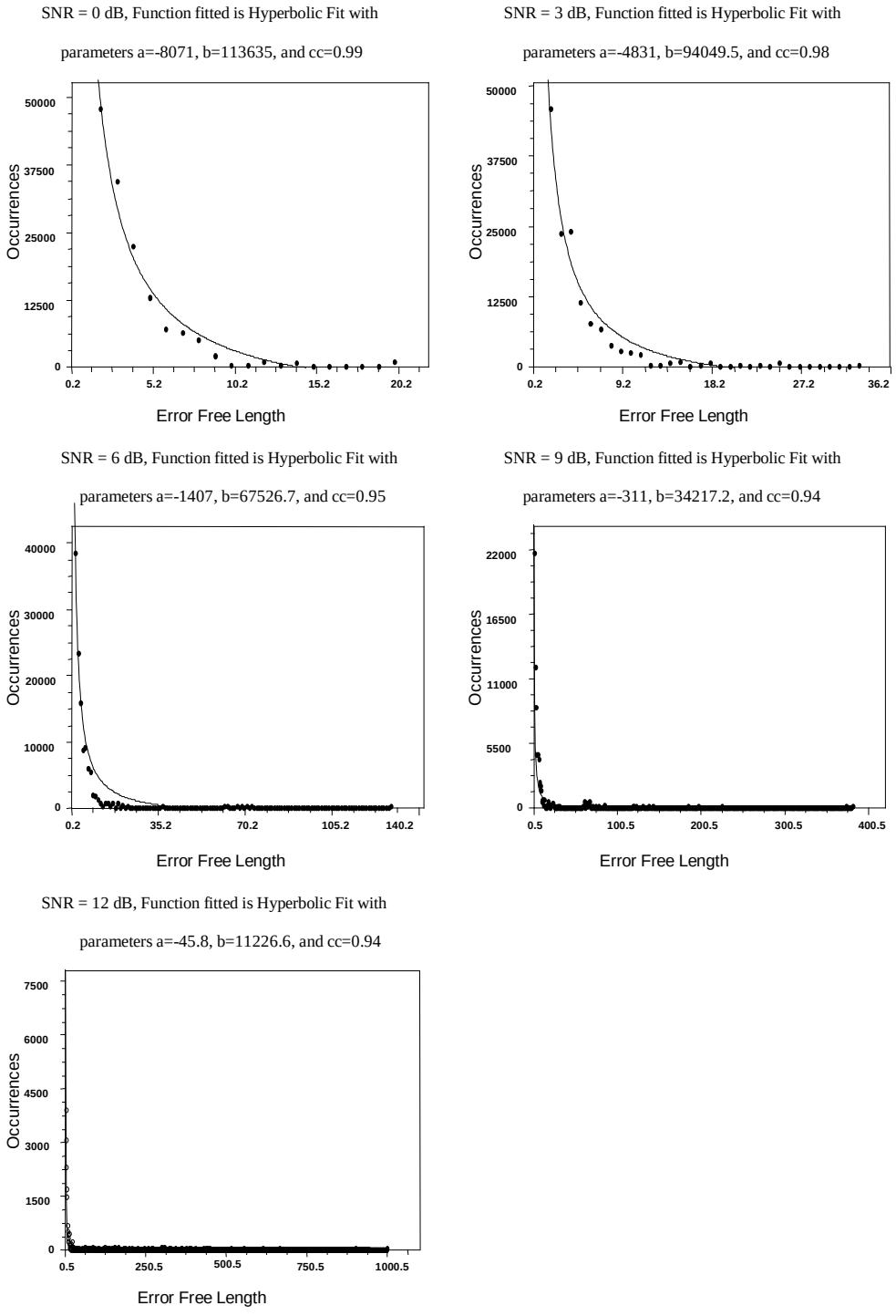

Figure 4.61: Error Free Length Histogram for Nakagami2.77 channel, interleaver size = 64, and Tx = 3, Rx = 3

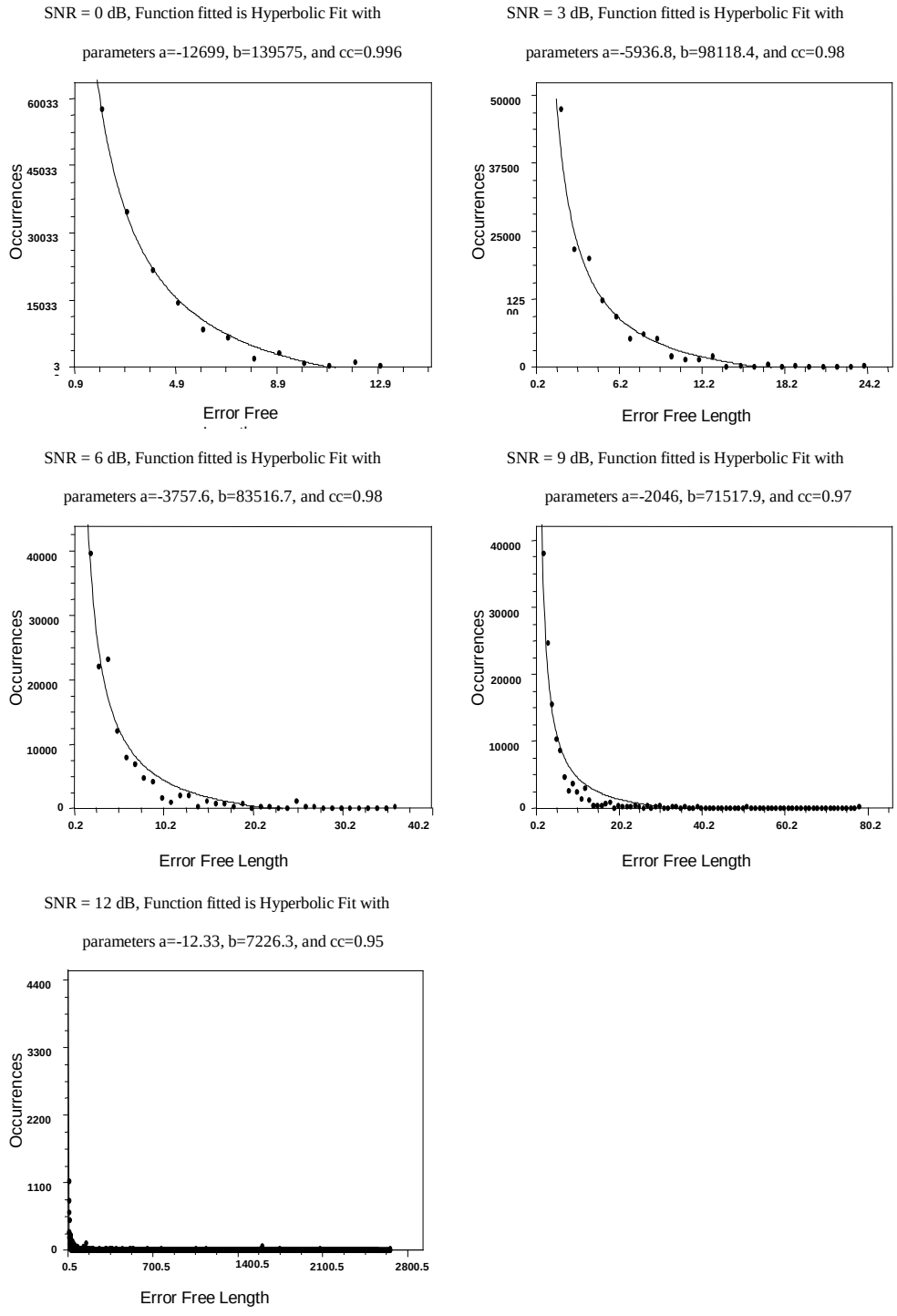

Figure 4.62: Error Free Length Histogram for Nakagami2.77 channel, interleaver size = 512, and Tx = 3, Rx = 3

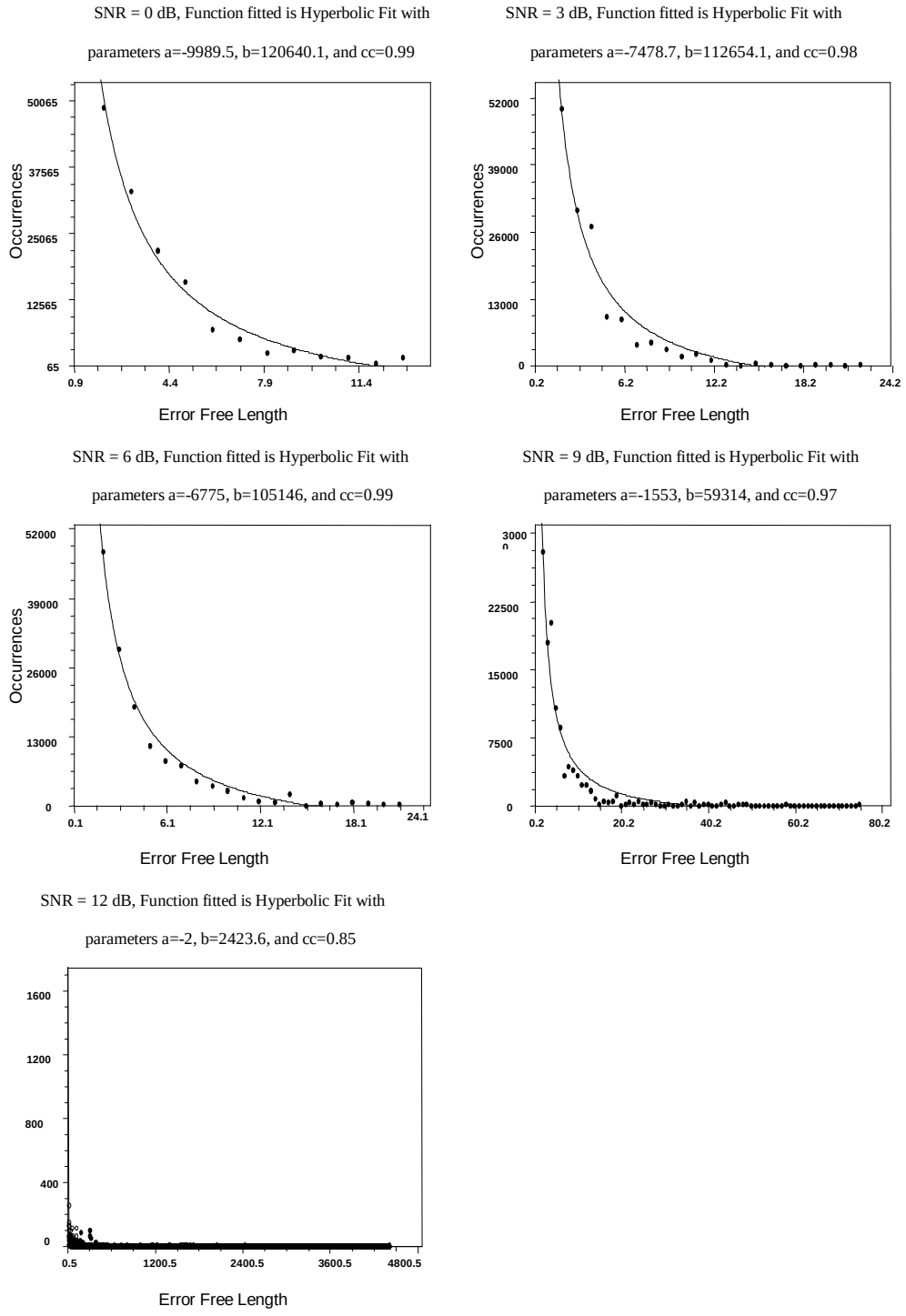

Figure 4.63: Error Free Length Histogram for Nakagami2.77 channel, interleaver size = 1024, and Tx = 3, Rx = 3

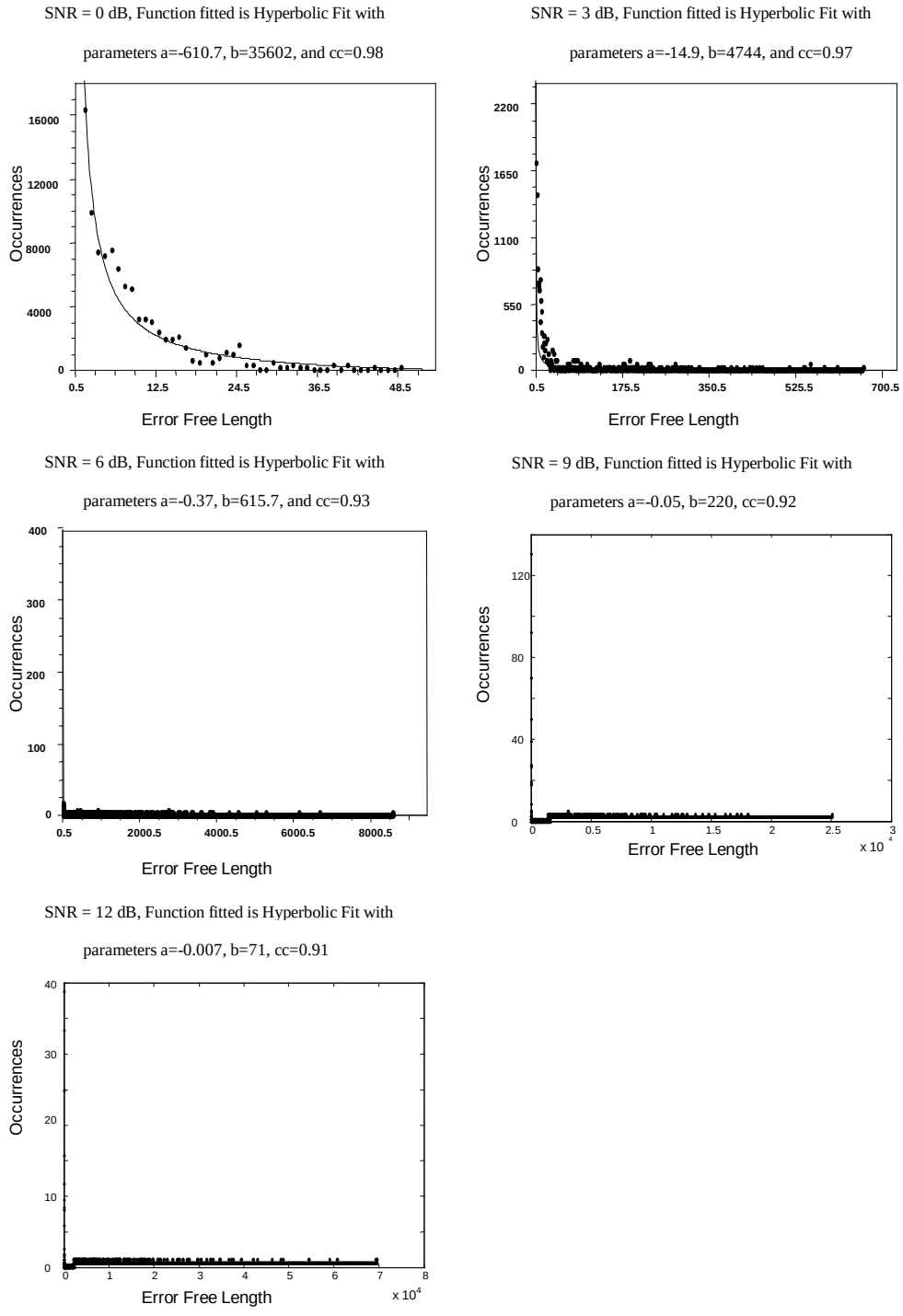

Figure 4.64: Error Free Length Histogram for Rayleigh channel, interleaver size = 64, and Tx = 6, Rx = 6

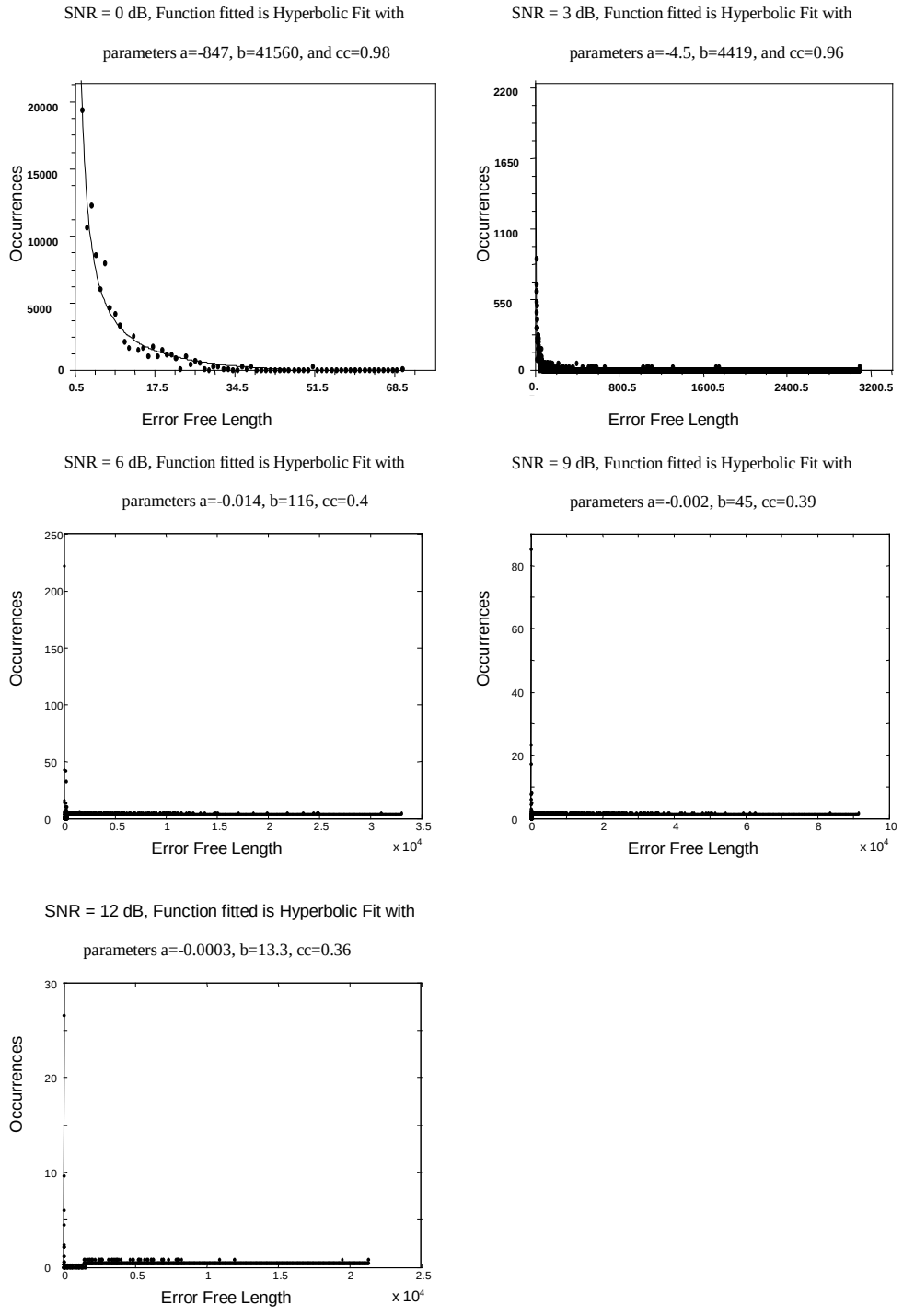

Figure 4.65: Error Free Length Histogram for Rayleigh channel, interleaver size = 512, and Tx = 6, Rx = 6

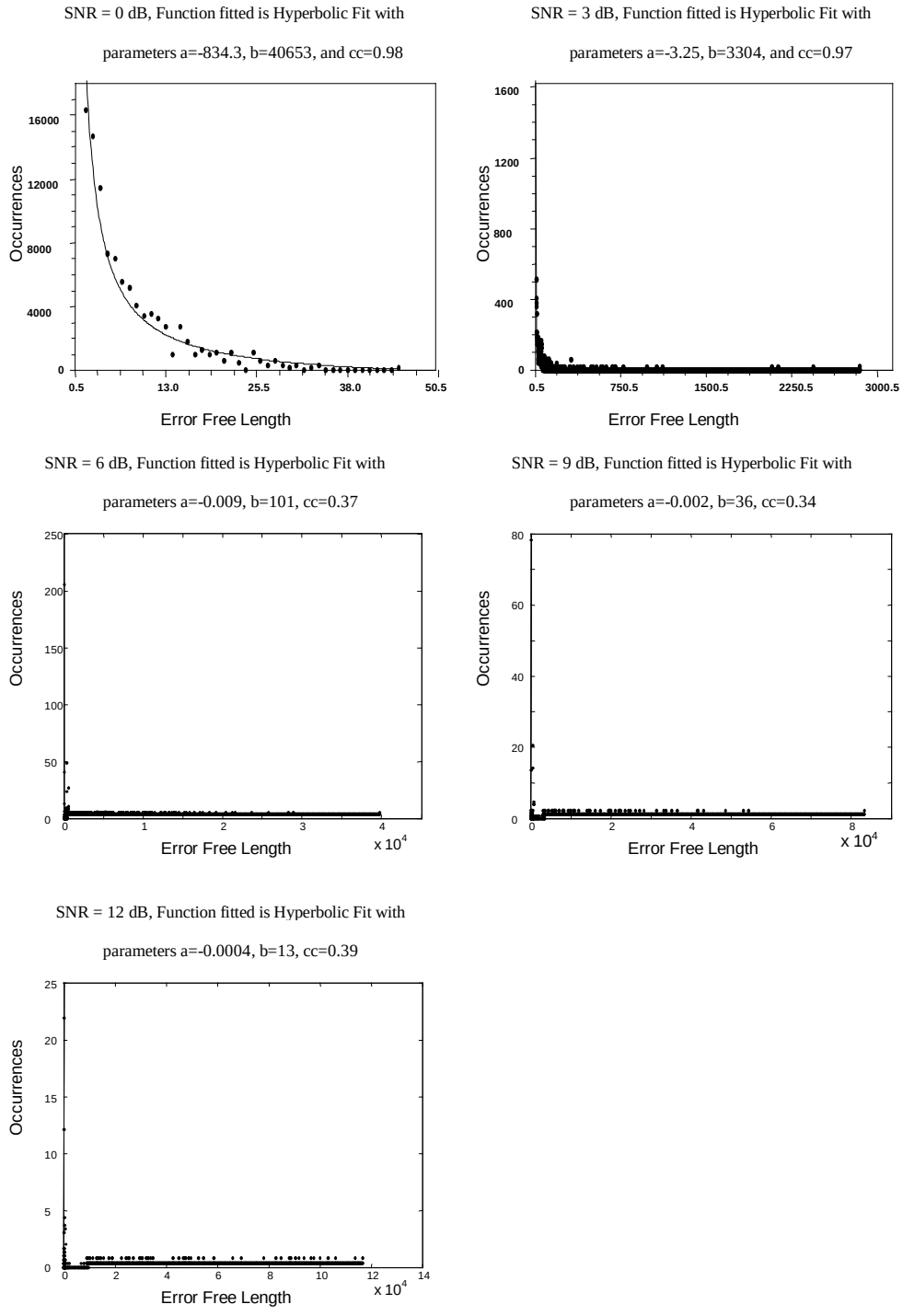

Figure 4.66: Error Free Length Histogram for Rayleigh channel, interleaver size = 1024, and Tx = 6, Rx = 6

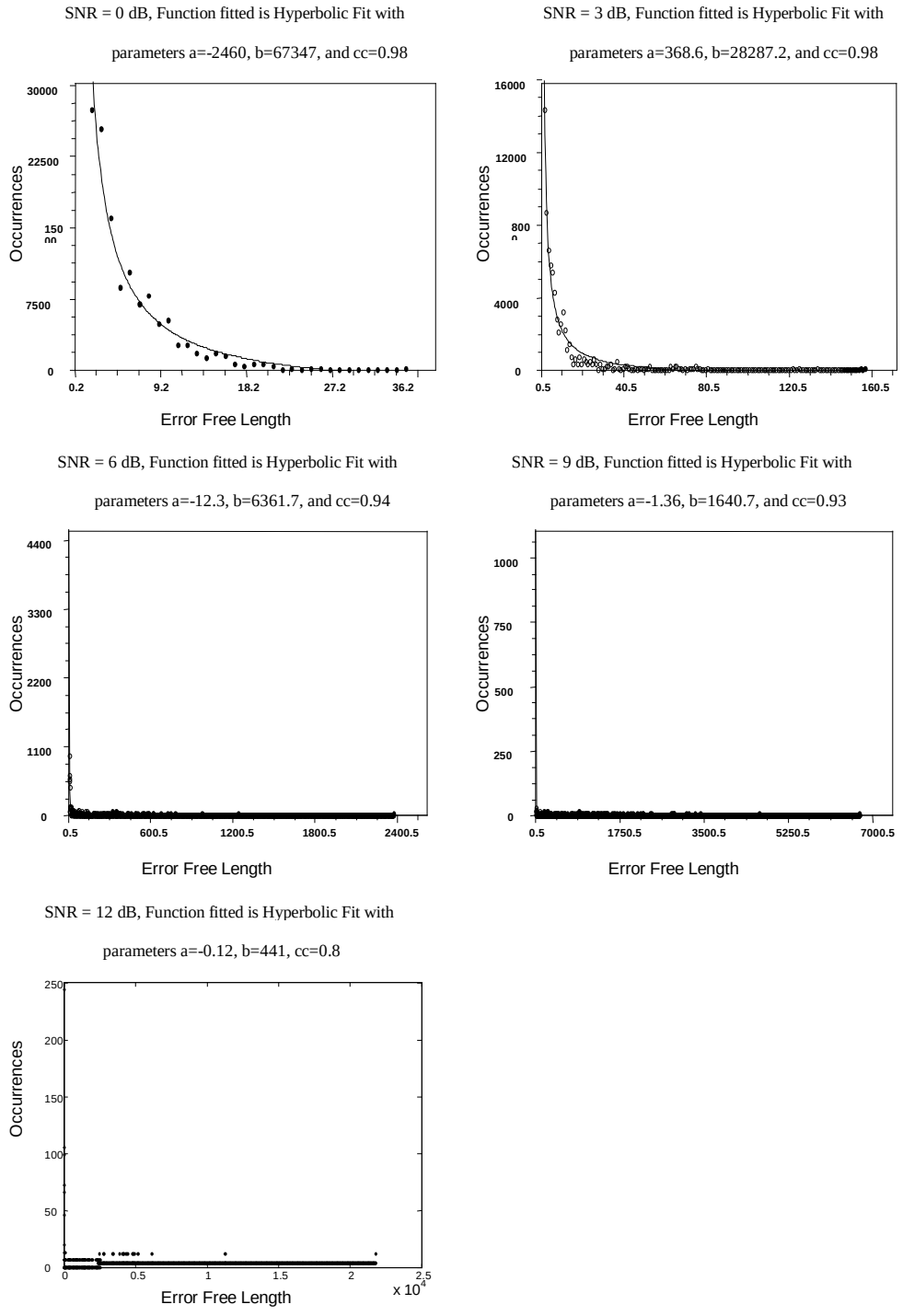

Figure 4.67: Error Free Length Histogram for Nakagami1.33 channel, interleaver size = 64, and Tx = 6, Rx = 6

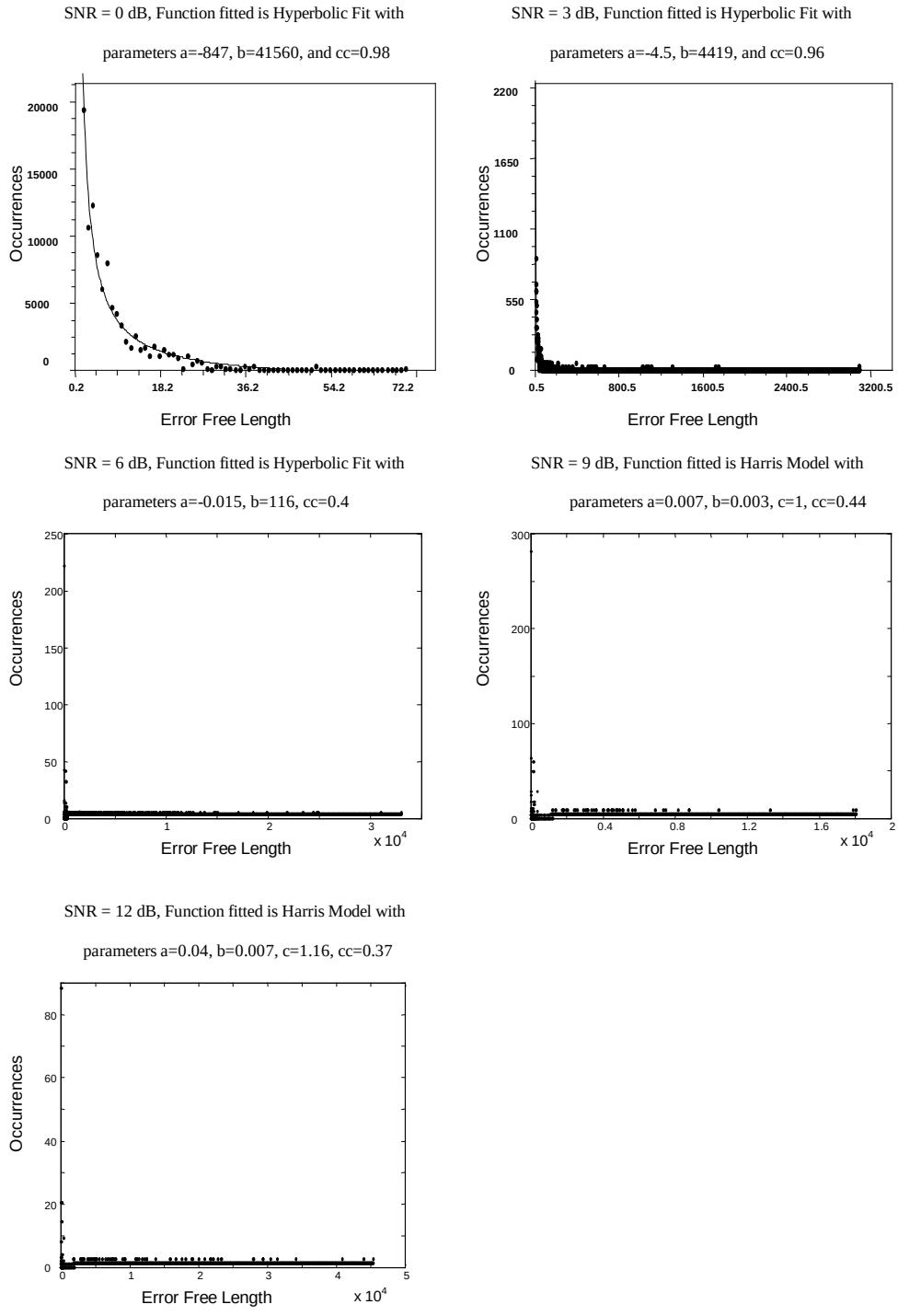

Figure 4.68: Error Free Length Histogram for Nakagami1.33 channel, interleaver size = 512, and Tx = 6, Rx = 6

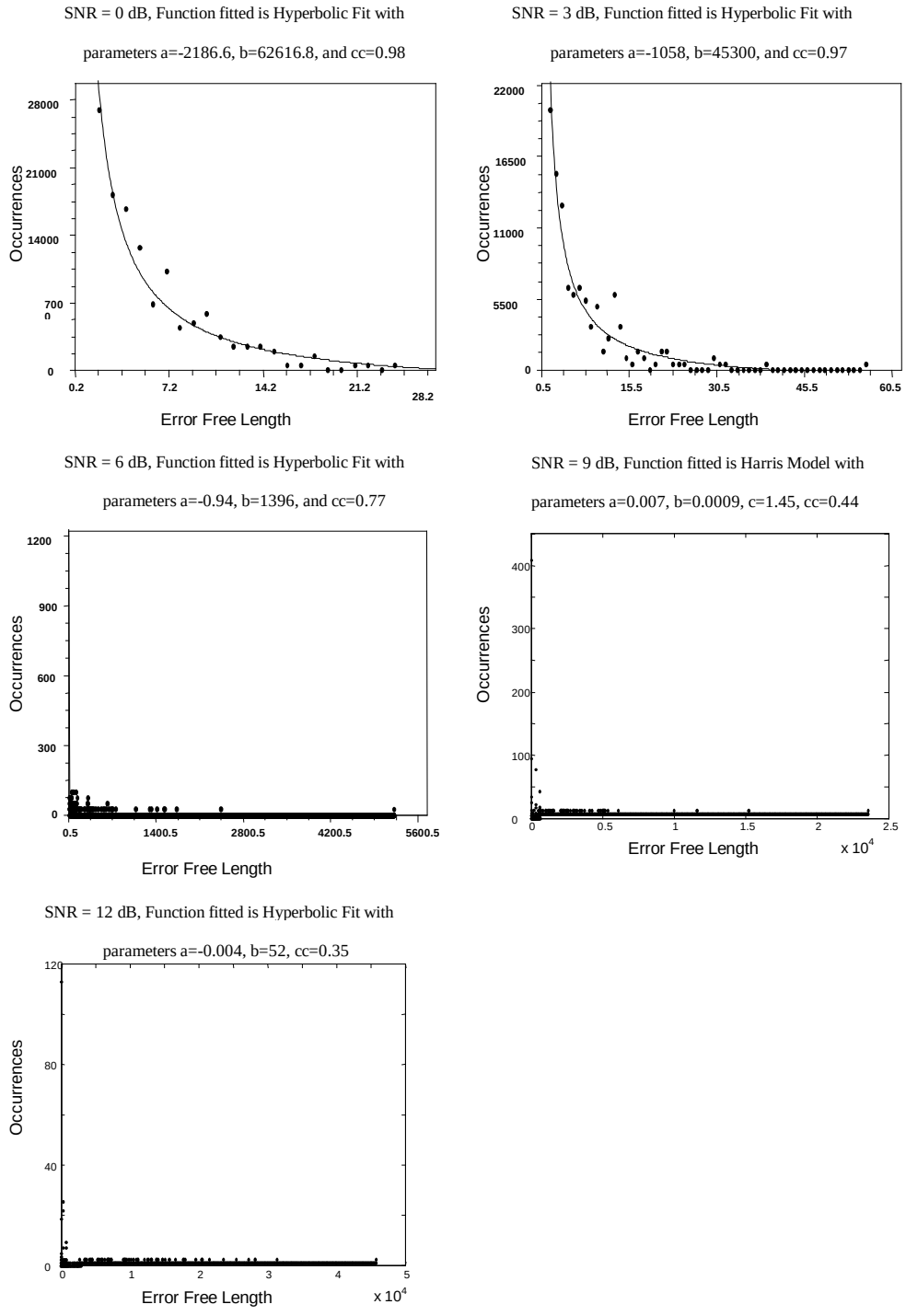

Figure 4.69: Error Free Length Histogram for Nakagami1.33 channel, interleaver size = 1024, and Tx = 6, Rx = 6

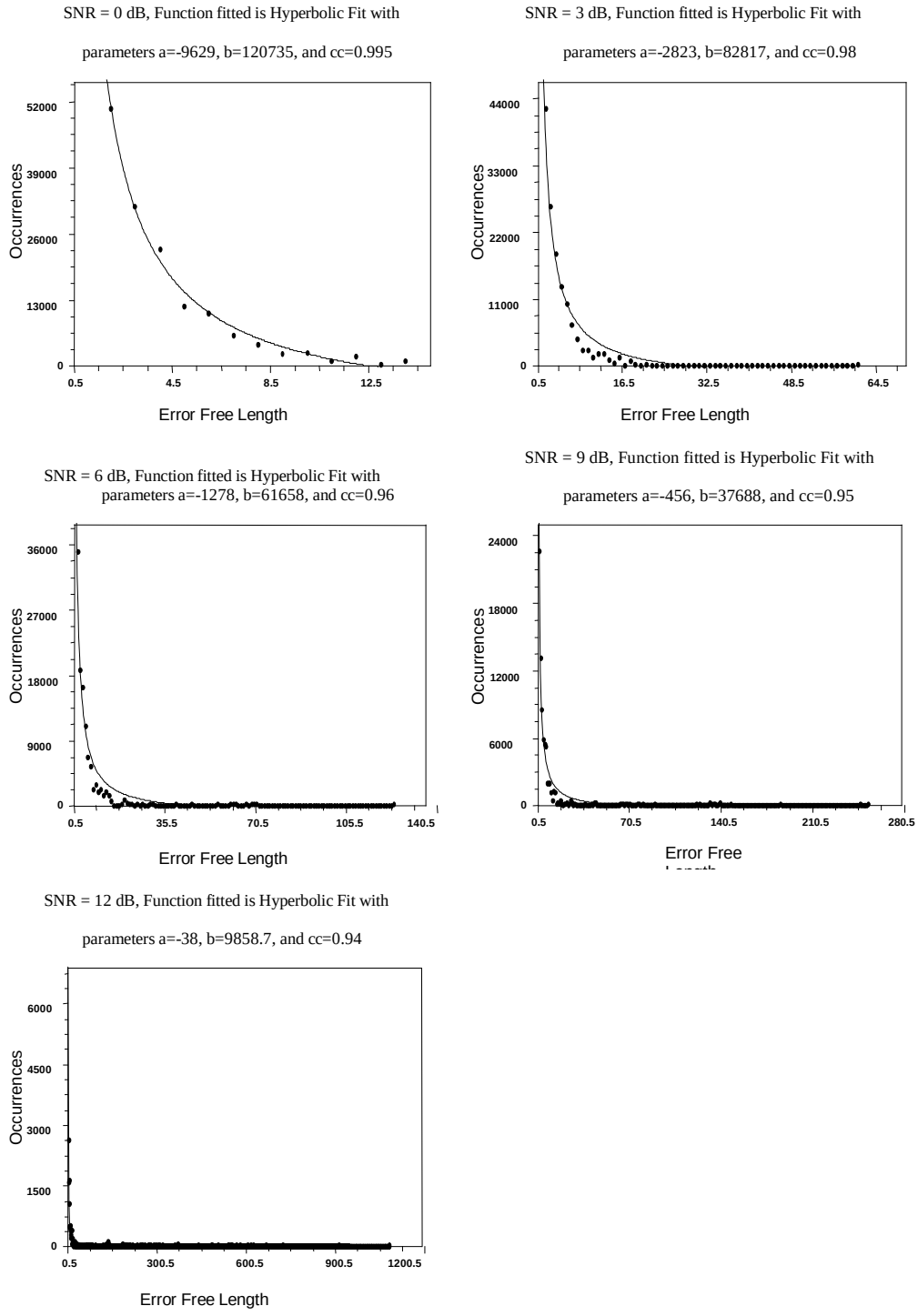

Figure 4.70: Error Free Length Histogram for Nakagami2.77 channel, interleaver size = 64, and Tx = 6, Rx = 6

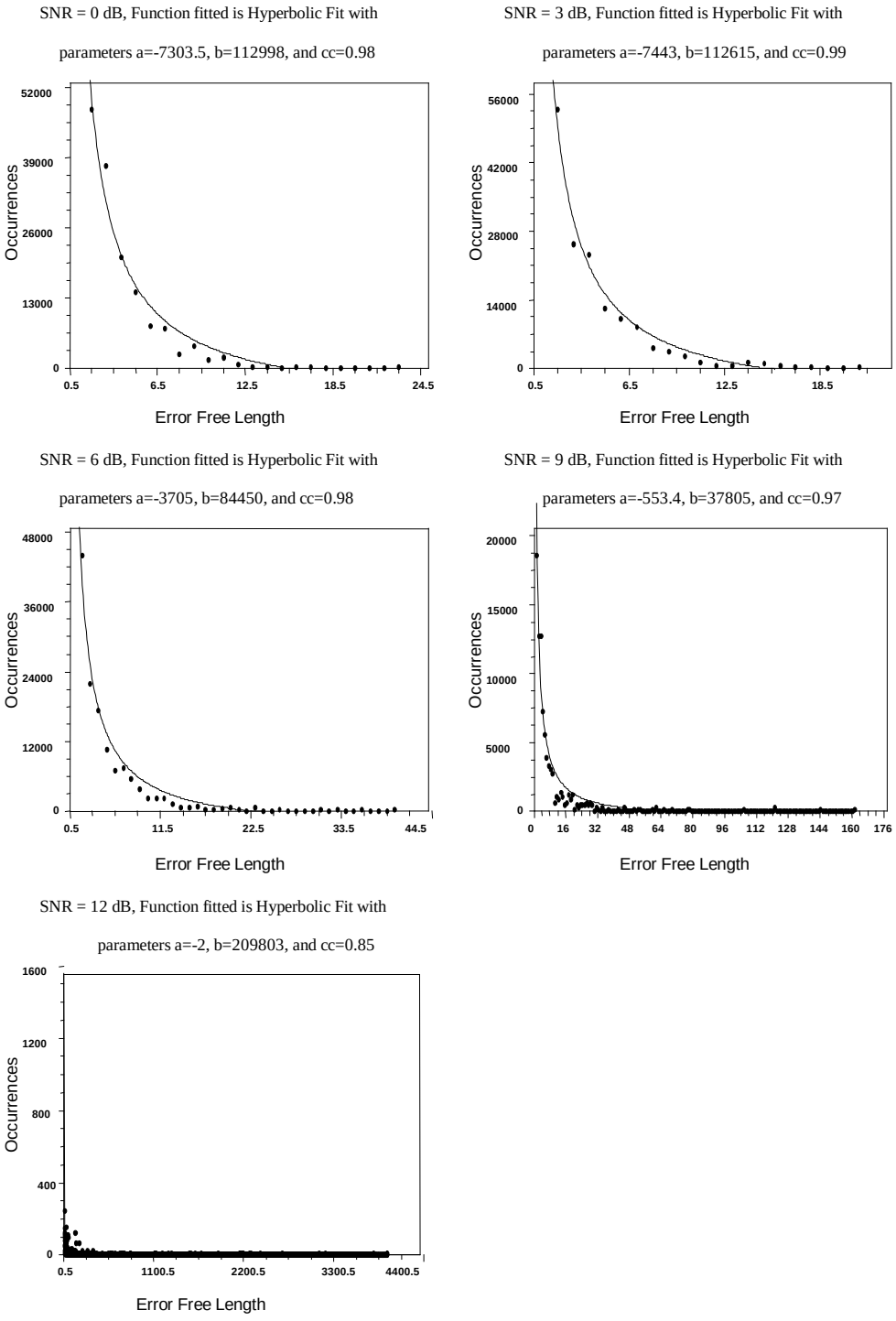

Figure 4.71: Error Free Length Histogram for Nakagami2.77 channel, interleaver size = 512, and Tx = 6, Rx = 6

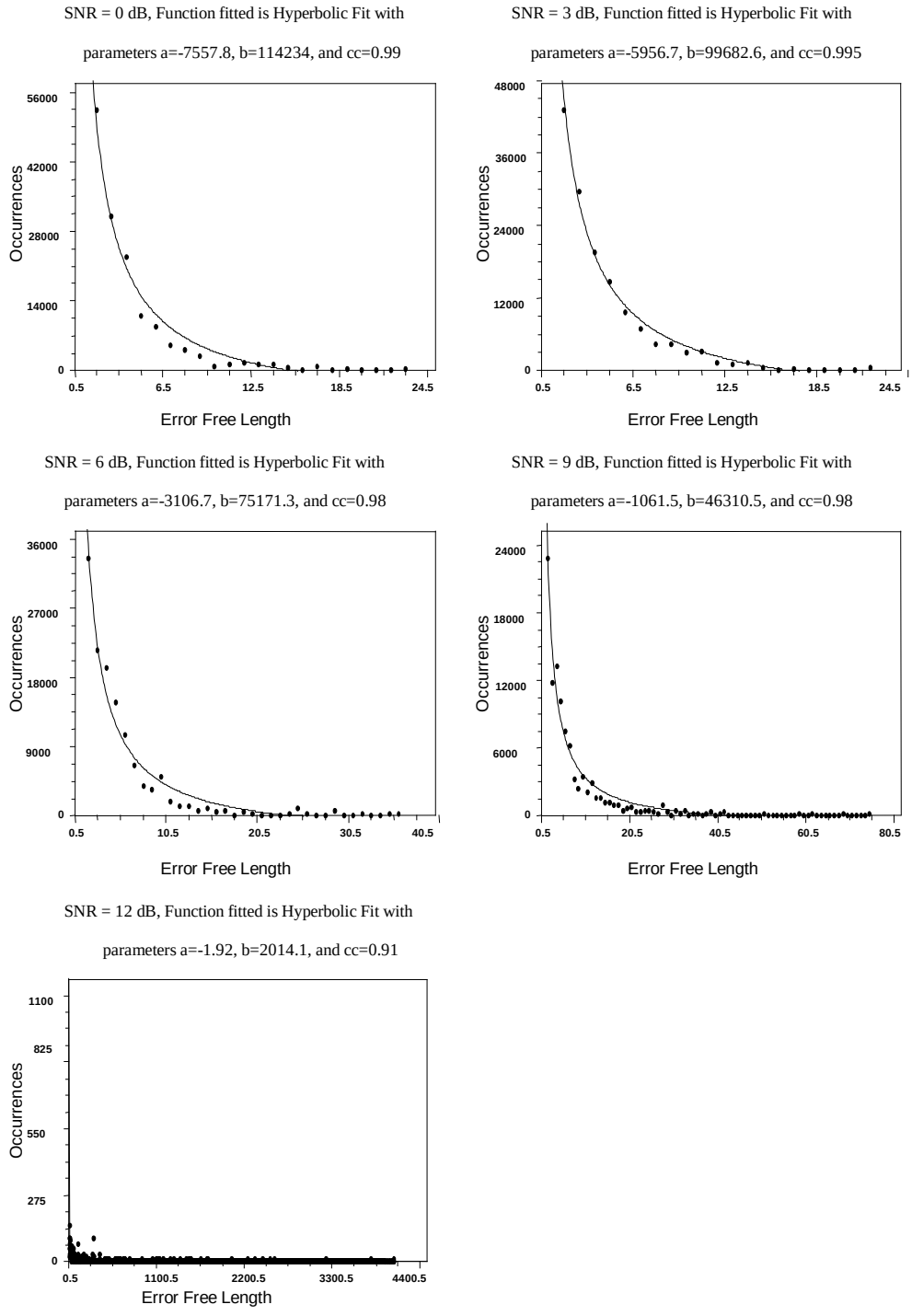

Figure 4.72: Error Free Length Histogram for Nakagami2.77 channel, interleaver size = 1024, and Tx = 6, Rx = 6

Average error free lengths (EFLs) increase with signal to noise ratios exponentially. Long interleavers randomize large block of data stream and can decorrelate long error bursts. It results in high probability of error correction and decorrelation of longer error burst, in turn gave longer error free gaps. Average EFLs increase from 4000 for IS = 64 (at 12 dB, (6,6) Rayleigh) to 10252 for IS = 1024. Setup (6×6) utilizes more transmitter receiver elements to a system than (3×3), the excess channels are used to improve performance and resulted in longer error free lengths. Rayleigh channel has strong scattering property, with $m = 1$ i.e. no correlation, results in increased probability of signal to be detected correctly. This results in high spectral efficiency that is enabled by the fact that a scattering environment makes the signal from every individual transmitter appear highly uncorrelated at each of the receive antennas. As a result, the signal corresponding to every transmitter has a distinct spatial signature at the receiver. These different spatial signatures allow the receiver to effectively separate, with adequate signal processing, the transmissions simultaneously and on the same frequency by the different transmit antennas. In a sense, the scattering environment acts like a very large aperture that makes it possible for the receiver to resolve the individual transmitters [45]. The high spectral efficiency is reduced if the signals arriving at the receivers are correlated. An shown in [46], the multiple element antenna MEA capacity is the sum of the individual subchannel capacities. The stronger the fading correlation, the higher the disparity between the capacities of these subchannels. As the fading correlation

becomes more severe, more and more subchannels have gains too small to convey information at any significant rate. In other words, signal detection of V-BLAST require Moore-Penrose psuedoinverse [4], that goes to singularity with correlation in matrix entries. This increase error in detecting signals with increase in correlation in channel paths. Incorrect detection of first symbol in a layer lead to further errors in the same layer, which can be termed as propagation of errors inherent to V-BLAST. This results in degradation with increase in m (correlation).

Comparing Fig. 4.73, 4.74, and 4.75 with the Fig. 4.16 i.e. for without coding case, shows average EFLs for coding are 1.5 to 11 times that of without coding for different interleaver depths. Low SNR Nakagami2.77 channels has smaller average error free lengths, as shown in Fig. 4.73, 4.74, 4.75. This results in no improvement by increasing interleaver size.

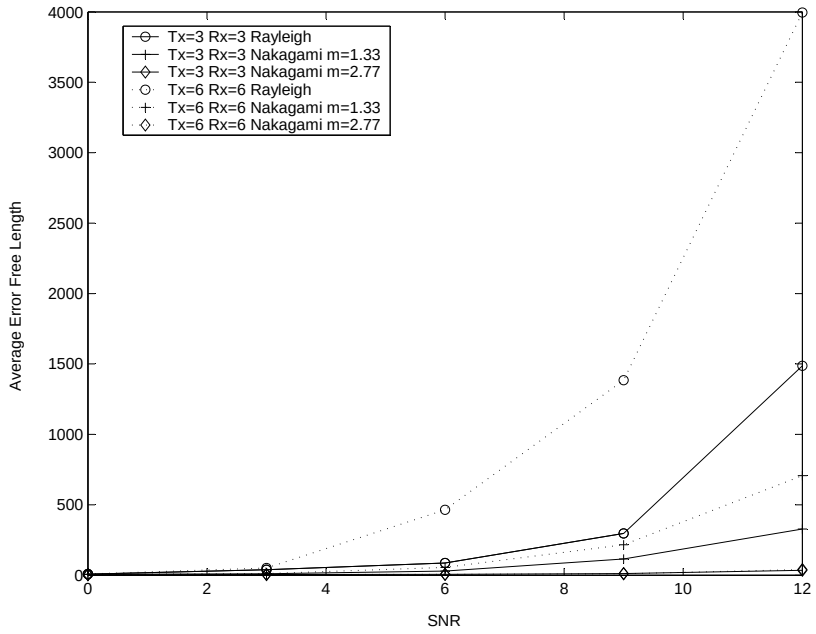

Figure 4.73: Average Error Free Length for interleaver depth = 64

4.5.3 Bit Error Rate

The plots 4.76, 4.77, 4.78 show BER for interleaver sizes 64, 512, and 1024 respectively. Coding gains are computed at 1×10^{-3}, 6×10^{-3}, 4×10^{-2} BER for Rayleigh, Nakagami1.33, and Nakagami2.77 channels respectively. Turbo coding gave 2, 4.5 dB gain for Rayleigh (3×3), (6×6) arrangements, 1-2 dB gain for Nakagami1.33 (3×3), (6×6) arrangements, and no improvement for Nakagami2.77 channels respectively for interleaver size 64. For Rayleigh channel, BER improvement is higher. Rayleigh channels have shorter error burst lengths and longer error free lengths, which gave more room for interleavers to spread the errors (which are al-

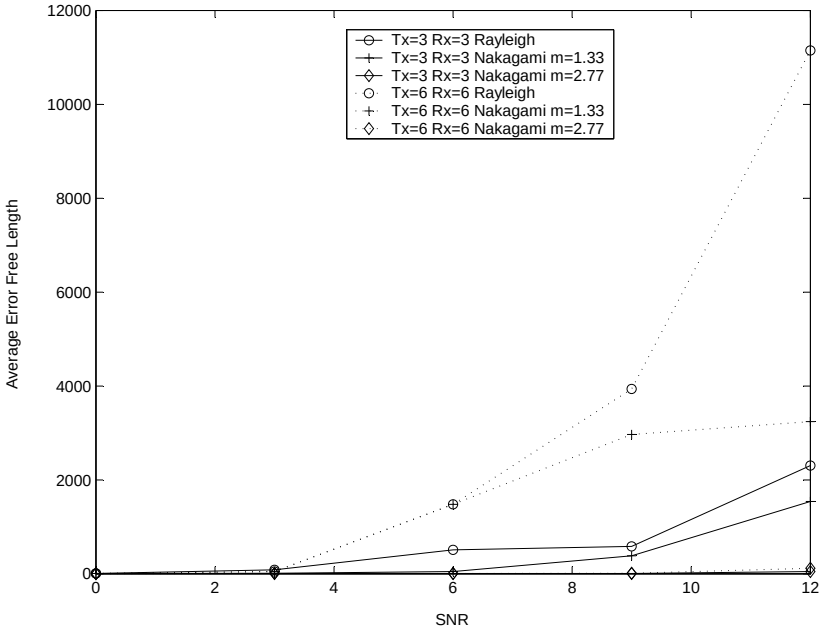

Figure 4.74: Average Error Free Length for interleaver depth = 512

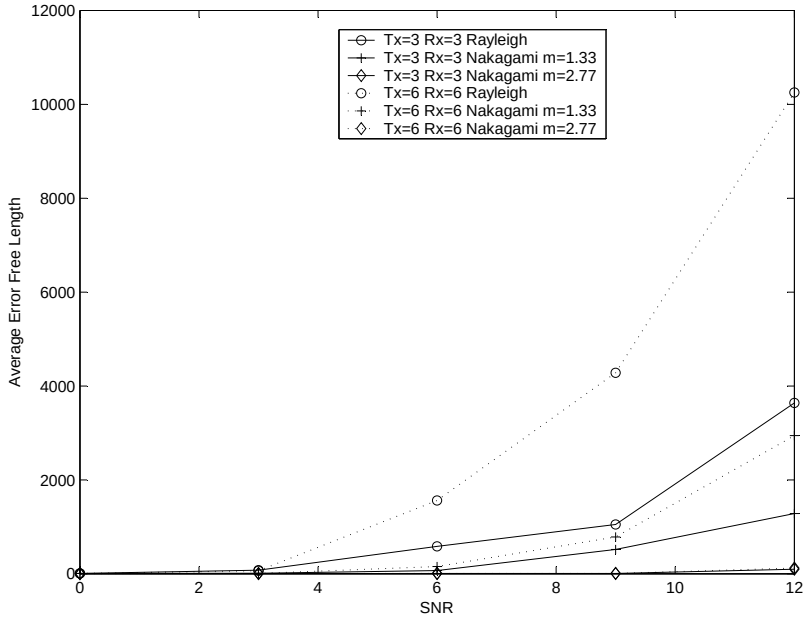

Figure 4.75: Average Error Free Length for interleaver depth = 1024

ready less than Nakagami channels as can be seen from BER performance in Fig. fig: T3R3wocber). This spreading of errors resulted in increased error correction or higher coding gains. For interleaver depth 512, it gave 8, 7 dB gain for Rayleigh (3×3), (6×6) arrangements, 5, 7 dB gain for Nakagami1.33 (3×3), (6×6) arrangements, and 1 dB improvement for Nakagami2.77 (6×6) arrangement respectively. Increasing interleaver size from 64 to 512 improved BER performance but further increase (i.e. 1024) does not provide improvement. Therefore, very small interleaving sizes is not desirable and very long interleaving sizes does not give further improvement. Error burst lengths are reduced and error free lengths are increased with interleaver size 512 than interleaver size 64 for Rayleigh and Nakagami1.33 channels while there is less improvement in these parameters over Nakagami2.77 channels. Therefore system performance is improved over Rayleigh and Nakagami1.33 channels while little improvement is observed over Nakagami2.77 channels. Gain attained from Turbo coding for interleaver depth 1024 is 7 dB for Rayleigh (3×3) and (6×6) arrangements, 5, 5.5 dB for Nakagami1.33 (3×3), (6×6) arrangements, and 1 dB improvement for Nakagami2.77 (3×3), (6×6) arrangements respectively. There is no significant improvement for error burst lengths and error free lengths in increasing interleaver size from 512 to 1024 over Nakagami2.77 channels. Therefor there is no significant improvement observed from interleaver size 512 to 1024. Increase in interleaving depth improves performance over Rayleigh channel. For Nakagami channels, very small and very long interleaver sizes degrade performance. Therefore,

interleaver depth can be made adaptive.

Due to constructive and destructive effects of multipath waves summing at various points in space, the signal receive does not pass through several fades in a small period of time. These fades result in occurrences of error burst lengths while inter-fade intervals where signal is strong results error free intervals. If interleaver is long enough to spread errors in the fade period over error free intervals to make that errors random, then coding can correct these error. Therefore, longer interleavers gave improvement in BER performance. An interesting observation stemming out of the results in the difficulty of V-BLAST with coding to reduce the BER in high m Nakagami channels, which are found in the micro cellular environment for both (3×3), (6×6) setups. The overall diversity level is limited by the diversity level obtained in the layer which is detected first. V-BLAST technique is affected severely with correlation between signal paths, which results in high probability of getting error in the first detected symbol. If first layer is detected wrong it can result in error propagation which restrict improvement even if more channel paths are used. That's why (6×6) setup gives very little improvement in performance.

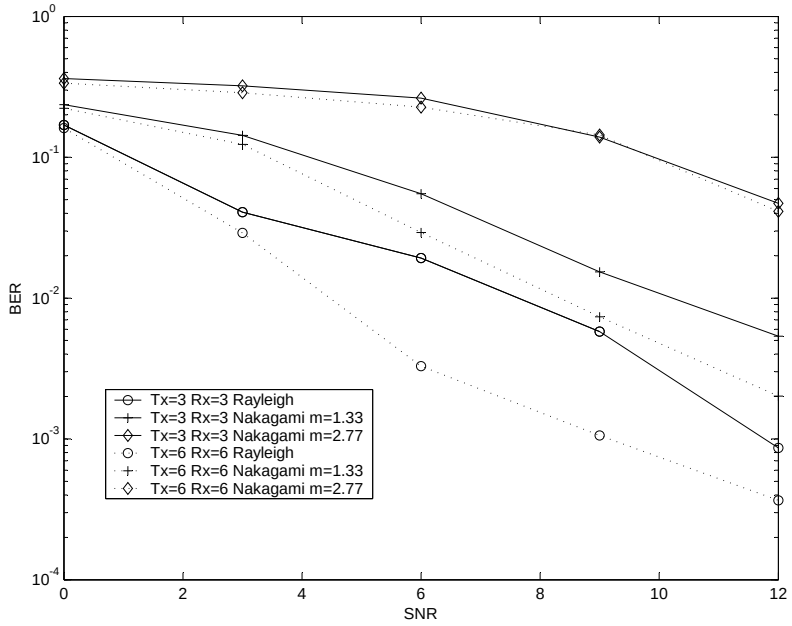

Figure 4.76: Average Bit Error Rate for interleaver depth = 64

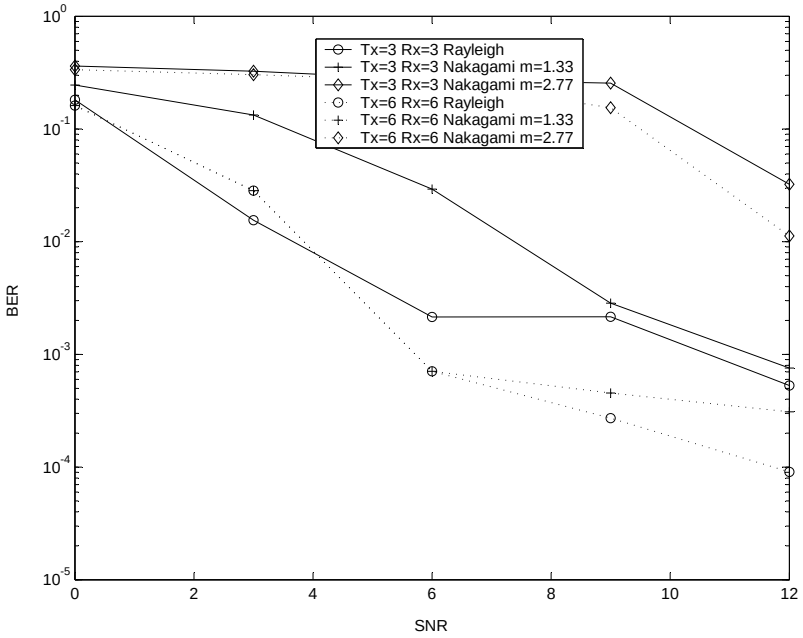

Figure 4.77: Average Bit Error Rate for interleaver depth = 512

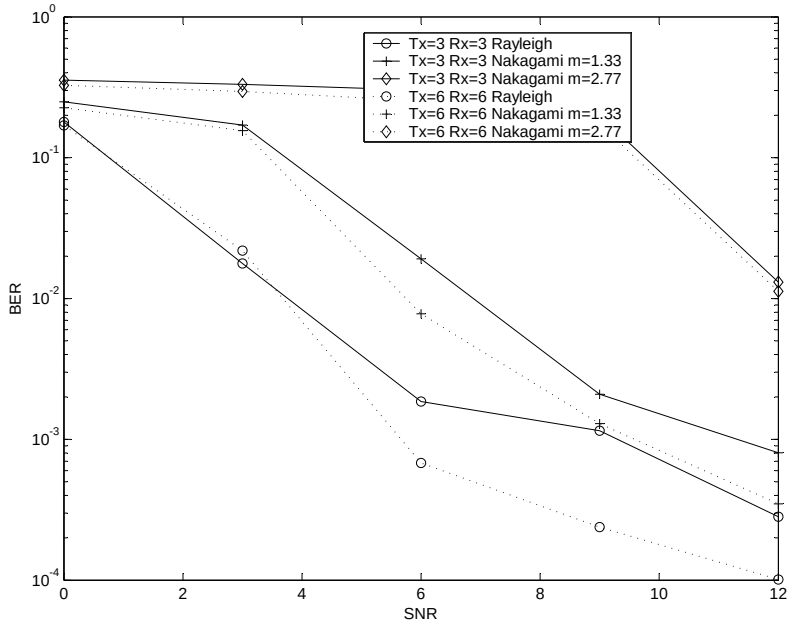

Figure 4.78: Average Bit Error Rate for interleaver depth = 1024

4.6 Receiver Structures of the BLAST System

Previous section described zero-forcing (ZF) V-BLAST detection. At each symbol time, the algorithm first detects the strongest [1] layer (transmitted signal), then cancels the effect of this strongest layer from each of the received signals, and then proceeds to detect the strongest of the remaining layers, and so on.

For M transmitters and N receivers, the diversity level is N - M + 1 when detecting the first layer. With each layer detected, the diversity level of the resulting system should increase layer by layer, until N for the last layer, since the detected layers have been cancelled while the receive antennas still keeps constant. However, the

[1] In the sense of SNR

diversity level of N - M + 1 for the first layer is too low in most cases, which largely limits the error performance of ZF V-BLAST. For example, if N = M, there would be no diversity gain for the first layer. To avoid this drawback, [9] provides a solution. In which, instead of detecting the first one layer, the first p layers (after ordering) are detected by using ML detection. Thus each of the first p layers attain a diversity of p. A dramatic performance improvement was observed in [9] even if $p = 2$. This detection algorithm, p-ML, would not be too complex since p is small.

4.6.1 MMSE Algorithm

Another way to improve detection performance especially for mid-range SNR values is to replace the zero-forcing (ZF) nulling proposed in [5] by the more powerful minimum mean-square error (MMSE) algorithm. In addition to nulling out the interferers the noise level on the channel is taken into account. A disadvantage is, however, that the SNR has to be known, and thus estimated, at the receiver. With ZF the nulling matrix corresponds just to the pseudo inverse of the channel matrix $G_i = \tilde{H}_i^{\S}$. Where § is pseudoinverse. The extension to MMSE nulling yields the following cancellation matrix.

$$G = (H^T H + \frac{\sigma_n^2}{\sigma_d^2} I)^{-1} H^T \tag{4.14}$$

where $\frac{\sigma_d^2}{\sigma_n^2}$ denoted the signal to noise ratio.

4.6.2 A Fast Square-Root Algorithm

One of the main computational bottleneck in the BLAST algorithm is a "nulling and cancellation" step. where the optimal ordering for the sequential estimation and detection of the received signals is determined. To reduce the computational cost of BLAST, [10] developed an efficient square-root algorithm for the nulling-vector optimal-ordering step. The main features of the algorithm include efficiency: the computational cost is reduced by an order of magnitude, effectively from $O(M^4)$ to $O(M^3)$, and numerical stability: the algorithm is division-free and uses only orthogonal transformations.

The algorithm avoids squaring and inverting things. It makes as much use as possible of unitary transformations. In order to avoid squaring H, the algorithm begins with the QR decomposition of the augmented channel matrix.

$$\begin{bmatrix} H \\ \sqrt{\alpha} I_M \end{bmatrix} = QR = \begin{bmatrix} Q_\alpha \\ Q_2 \end{bmatrix} R \tag{4.15}$$

where Q is an (N+M) $\times$ M matrix with orthonormal columns, and R is M $\times$ M and nonsingular. Therefore,

$$P^{1/2} = R^{-1} \quad and \quad H_\alpha^{\S} = P^{1/2} Q_\alpha^T \tag{4.16}$$

where $P^{1/2}P^{*1/2} = P$, and § is pseudoinverse. Thus, given $P^{1/2}$ and Q_α, both pseudoinverse and the error covariance matrix can be computed.

4.6.3 Decorrelating Decision Feedback Method

A square-root algorithm based on QR decomposition of the channel matrix and unitary transformations described in the previous subsection is used to avoid the repeated computation of the nulling vectors. Instead, the QR decomposition is computed only once. Not only is computation complexity reduced, but also the numerical robustness is improved by this square-root algorithm. Complexity of the algorithm is reduced by the decorrelating decision feedback multiuser detection algorithm originally proposed for code division multiple access (CDMA) systems [47]. In this method, the received signal vector $\mathbf{x}$ is correlated with the conjugate transpose of the channel matrix. This correlation is analogous to the matched filter bank front-end of a CDMA multiuser receiver. The correlator output $y \in C^M$ is:

$$y = H^T x = Rs + z \tag{4.17}$$

where $R = H^T H$ is a M × M cross-correlation matrix, and z is a zero-mean Gaussian noise vector with auto-correlation $\sigma^2 R$.

The cross-correlation matrix can be Cholesky decomposed as $R = LL^T$, where L is a lower triangular matrix and L^T is its conjugate transpose. A filter with impulse

response L^{-1} is applied to the correlator outputs y of (4.17) to whiten the noise:

$$\check{y} = L^{-1}y = L^T s + n \tag{4.18}$$

Since L^T is upper triangular, the k^{th} component of $\check{y}$ can be expressed as:

$$\check{y}_k = L^T_{k,k} s_k + \sum_{i=k+1}^{M} L^T_{k,i} s_i + n_k \tag{4.19}$$

which contains only interference from (M - k) signals.

The last component $\check{y}_M$ contains no interference, so a decision for this transmitted signal can be made first: $\hat{s}_M = dec(\check{y}_M)$. The next signal can be detected by subtracting the interference contribution from the M^{th} signal using the previous decision, i.e., $\hat{s}_{M-1} = dec(\check{y}_{M-1} - L^T_{M-1,M}\hat{s}_M)$. This procedure is repeated until all signals are detected.

The above decorrelating decision-feedback method first cancels the interference using the feedback of previous decisions, and then makes a decision on the current signal. The detection and decision-feedback are performed in decreasing order of received signal energies in the original decorrelating decision-feedback CDMA multiuser detector in [47]. The Cholesky decomposition is calculated only once, so repeated calculation of the pseudo-inverse is avoided.

4.6.4 Modified Decorrelating Decision Feedback Method

Wei Zha *et al* proposed modified decorrelating decision feedback method in [48] to further reduce the complexity of algorithms presented in [10] and [48]. The original cross-correlation matrix R, or its corresponding Cholesky decomposition matrices L and L^T, have to be reordered for optimal detection ordering. In this algorithm the detected signal has the largest SNR at every step.

The inverse of the cross-correlation matrix is $R^{-1} = L^{-T}L^{-1}$, where L^{-1} can be easily calculated from the lower triangular matrix L by back-substitution, and L^{-T} is the conjugate transpose of L^{-1}. The signal to be detected with the largest SNR corresponds to the signal with the smallest diagonal entry of R^{-1}. Note that no need to calculate R^{-1} to find the smallest diagonal entry, since the diagonal entries of R^{-1} are equal to the column norms of L^{-1}.

First find the smallest column norm of L^{-1}, and then reorder the columns of L^{-1} by interchanging the smallest column-norm column with the last (M^{th}) column. The rows of L, corresponding to columns of L^{-1}, as well as both the corresponding rows and columns of R are interchanged in the same way. Interchanging two columns of a matrix can be performed by post-multiplication by a unitary permutation matrix P, and interchanging two rows of a matrix can be performed by pre-multiplication by a unitary permutation matrix P^T, so the matrices after reordering are:

$$P^T R P = (P^T L)(L^T P) \tag{4.20}$$

Correlation in channel paths degrade performance so why to have high complexity when channel paths are correlated. A suboptimum but less complex detection can be used. Turbo code rate may also change with environment. Therefore receiver can be made adaptive. Antenna spacing can be increased as far as possible to decorrelate channel paths.

Further work is terminated from this point due to saturation has come in finding ways to avoid zero-forcing (nulling and interference cancellation). Shortage of time and deviation from the direction of investigation of error performance of the thesis also played a role in stopping the work towards this direction.

Chapter 5

Conclusion and Future Work

This chapter concludes the thesis by summarizing important contributions and identifies some future avenues of research that originated from this work.

5.1 Conclusion

We have shown error statistics of V-BLAST system. The study of statistical distribution of errors is a prerequisite in the design of appropriate coding techniques to effectively control errors. The analysis contains error burst length and error free length histograms, average error burst length and average error free length, and BER. These parameters are evaluated over Rayleigh, Nakagami1.33, Nakagami2.77 channels and (3×3), (6×6) transmitter receiver arrangements. A benchmark system having single transmitter and single receiver is analyzed for comparison.

Increase in mobile velocity reduces duration of fades and non fade intervals. This reduction in fade and non fade durations resulted shorter average error burst lengths and average error free lengths. The highest m channel (i.e. Nakagami2.77) resulted in half the average error burst length than the lowest m channel (i.e. Rayleigh). BER of single transmitter single receiver arrangement is unaffected with the change in Doppler. At approx. 10^{-2} BER, Nakagami2.77 showed 5 dB improvement over Nakagami1.33 while Nakagami1.33 showed around 2 dB improvement over Rayleigh channel.

Statistical analysis of V-BLAST system is performed over Rayleigh, Nakagami1.33, and Nakagami2.77 channels and for 10 Hz, 20 Hz, and 50 Hz Doppler frequencies. Average error burst length, error free length, and BER are measured. Modelling of the distribution of error burst length, and error free length is also performed. The results found for V-BLAST system are listed below.

Frequency of occurrences of error bursts decreases exponentially with increase in length and signal power. Burst length is reduced with signal-to-noise ratio. V-BLAST performance is degraded by correlation in channel paths. Correlation reduces independence in channel paths which in turn increases average error burst lengths. Error burst length occurrences are increased for Nakagami2.77 channel due to transformation of longer error burst into smaller error bursts at high signal powers. Rayleigh channel has the least number of longer error bursts while Nakagami2.77 has the most. Ratio of longer burst lengths to smaller burst lengths increases expo-

nentially (having 0.9 to 1 cross correlation) from Rayleigh to Nakagami2.77 channel. Tx = 6, Rx = 6, arrangement has shorter average error burst than Tx = 3, Rx = 3. Hyperbolic function perfectly models the error free length. An interesting observation is found that the parameter 'a' of Hyperbolic fit is exponentially increases while parameter 'b' is exponentially decreases with SNR. This ensures the finding of error free intervals at any SNR other than the given with a good approximation. Lower m channels resulted in longer error free intervals because of independence of channel paths. Independent paths improved symbol detection. Arrangements with larger number of channels utilized (i.e. Tx = 6, Rx = 6) and uncorrelated paths (i.e. Rayleigh channel) give better BER performances. Error burst length, error free length, and bit error rate of V-BLAST system are unaffected by speed of mobile. In comparison with benchmark system, Rayleigh channel in V-BLAST system resulted in 2 times shorter error burst length, 3 times higher error free lengths, and 6dB gain at 10^{-2} BER. Correlated channels degraded in V-BLAST systems. Nakagami2.77 channel in V-BLAST system resulted 2-3 times higher error burst lengths, 100 times smaller error free lengths, and 10 dB loss at 4×10^{-1} BER.

V-BLAST system performance is analyzed over Rayleigh, Nakagami1.33, and Nakagami2.77 channel at 10 Hz Doppler when turbo coding is applied. This exercise is taken up to evaluate the effectiveness of Turbo Coding in V-BLAST. A comparison is also made between the statistics with and without coding. Cyclic shift type interleaver of depth 64, 512, and 1024 are used.

Error burst length distributions of V-BLAST are determined and modelling of distributions of error burst lengths is performed. Nakagami2.77 channel has the highest correlation among all channels under consideration. This correlation in channel paths gives worse detection performance for V-BLAST . This resulted in very long error bursts. As Nakagami parameter, m increases, error burst length increases and even the average probability of error degrades. Very small interleaving sizes are not desirable and very long interleaving sizes do not result in any improvement. For stronger signals, not only error burst lengths become shorter also their occurrences reduced. With the increase in interleaver size, error burst length and their occurrences increased. Tx = 6, Rx = 6 arrangement has smaller error Burst lengths higher error free lengths and better BER performance over Tx = 3, Rx = 3 arrangement. Rayleigh channel performs the best results in terms of higher capacity. It resulted the smallest error burst lengths, the highest error free lengths, and the least bit error rates. Comparing with the without coding case, error burst lengths and their occurrences are tremendously reduced with coding. Error burst length occurrences (EBLOs) are reduced with coding in high SNRs like 3, 6, 9 12 dB. While at 0 dB EBLOs are increased. Rate of decrease of EBLOs is higher (for IS=64, 512, 1024, and Rayleigh, Nakagami1.33 channels) *w.r.t* SNR in the setup (6×6) than in the setup (3×3). Therefore, at higher signal powers, large array of transmitters and receivers is beneficial. The most precise representative model for any error free length distribution is hyperbolic. Occurrences of error free lengths increased with decrease

in m(correlation) in channel paths. Turbo coding gave 2-8 dB gain for Rayleigh and Nakagami1.33 channels. There is very little improvement in Nakagmai2.77 channel. Increase in interleaving depth improves performance over Rayleigh channel. For Nakagami channels, very small and very long interleaver sizes degrade performance. Therefore, interleaver depth can be made adaptive.

Receiver can be made adaptive. Different detection schemes and variable turbo code rate may be used with environment. Increasing antenna spacing may be used to decorrelate the signal paths as far as possible.

Error burst lengths, error free lengths and their models can lead to development of other coding schemes specific to V-BLAST e.g. a serial concatenated code. An interesting observation stemming out of the results is the difficulty of V-BLAST with coding to reduce the error burst lengths and bit error rate in Nakagami2.77 channels, which are found in the micro cellular environment. Does it mean that it may be more difficult to implement V-BLAST in typical Urban areas? More work on this aspect will be a good contribution to wireless communications.

5.2 Future Work

During the course of this thesis, it was found that, future research can be directed towards the following areas.

Performance improvement can be made for Nakagami channels that are common

in wireless environment by decorrelating the channel paths for example by using singular value decomposition. Development of methods for channel estimation can also be a good addition. Methods like LSE, LMMSE estimation, or application of neural network are potential candidate for estimation of channels. Capacity of V-BLAST system can be calculated with inaccurate channel estimation. Instead of known channel transfer characteristic, channel can be equalized and the performance of the two scenarios can be compared. That can give a comparison of V-BLAST system for a pure theoretical versus a practical scenario. Very high data processing requirement for Diagonal-BLAST restrict researchers to enter in this area. Bit error rate performance of D-BLAST system can be evaluated. Statistical analysis of errors can be performed for Diagonal-BLAST. Error performance of V-BLAST system can also be investigated over CDMA which can be a step towards the application of BLAST technique in 3G systems. Detection algorithm for Nakagami channels can be devised so that V-BLAST can efficiently be used in micro cellular environment.

Bibliography

[1] Theodore S. Rappaport, *Wireless Communications*. New Jersey: Prentice Hall PTR, 1996.

[2] T. Ojanperä, R Parasad, "An overview of Third Generation Wireless Personal Communications: A European Perspective," *IEEE Pers. Communications*, vol. 5, No. 6, pp. 59–65, December 1998.

[3] V. Tarokh, N. Seshadri, A. R. Calderbank, "Space Time Codes for High Data Rate Wireless Communications: Performance Criteria and Code Construction," *IEEE Transaction Inf. Theory*, vol. 44, pp. 744–765, March 1998.

[4] P.W. Wolniansky, G.J. Foschini, G.D. Golden, R.A. Valenzuela, "V-BLAST: An Architecture for Realizing Very High Data Rates Over the Rich-Scattering Wireless Channel," *ISSSE 98. URSI International Symposium on Signals, Systems, and Electronics*, pp. 295–300, September 1998.

[5] G. J. Foschini, "Layered Space-Time Architecture for Wireless Communication in a Fading Environment When Using Multi-Element Antenna," *Bell Labs Technical Journal*, pp. 41–59, 1996.

[6] G. Foschini and M. Gans, "On Limits of Wireless Communications in a Fading Environment when using Multiple Antenna," *Wireless Personal Communications*, vol. 6, pp. 311–335, March 1998.

[7] G.D. Golden, G.J. Foschini, R.A. Valenzuela and P.W. Wolniansky, "Detection algorithm and initial laboratory results using V-BLAST space-time communication architecture," *IEE Electronic Letters*, pp. 14–16, January 1999.

[8] Stephen Baro, Gerhard Bauch, Aneta PAvlic, Andreas Semmler, "Improving BLAST Performance using Space-Time Bloce Codes and Turbo Decoding," *IEEE Global Telecommunications Conference*, pp. 1067–1071, November 2000.

[9] Won-Joon, Rohit Negi and Hohn M. Cioffi, "Combined ML and DFE Decoding for the V-BLAST System," *IEEE International Conference on Communications*, pp. 1243–1248, June 2000.

[10] Babak Hassibi, "A Fast Square-Root Implementation for BLAST," *Conference Record of the Thirty-Fourth Asilomar Conference onSignals, Systems and Computers, 2000*, vol. 2, pp. 1255–1259, October 2000.

[11] Xiaodong Li, Howard Huang, G.J. Foschini, and Reinaldo A. Valenzuela, "Effects of Iterative Detection and Decoding on the performance of BLAST," *Global Telecommunications Conference, 2000. GLOBECOM '00. IEEE*, vol. 2, pp. 1061–1066, November 2000.

[12] M.O. Damen, K. Abed Meraim and S. Burykh, "Iterative QR Detection for BLAST," *Wireless Personal Communications*, vol. 19, pp. 179–191, December 2001.

[13] Mathini Sellathurai and Simon Haykin, "TURBO-BLAST for High-Speed Wireless Communication," *Wireless Communications and Networking Conference, 2000. WCNC. 2000 IEEE*, vol. 1, pp. 315–320, September 2000.

[14] Howard Huang, Harish Viswanathan, and G.J. Foschini, "Achieving High Data Rates in CDMA Systems Using BLAST Techniques," *IEEE Global Telecommunications Conference*, vol. 5, pp. 2316–2320, December 1999.

[15] Seong Taek Chung, Angel Lozano, and Howard C. Huang, "Approaching Eigenmode BLAST Channel Capacity Using V-BLAST with Rate and Power Feedback," *Vehicular Technology Conference IEEE*, vol. 2, pp. 915–919, October 2001.

[16] Dmitry Chizhik, Farrokh Rashid Farrokhi, Jonathan Ling, Angel Lozano, "Antenna Separation and Capacity of BLAST in Correlated Channels," *IEEE-APS Conference on Antennas and Propagation for Wireless Communications*, pp. 183–185, November 2000.

[17] F.R. Farrokhi, G.J. Foschini, A. Lozano, R.A. Valenzuela, "Link-Optimal BLAST Processing With Multiple-Access Interference," *Vehicular Technology Conference, IEEE*, vol. 1, pp. 87–91, September 2000.

[18] J. G. Proakis, *Digital Communications*. McGraw Hill Inc., 1995.

[19] S. Haykin, *Communication Systems*. John Wiley and Sons, 2nd ed., 1983.

[20] P. A.Bello, "Characterization of randomly time-varying linaer channels," *IEEE Trans on Communication*, vol. 11, pp. 360–393, December 1963.

[21] R. H. Clarke, "A statistical theory of mobile-radio reception," *Bell System Technical Journal*, vol. 47, pp. 957–1000, July-August 1968.

[22] W. C. Jakes, *Microwave Mobile Communication*. Newyork: Willey, 1974.

[23] Seymour Stein, J. Jay Jones, *Modern Communication Principles*. New York: McGraw Hill Book Company, 1967.

[24] Roger L. Peterson, Rodger E. Zeimer, David E. Borth, *Introduction to Spread Spectrum Communications*. Singapore: Prentice Hall International Inc., 1967.

[25] Sweeney P., *Error Control Coding: an Introduction*. UK: Prentice Hall International Ltd., 1991.

[26] Clark G., Cain J., *Error Control Coding for Digital Communications*. New York: Plenum Publishing Corporation, 1998.

[27] Lin, Shu, Costello Jr., *Error Control Coding: Fundamentals and Applications*. 1983.

[28] B. Sklar, *Digital Communications: Fundamentals and Applications*. Prentice Hall, 1988.

[29] Luis M. Correia, *Wireless Flexible Personalised Communications*. New York: John Wiley and Sons, 1967.

[30] Pieter van Rooyen, Michiel Lötter, Danie van Wyk, *Space Time Processing for CDMA Mobile Communications*. Massachusetts: Kluwer Academic Publishers, 2000.

[31] A. J. Viterbi, "Convolutoinal Codes and Their Performance in Communication Systems," *IEEE Trans. Commun.*, vol. 34 No. 4, pp. 353–354, October 1971.

[32] Claude Berrou, Alain Glavieux, "Near Optimum Error Correcting Coding and Decoding: Turbo-Codes," *IEEE Transaction on Communications*, vol. 44 N0. 10, pp. 1261–1271, October 1996.

[33] Ali Mugaibel, Maan Kousa, "Understanding Turbo Codes," *Proceedings of 6th Annual IEEE TEM*, pp. 163–167, April 1999.

[34] Branka Vucetic, Jinhong Yuan, *Turbo Codes: Principles and Applications*. Massachusetts: Kluwer Academic Publishers, 2000.

[35] Andrew K.,Heegard C., Kozen D, "A Theory of Interleavers," *Technical Report, Computer Science Department, Cornell University*, June 1997.

[36] M. Patzold, U. Killat, F. Laue, and Y. Li, "On the statistical properties of deterministic simulation models for mobile fading channels," *IEEE Transactions on Vehicular Technology*, vol. 47, pp. 254 –269, February 1998.

[37] P. Hoeher, "A statistical discrete-time model for the WSSUS multipath channel," *IEEE Transactions on Vehicular Technology*, vol. 41, pp. 461–468, November 1992.

[38] Marius F. Pop and Norman C. Beaulieu, "Limitations of Sum-of-Sinusoids Fading Channel Simulators," *IEEE Transection on Communications*, vol. 49, No. 4, pp. 699–708, April 2001.

[39] G. L. Stuber, *Principles of Mobile Communication*. Boston: Kluwer Academic Press, 1996.

[40] S. Aun Abbas, Asrar U. Sheikh, "A Geometric Theory of Nakagami Fading Multipath Mobile Radio Channel with Physical Interpretations.," *Vehicular Technology Conference, IEEE*, vol. 2, pp. 637–641, April 1996.

[41] Laveen N. Kanal, A. R. K. Sastry, "Models for Channels with Memory and Their Applications to Error Control," *Proceedings of The IEEE*, vol. 66, No. 7, pp. 724–743, July 1978.

[42] J. G. D. Forney, *Concatenated Codes*. Cambridge: MA: MIT Press, 1966.

[43] C. Berrou, A. Glavieux, P. Thitimajshima, "Near Shanon limit error-correcting coding and decoding: Turbo-codes(1)," *Proc. ICC'93, Geneva, Switzerland*, pp. 1064–1070, May 1993.

[44] Patrick Robertson, "Illuminating the structure of code and decoder of parallel concatenated recursive systematic (turbo) codes," *Globel Telecommunications Conference, GLOBECOM'94*, vol. 3, pp. 1398–1303, December 1994.

[45] Dmitry Chizhik, Gerard J. Foschini, Michael J. Gans, Reinaldo A. Valenzuela, "Keyholes, Correlations, and Capacities of Multielement Transmit and Receive Antennas," *IEEE Transactions on Wireless Communications*, vol. 1, No. 2, pp. 361–368, April 2002.

[46] Da-Shan Shiu, Gerard J. Foschini, Michael J. Gans, Joseph M. Kahn *IEEE Transactions on Communications*, vol. 48, pp. 502–513.

[47] A. Duel-Hallen, "Decorrelating decision-feedback multiuser detector for synchronous code-division multiple-access channel," *IEEE Transactions on Communications*, vol. 41, pp. 285 –290, February 1993.

[48] Wei Zha, Steven D. Blostein, "Modified decorrelating decision-feedback detection of BLAST space-time system ," *IEEE International Conference on Communications*, vol. 1, pp. 335 –339, April 2002.

[49] S. Loyka, "Channel Capacity of two-antenna BLAST architecture," *IEE Electronic Letters*, vol. 35, pp. 1421–1422, August 1999.

[50] S. Loyka and J. Mosig, "Channel capacity of n-antenna BLAST architecture," *IEE Electronic Letters*, vol. 36, pp. 660–61, March 2000.

[51] A. Lozano, F.R. Farrokhi, R.A. Valenzuela, "Link spectral efficiency of blast in ricean wireless channels," *Bell Laboratories (Lucent Technologies)*.

[52] Catherine Z.W.H.Sweatman, J.S. Thompson, B. Mulgrew and P.M. Grant, "A Comparison of Detection Algorithms including BLAST for Wireless Communication using Multiple Antennas," *IEEE International Symposium on Personal, Indoor and Mobile Radio Communications PIMRC*, vol. 1, pp. 698–703, September 2000.

[53] Mathini Sellathurai and Simon Haykin, "Joint Beamformer Estimation and Co-Antenna Interference Cancellation for TURBO-BLAST," *IEEE Proceedings on Acoustics, Speech, and Signal Processing*, vol. 4, pp. 2453–2456, May 2001.

[54] Mathini Sellathurai and Simon Haykin, "A Simplified Diagonal BLAST Architecture with Iterative Parallel-Interference Cancellation Receivers," *IEEE International Conference on Communications*, vol. 10, pp. 3067–3071, June 2001.

[55] S. Sfar, R.D. Murch, and K.B. Letaief, "Performance of Packetized Layered Space-Time Detection Over Wireless Links," *IEEE Proceedings on Computers and Communications*, pp. 592–596, July 2001.

Vitae

- Sajid Anwar Khan.
- Born in Karachi, Pakistan on January 28, 1975.
- Received Bachelor of Engineering (B.E) degree in Electrical Engineering from N.E.D University of Engineering and Technology, Karachi, Pakistan in 1998.
- Joined King Fahd University of Petroleum and Minerals in January 2001.
- Publication: Sajid Anwar Khan and Dr. Asrar U. H. Sheikh, 'Error Performance of Vertical-BLAST over Rayleigh and Nakagami Fading Channels', submitted in IEEE-PIMRC Conference, September 2003, Beijing, China.
- Email: sajidk@kfupm.edu.sa